

17 March 2023

21481693-016-L-Rev0

James Evans

BHP Billiton Pty Ltd
Level 36, 125 St Georges Terrace
PERTH WA 6000

OREBODY 29/30/35/WR DEWATERING AND PER- AND POLYFLUOROALKYL SUBSTANCES MIXING ASSESSMENT

Dear James

1.0 INTRODUCTION

BHP Billiton Iron Ore (BHP) engaged Golder Associates Pty Ltd (Golder) to undertake groundwater modelling for areas within their Eastern Pilbara operations to evaluate the potential for per- and polyfluoroalkyl substances (PFAS) to migrate towards orebodies during dewatering activities. This letter provides the findings related to Orebody 29 (OB29), Orebody 30 (OB30), and Orebody 35 (OB35) for an updated dewatering scenario following a 24m/year drawdown rate as well as a 12m/year dewatering scenario to account for potential uncertainties in the future dewatering scheme.

1.1 Objectives and Scope of Work

The key objectives of this stage of the modelling works are:

- Provide an assessment of the potential mixing of groundwater impacted by PFOS and sum of PFOS and PFHxS (PFOS+PFHxS) prior to abstraction (i.e., the potential mixing that will occur in situ as part of abstraction required for mining) for OB29.
- Estimate the potential volume of impacted water that may be captured by abstraction bores.
- Estimate the potential concentrations of PFOS and PFOS+PFHxS in surplus groundwater that may be discharged to Ophthalmia Dam.

1.2 Assessment Criteria

In evaluating the potential risk associated with PFAS in abstracted groundwater, the modelling results were compared to the following PFAS NEMP (2020) criteria:

- The 95% species protection for freshwater for PFOS which is 0.13 µg/L.
- The 99% species protection for freshwater for PFOS which is 0.00023 µg/L.
- The drinking water criterion for PFOS+PFHxS which is 0.07 µg/L.

1.3 Site Setting

The study site is located southwest of Newman, Western Australia, approximately 12,000 km northeast of Perth. The operations in the area comprise the Whaleback Pit, OB29, OB30 and OB35; however, this report only focused on OB29, OB30, OB35 and the undeveloped area of Western Ridge, located to the southwest of OB35 (Figure A). Several areas within the study site have been identified as potentially contaminated, with initial releases anticipated to have occurred several decades ago. Of concern are impacts of PFAS which have been identified in groundwater. Groundwater sampling since 2020 has identified that PFOS and PFOS+PFHxS are present at concentrations above PFAS National Environmental Management Plan (NEMP) 2020 criteria (NEMP 2020).

Concerns have been raised that dewatering during mining activities at OB29, OB30 and OB35 could mobilise these species into abstraction bores which, when discharged to Ophthalmia Dam, may exceed the relevant ecological risk criteria.

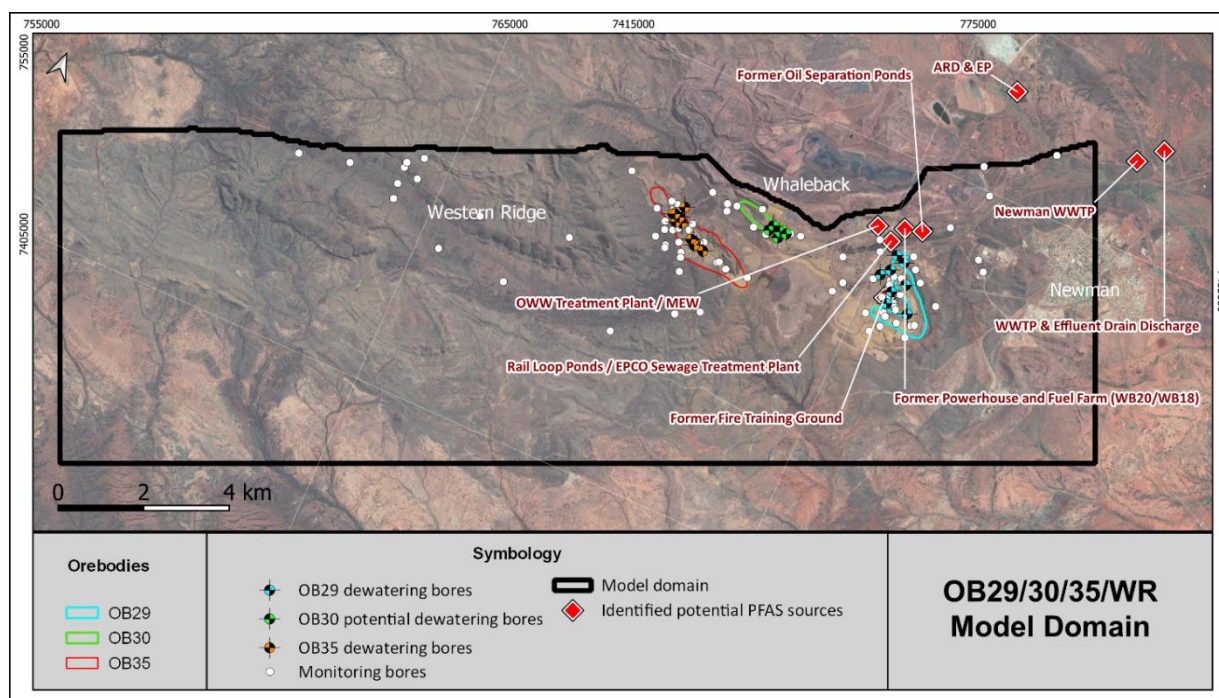


Figure A: Site Plan and Model Domain

2.0 MODELLING METHODOLOGY

The groundwater modelling has been completed in a staged approach and builds on the following previous scopes of work:

- A methodology was developed to assess the potential PFAS mixing at the dewatering bores of OB29, OB30 and OB35. The methodology uses the outputs of an updated groundwater model to assess the potential mixing rates. FlowSource software is used to process model outputs to estimate the volumes of water coming from impacted zones (as described in Golder 2020a and b). Overall, this methodology uses the flow budgets per each cell to calculate its contribution to a predefined destination cell (e.g., dewatering bores). In this way, FlowSource facilitates the calculation of the volumetric contribution for both impacted and clean areas, thus allowing for the assessment of the in-situ mixing. For a detailed description of the FlowSource methodology refer to Subsection 6.1. This methodology was peer-reviewed by a Department of Water and Environmental Regulation accredited Contaminated Sites Auditor. The mixing assessment presented in this letter has been carried out following this methodology.

- A groundwater model for an area containing OB29, OB30, OB35, and WR was developed by BHP to assess the dewatering volumes for the purpose of a 5C application (BHP 2020). The model was subsequently extended to include the latest observed dewatering rates and the head observations. The model was then calibrated to match the newer head and drawdown observation data.
- Forward simulations were carried out to forecast groundwater flow in the region until 2056. The groundwater model, including its predictive phase, was developed by BHP (BHP, 2020) using MODFLOW 2005 (Harbaugh, 2005), the dewatering scenario is based on the 5C licence modelling work.
- Geostatistical kriging methodology was used to develop a plume map of PFOS and PFOS+PFHxS. The plumes were developed using the maximum historical concentration for each species at all locations. Additional data was incorporated from recently installed monitoring bores during 2021 and 2022.

2.1 Base Case Groundwater Model and Model Variations

The groundwater model for the dewatering volumes for a 5C application for OB29 was extended to the west to include the entirety of OB35 and WR. The groundwater model has a general head boundary condition (GHB) along the northeastern boundary as the main groundwater inflow. Dewatering bores correspond to the main groundwater outflow from the model. The bores were simulated using the MNW2 package.

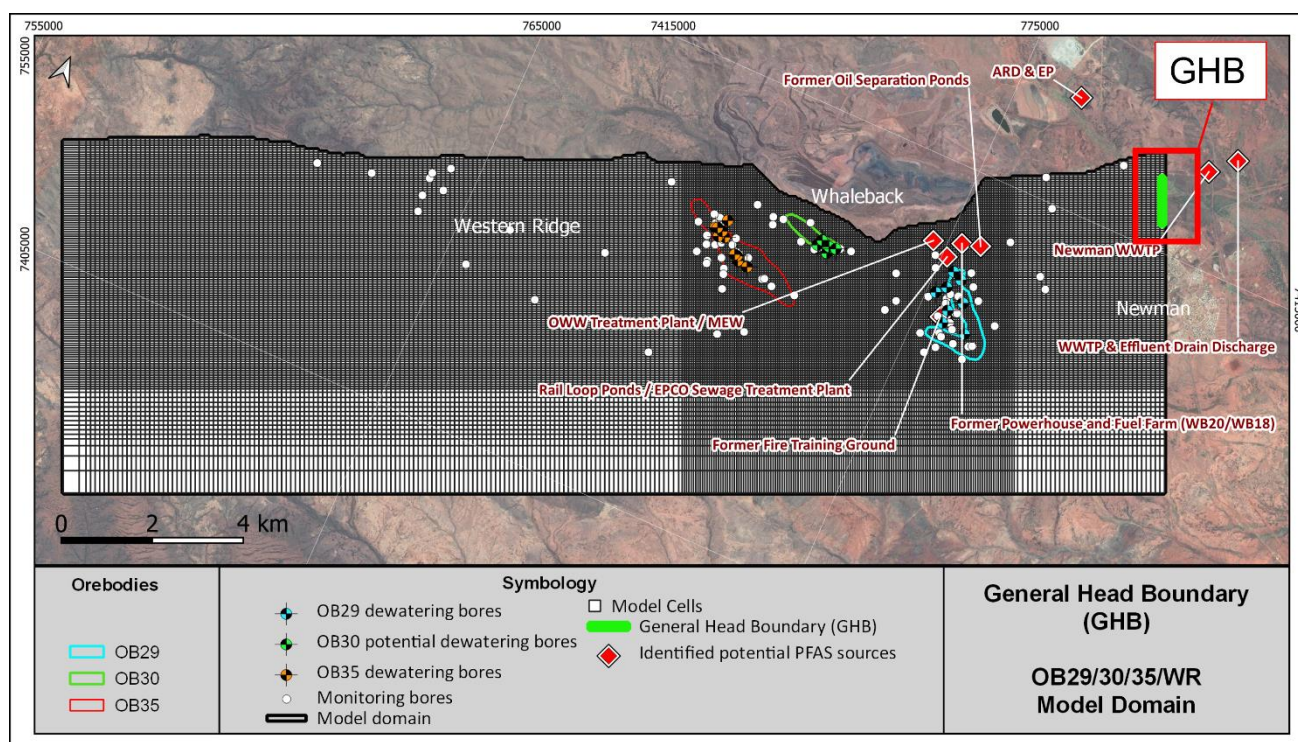


Figure B: Boundary Conditions in the OB29/30/35/WR Groundwater Model

Additional upgrades to the groundwater model hydraulic properties were included during the calibration process. After an initial attempt to calibrate the observed heads and dewatering, the software PEST_HP (Doherty, 2010) was used to continue the calibration in an automated yet controlled fashion. Hydraulic conductivities were updated during this process.

The calibrated version of this model is identified as “Base case”. The geological framework of the Base Case model version was later modified to account for potential uncertainties in the geological understanding between OB29 and OB30. Three additional model variations were constructed and calibrated: a) “Dolomite extended”, which correspond to Dolomitic regional aquifer being located to the north instead of the south of OB30 (Figure C); b) “Connecting fracture”, which incorporates a high transmissive, elongated zone connecting OB29 and OB30 (Figure D); and c) “Dolomite+Fracture”, which incorporates both features (Figure E).

The head distribution during the last time step from each model variation (“Base case”, “Dolomite extended”, “Connecting Fracture”, “Dolomite+Fracture”) in the historical model provided the initial condition for the predictive model variations. For all the model variations, the OB29 dewatering bores were extended down to Layer 4 to be able to match the dewatering targets.

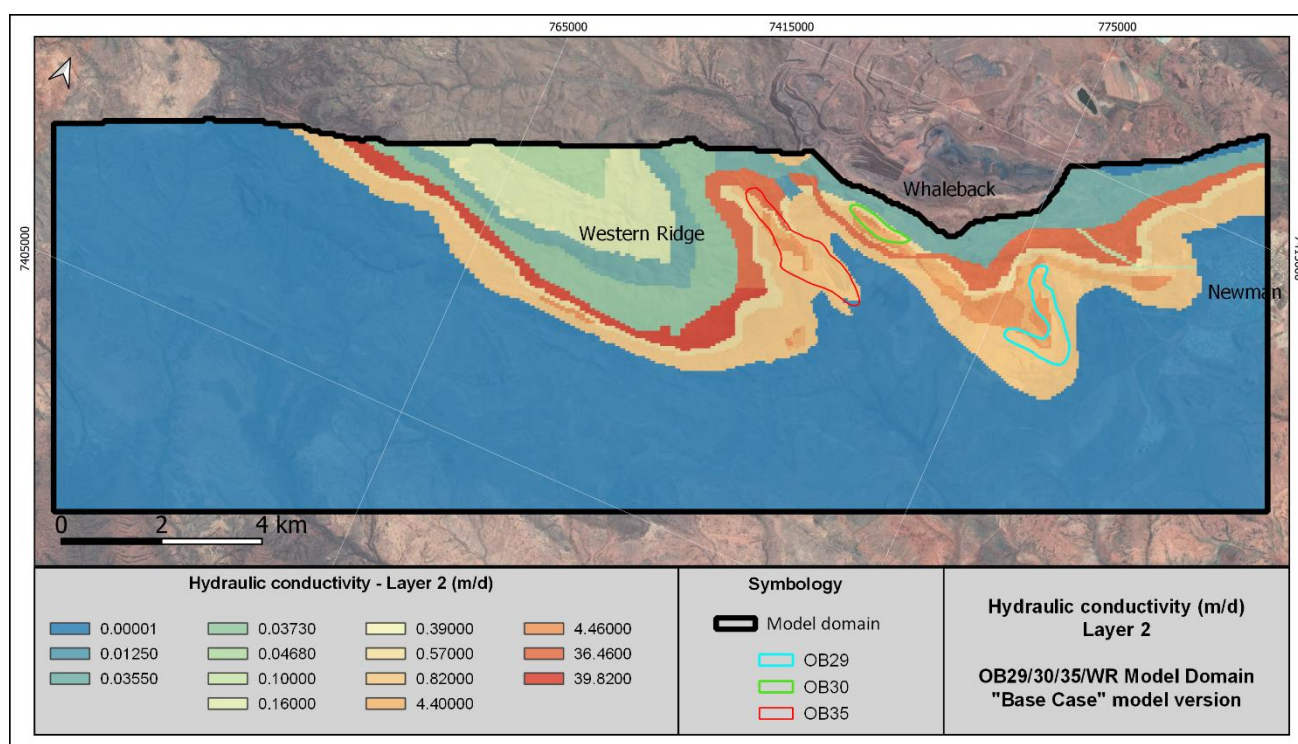


Figure C: Hydraulic conductivity zones (Layer 2) – OB29/30/35/WR “Base Case” model version

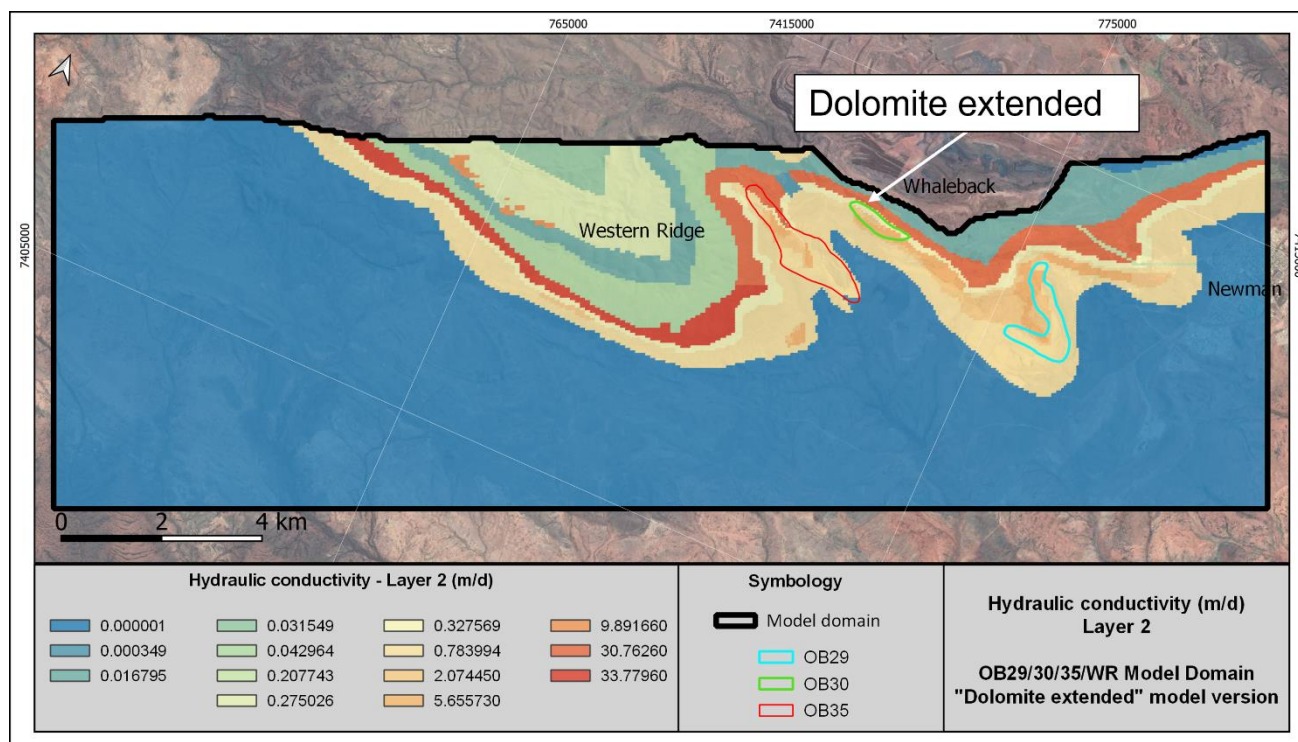


Figure D: Hydraulic conductivity zones (Layer 2) – OB29/30/35/WR “Dolomite Extended” model version

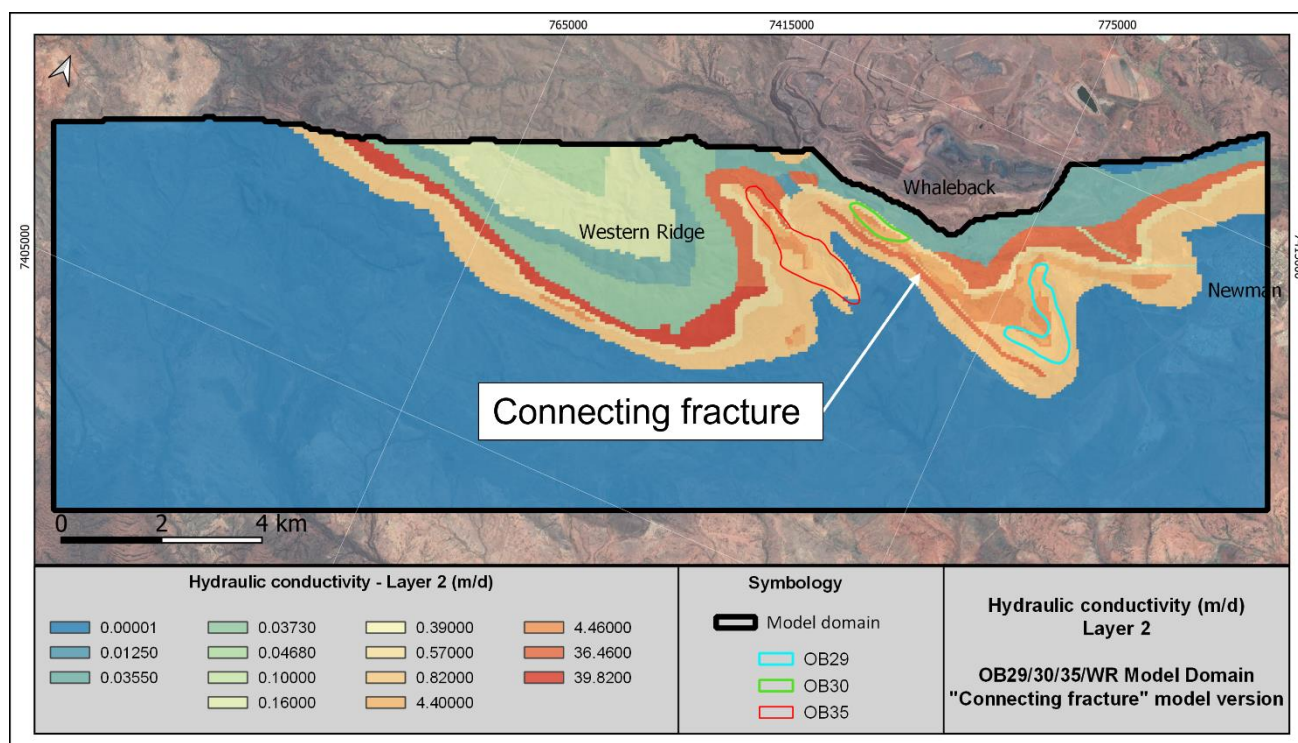


Figure E: Hydraulic conductivity zones (Layer 2) – OB29/30/35/WR “Connecting Fracture” model version

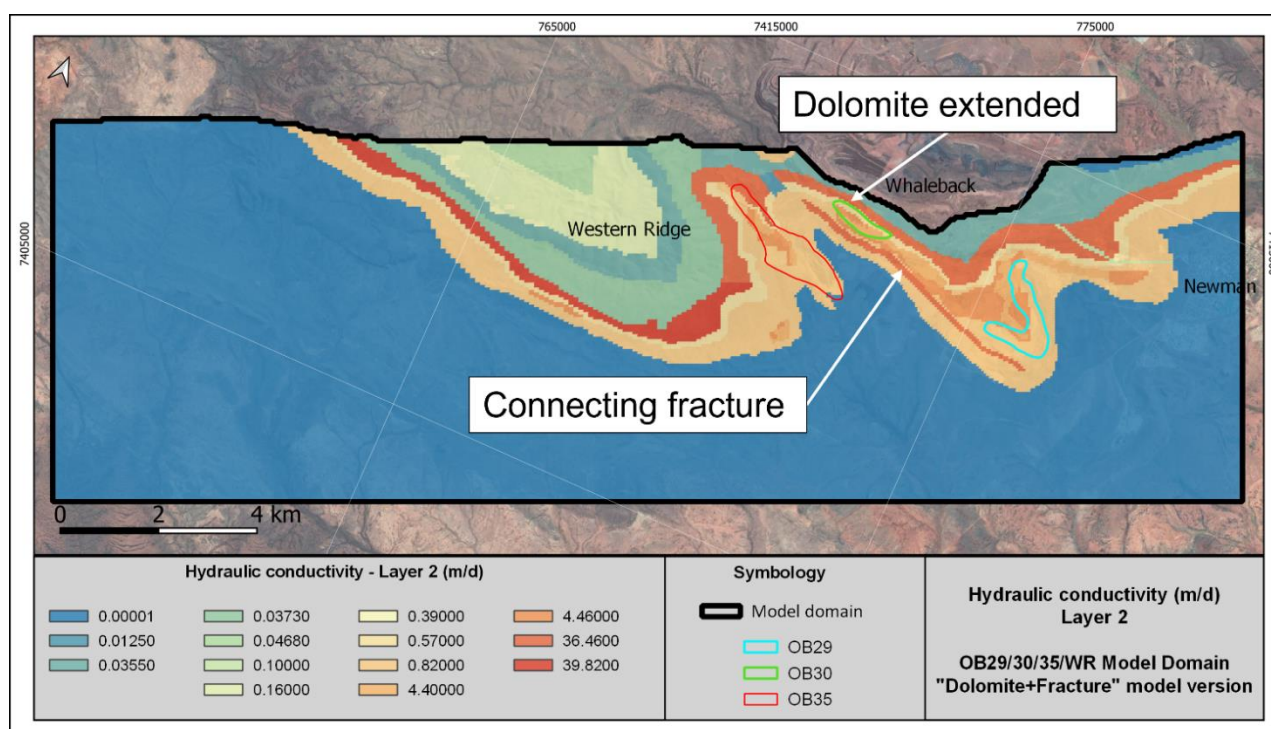


Figure F: Hydraulic conductivity zones (Layer 2) – OB29/30/35/WR “Dolomite+Fracture” model version

2.2 Modelling Assumptions

As part of these simulations, the following assumptions have been made:

- The concentrations of PFOS and PFOS+PFHxS were assumed to remain constant in the areas close to the identified potential sources (see Section 4.0) within the model domain. The plume was allowed to degrade outside of these defined sources (source release mechanism; Section 5.0).
- Calculations completed using FlowSource assume steady state flow for each time step. To account for the transient conditions, the Volume From and Volume Through metrics from FlowSource have been calculated at each time-step and each stress period. Although FlowSource metrics are calculated under transient stresses, the calculated volumetric contribution still represents a steady-state condition, therefore the calculations assume that all the abstracted water within the steady-state capture zone arrives instantaneously to the dewatering bore during the time step. Furthermore, this methodology does not consider contaminant transport travel times, which are controlled by factors such as porosities, dispersivity, diffusion, or retardation. Accordingly, it is considered that the calculations represent a conservative approach of the predicted concentrations.

2.3 Development Of Contaminant Plume

The mixing assessment requires an interpretation of contaminant distribution in the groundwater system. The derived plume characterisation supports the calculation of concentrations at the dewatering bores as well as the calculation of mixing factors.

For the purpose of developing the contaminant plume or “map”, data provided by BHP from monitoring bores within and just outside the modelling domain have been used. Due to the large aerial extent and limited sample coverage in some areas, interpolation control points were used to develop a more realistic interpretation of the plume extent. These control points were based on known areas of lower hydraulic conductivity (i.e., the Jeerinah Formation) as well as areas that are anticipated to have lower concentrations as these areas are undeveloped.

Historical maximum concentrations at each sampling location were used to develop the contaminant plume. Bores with PFOS and PFOS+PFHxS concentrations below the limit of reporting (LOR) of $<0.0002 \mu\text{g/L}$ were assigned a concentration of $0.0001 \mu\text{g/L}$, i.e., half the LOR of PFOS in the respective plume map development. This approach ensures the calculations result in a conservative approach that likely overestimates the background contamination at the site.

The resulting 2D plume maps for PFOS and PFOS+PFHxS are presented in Figure G and Figure H, respectively.

The vertical delineation for the plume was based on the limited information available but included a series of assumptions based on both direct field data analysis and calibration based on the predicted concentrations. As part of the plume thickness determination, the assumptions related to each orebody are outlined in the following sections.

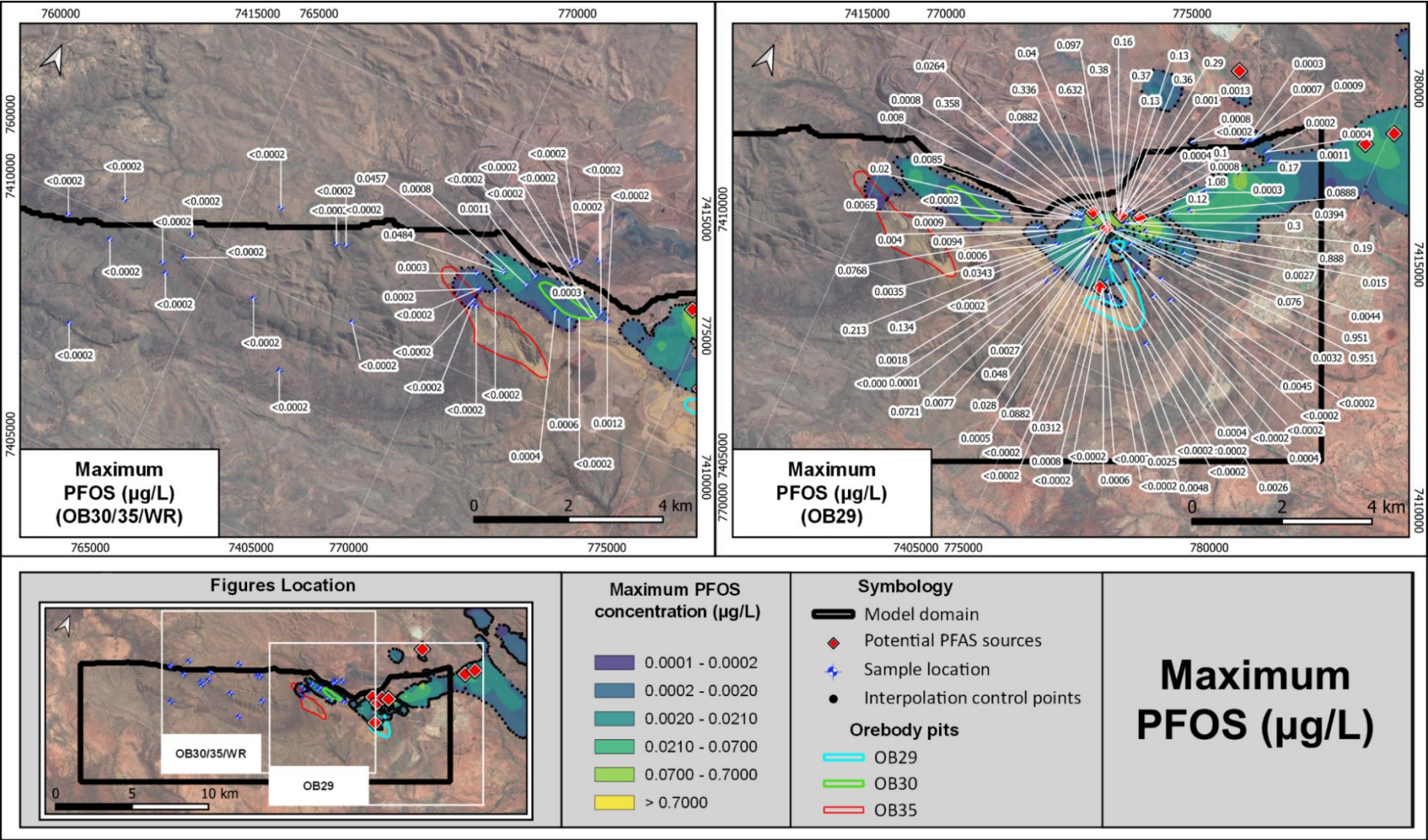


Figure G: Maximum PFOS Concentrations and PFOS Plume Map

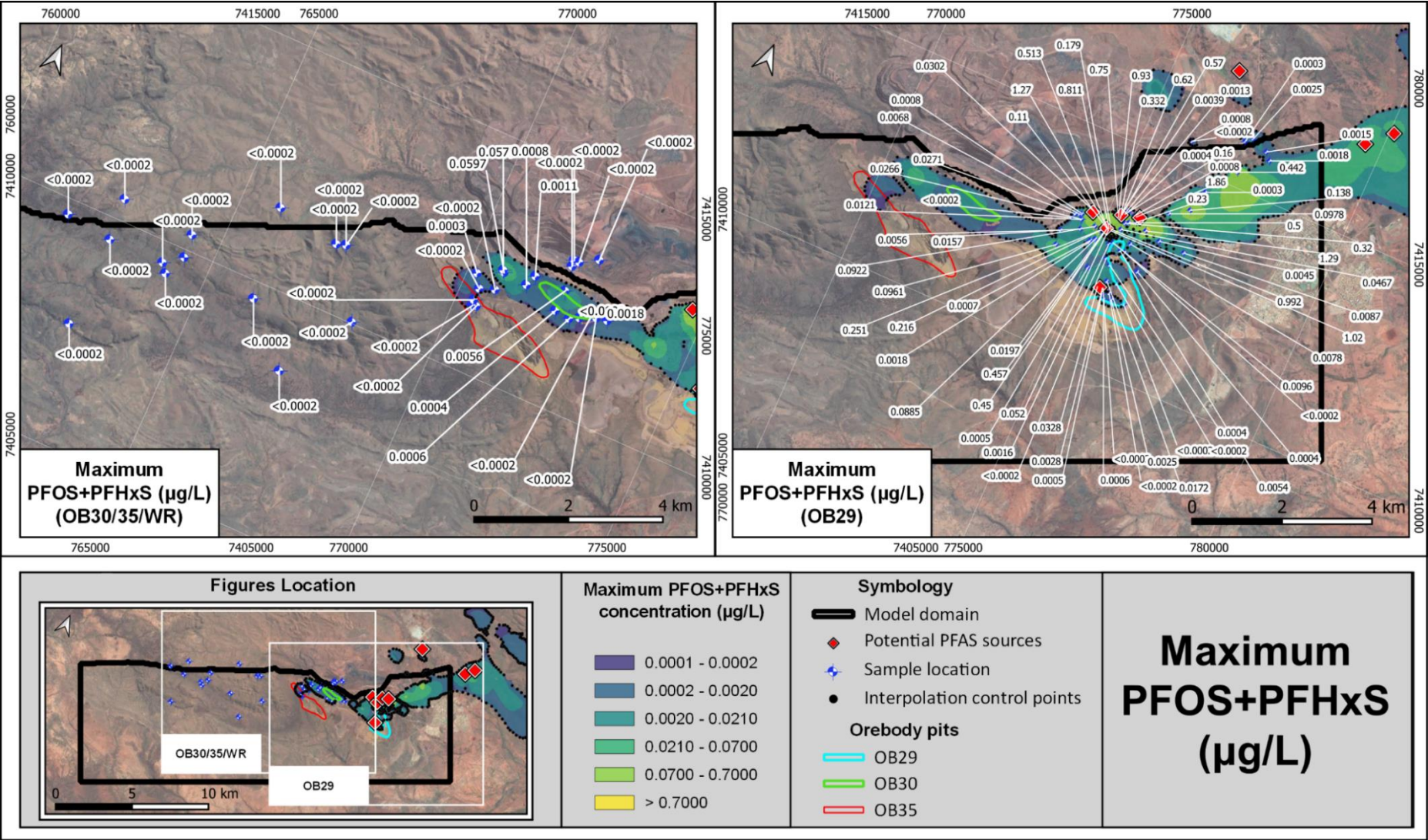


Figure H: Maximum Sum of PFOS+PFHxS Concentrations and Sum of PFOS+PFHxS Plume Map

2.3.1 OB29

- The plume thickness in OB29 was defined as 60 m. This definition was underpinned by both field data analysis and calibration from the predicted concentrations.
- Results from a vertical delineation field campaign in monitoring bores in OB29 during 2022 were analysed to define the plume thickness for the mixing assessment. An overview of these results is shown in Figure J. Overall, it can be observed that PFOS and PFOS+PFHxS were detected at depths between ~1 to ~91 m below the water table (m BWT). The deepest detection of PFOS and PFOS+PFHxS was observed at the bore HWHB1549M (~91 m BWT), west of OB29, where concentrations of both PFOS and PFOS+PFHxS were relatively low (0.0003 µg/L for both). However, higher concentrations were found in the bore HWHB1521M, northeast of OB29, at a depth of ~54 m BWT (0.0029 and 0.0078 µg/L for PFOS and PFOS+PFHxS, respectively).

An uncertainty analysis was also conducted by varying the plumes thickness during the mixing assessment while comparing the initial predicted concentrations to both the observed concentration at the individual dewatering bores and an averaged concentration from the existing dewatering bores in OB29 (Table 1). The sensitivity analysis considered four different plume thicknesses: 1, 10, 30, and 60 m. The results of this process showed that, for OB29, variations of the plume thickness between 10 and 30 m, and 30 and 60 m can result in up to one order of magnitude of difference in the predicted concentrations. A comparison with the observed concentrations at the individual bores (Attachment A) and the combined abstracted water from OB29 (Figure I) suggests that a plume thickness of ~60 m tends to better honour the data (Table 4).

Table 1: PFOS and PFOS+PFHxS Concentrations at Dewatering Bores in OB29

Name	PFOS (µg/L)	PFOS+PFHxS (µg/L)	Sampling Date
HWHB0049P	0.0004	0.0004	7/5/2020
HWHB0050P	0.0005	0.0005	7/4/2020
HWHB0051P	0.0026	0.0054	25/3/2020
HWHB0052P	0.0048	0.0172	23/1/2020
HWHB0057P	<0.0002	<0.0002	7/9/2020
HWHB0058P	0.0045	0.0096	21/3/2019
HWHB0059P	<0.0002	<0.0002	26/3/2020
HWHB0060P	<0.0002	0.0005	25/3/2020
Average	0.0016	0.0042	-

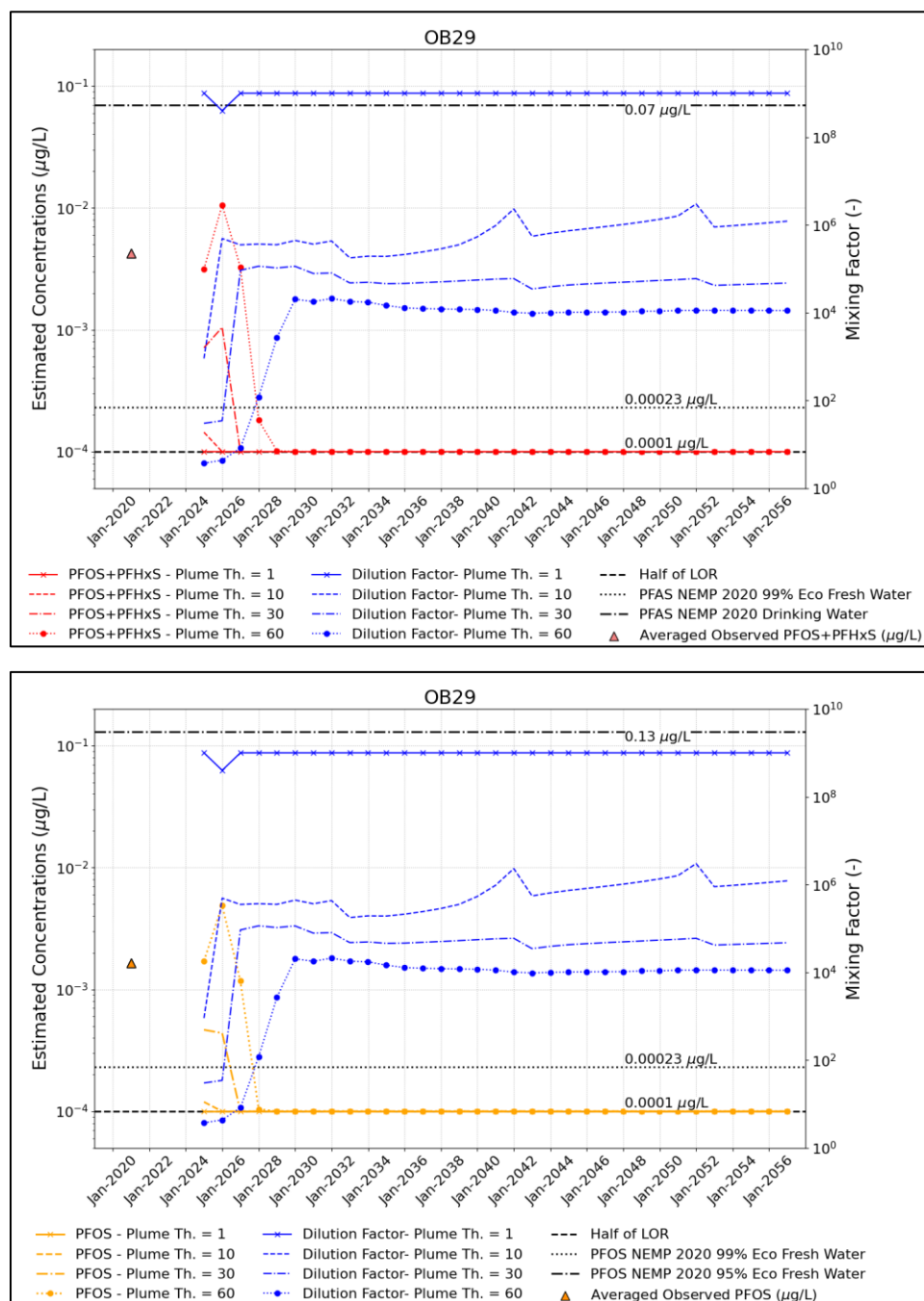


Figure I: Mixing Assessment Results of the Combined Abstracted Water in OB29 using Plume Thickness of 1, 10, 30 and 60 m.

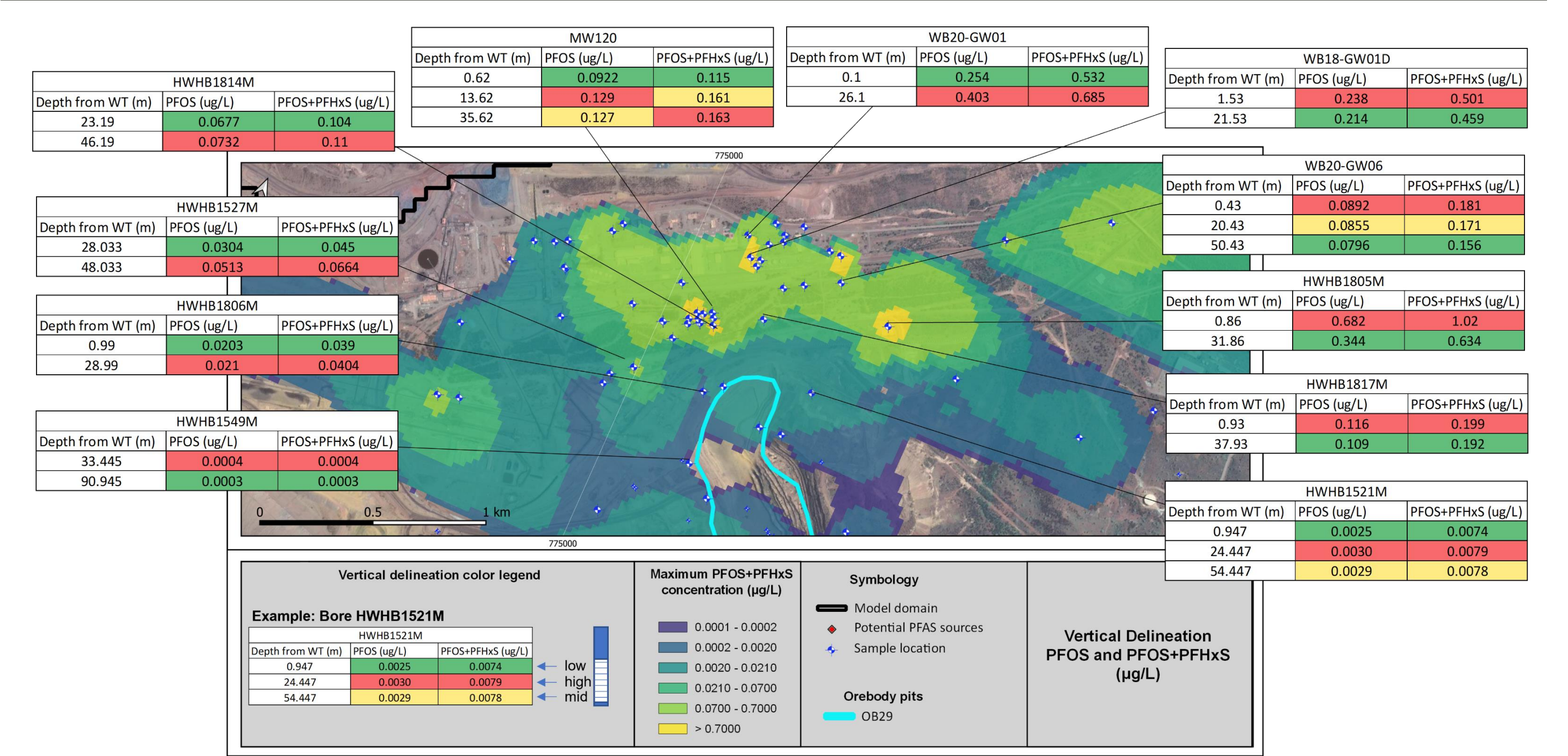


Figure J: Vertical Delineation Results from March 2022 Sampling Campaign in OB29

2.3.2 OB30

An uncertainty analysis was also conducted for OB30 by varying the plumes thickness of 1, 10, 30 and 60 m. The results of this process showed that, for OB30, variations of the plume thickness between 1 and 10 m can result in more than one order of magnitude of difference in the predicted concentrations. A comparison with the observed concentrations at the individual bores (Attachment A) and the combined abstracted water from OB30 (Figure K). A comparison with the observed concentrations at the individual bores (Attachment A) and the combined abstracted water from OB29 (Figure K) suggests that a plume thickness of ~30 m tends to better honour the data (Table 2).

Table 2: PFOS and PFOS+PFHxS Concentrations at Monitoring Bores Within and Around OB30

Name	PFOS (µg/L)	PFOS+PFHxS (µg/L)	Sampling Date
HEL0102M	0.0457	0.0597	20/7/2022
HWHB0802M	0.0484	0.0577	10/7/2021
HWHB1607M	0.0008	0.0008	10/7/2021
HEL0103M	0.0011	0.0011	4/7/2020
HWHB1616M	0.0003	0.0056	5/5/2021
HWHB1631M	0.0006	0.0006	4/8/2021
HWHB1608M	0.0004	0.0004	4/8/2021
HWHB1609M	0.0012	0.0018	4/8/2021
EL0006DM	<0.0002	<0.0002	11/7/2021
HEL0104M	<0.0002	<0.0002	19/7/2022
HWHB1610M	<0.0002	<0.0002	4/8/2021
HEL0101M	<0.0002	<0.0002	19/7/2022
Average	0.0082	0.0107	-

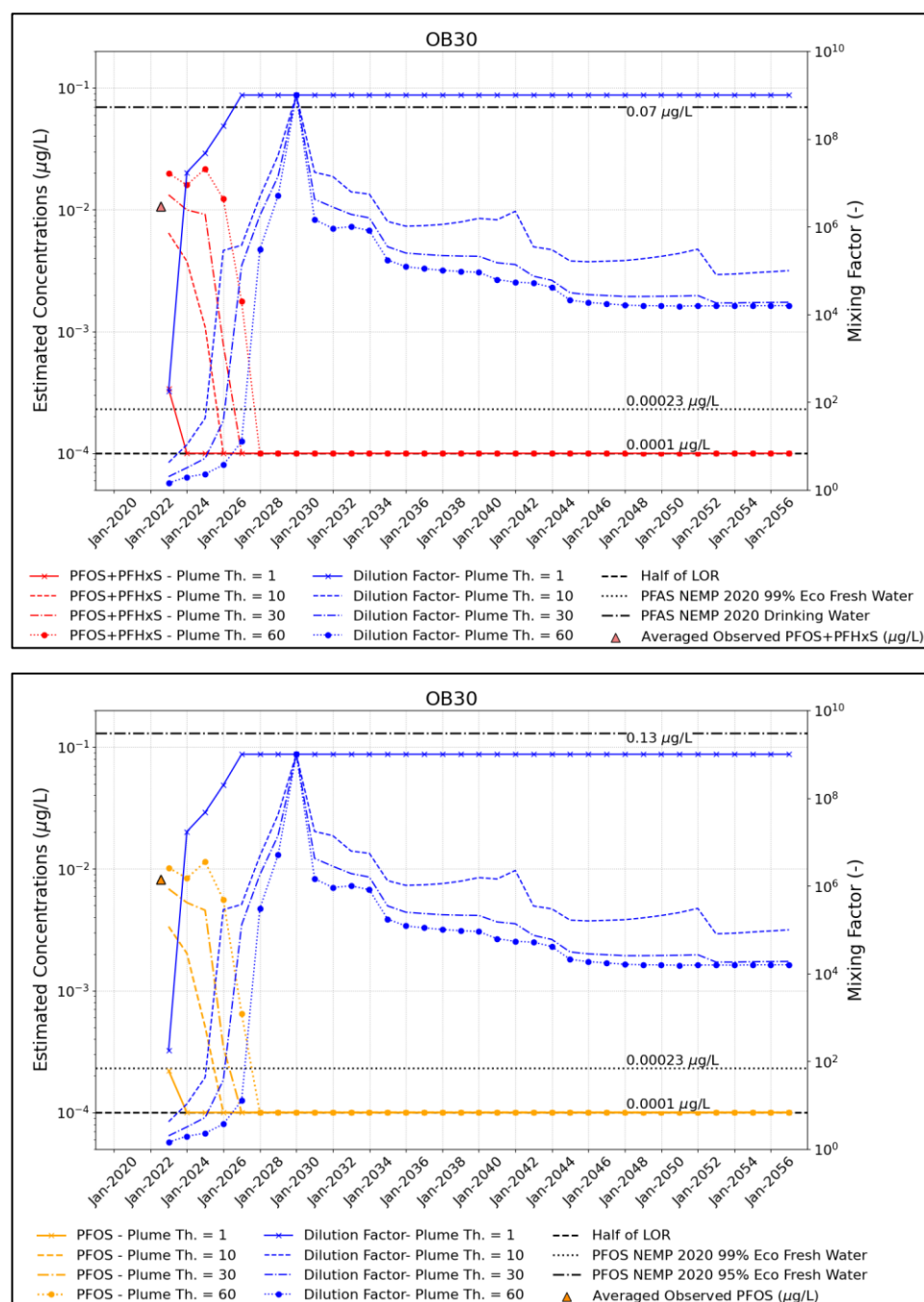


Figure K: Mixing Assessment Results of the Combined Abstracted Water in OB30 using Plume Thickness of 1, 10, 30 and 60 m

2.3.3 OB35

A sensitivity analysis was also conducted for OB35 by varying the plumes thickness of 1, 10, 30, and 60 m. The results of this process showed that, for OB35, variations of the plume thickness between 1 and 10 m can result in nearly one order of magnitude of difference in the predicted concentrations. A comparison with the observed concentrations at the individual bores (Attachment A) and the combined abstracted water from OB30 (Figure L). A comparison with the observed concentrations at the individual bores (Attachment A) and the combined abstracted water from OB29 (Figure L) suggests that a plume thickness of ~1 m tends to better honour the data (

Table 3: PFOS and PFOS+PFHxS Concentrations at Dewatering Bores in OB35

Name	PFOS (µg/L)	PFOS+PFHxS (µg/L)	Sampling Date
HEK0003P	<0.0002	<0.0002	4/7/2020
HEK0004P	<0.0002	<0.0002	9/7/2020
HEK0005P	<0.0002	<0.0002	9/7/2020
HEK0006P	<0.0002	<0.0002	4/7/2020
Average	<0.0002	<0.0002	-

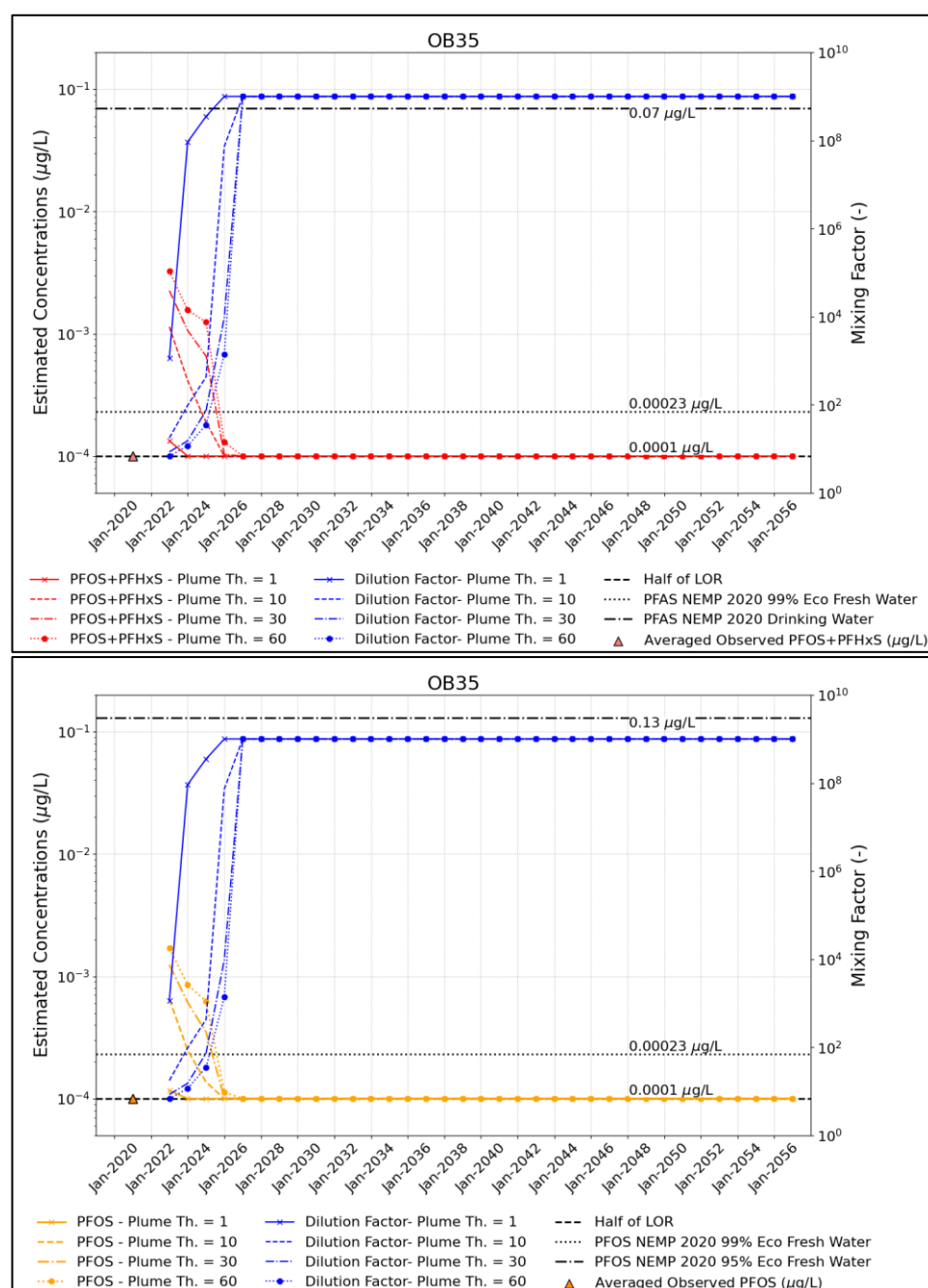


Figure L: Mixing Assessment Results of the Combined Abstracted Water in OB35 using Plume Thickness of 1, 10, 30 and 60 m.

2.3.4 Summary of Plume Thickness Uncertainty Analysis

From the uncertainty analysis and the vertical delineation data presented in the previous section, the most representative plume thickness for each orebody is presented in Table 4.

Table 4: Most Representative Plume Thickness for each orebody

Orebody	Plume thickness (m)	Supporting information
OB29	60	<ul style="list-style-type: none"> Field vertical delineation Comparison of predicted concentrations and averaged observations
OB30	30	<ul style="list-style-type: none"> Comparison of predicted concentrations and averaged observations
OB35	1	<ul style="list-style-type: none"> Comparison of predicted concentrations and averaged observations

3.0 DEFINITION OF POTENTIAL SOURCES

A previous review of historical operations/activities in and around OB29 where PFAS-containing chemicals were used, identified five potential sources of PFAS contamination to groundwater. For the purposes of the modelling, these sources were conservatively considered to be constant sources of PFAS to groundwater. Four of the sources were associated with the elevated concentrations of PFAS directly north of OB29. These sources are identified as: 1) Oily Waste Water (OWW) Treatment Plant / Mobile Equipment Workshop (MEW), 2) Rail Loop Ponds / EPCO sewage treatment plant, 3) Former powerhouse and fuel farm (WB20/WB18) and 4) Former oil water separation ponds (WB20). The fifth source is located to the west of OB29, and it was identified as 5) Former Fire Training Ground (WB26) (Figure M).

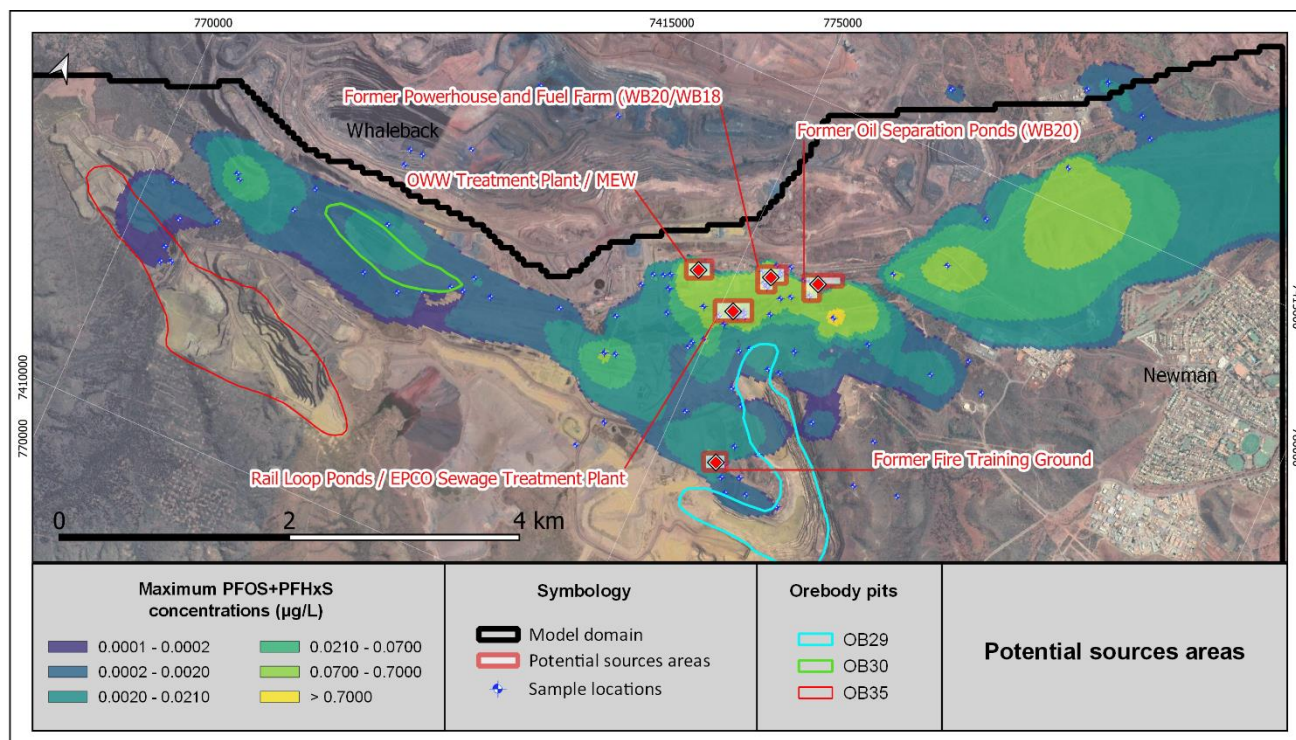


Figure M: Defined Potential PFAS Sources Areas within the model domain

4.0 PLUME DEPLETION

The mixing assessment methodology is based on a constant source release mechanism, which considers that areas defined as sources (Section 3.0) will continue to release contaminants during the entire simulated period. Concentrations in model cells outside of the source areas are allowed to deplete with time. The source of PFAS outside of the immediate source areas are unknown and it is considered that these areas may be diffuse PFAS impacts associated with past exploration or contaminant migration resulting from mining-related activities.

The plume depletion is performed using the Volume Through metric from FlowSource, which accounts for the groundwater that passes through a model cell. The plume is considered to 'deplete' when the Volume Through metric is greater than the water content in the cell whereby the PFOS and PFOS+PFHxS concentrations are reduced to half the LOR (0.0001 µg/L).

5.0 ASSESSMENT OF PUMPING SCENARIO

The projected dewatering rates for the individual dewatering bores were assigned to match the dewatering targets presented in Figure N. The objective dewatering targets are 412, 432, and 436 mAHD, for OB29, OB30 and OB35, respectively. The Base Case model and the geological scenarios were simulated using a drawdown rate of 24 m/year to reach the previously indicated objective dewatering targets. In order to account for potential uncertainties in the dewatering program, a second dewatering scenario was simulated using the Base Case model. This scenario used a drawdown rate of 12 m/years to reach the objective dewatering targets, presented in Figure O. The simulated dewatering bores in OB29 were extended to layer 4 to be able to reach the dewatering targets for all the described scenarios.

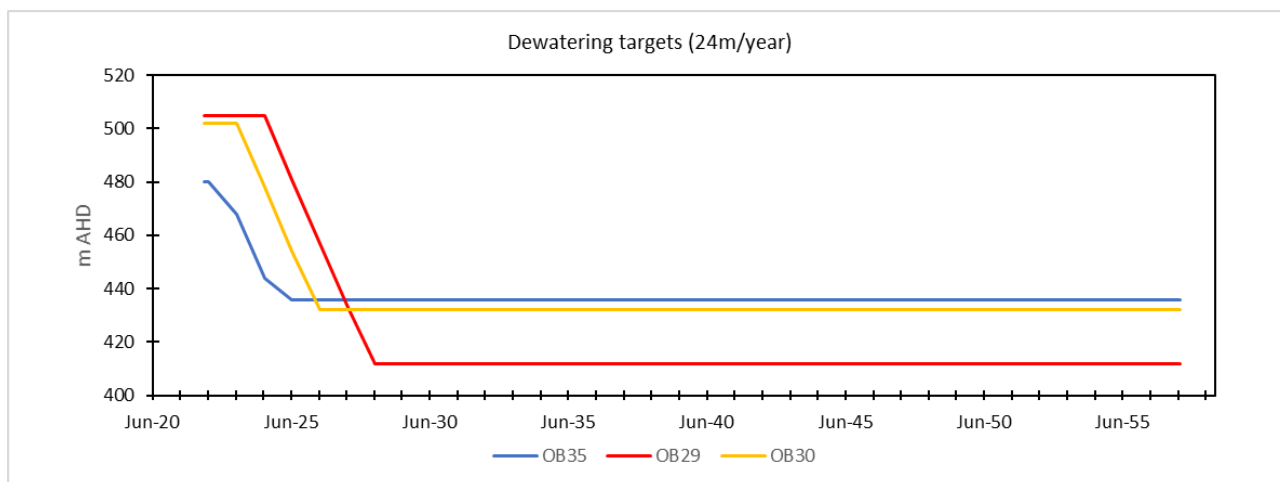


Figure N: Dewatering Targets for the 24 m/year Dewatering Scenario

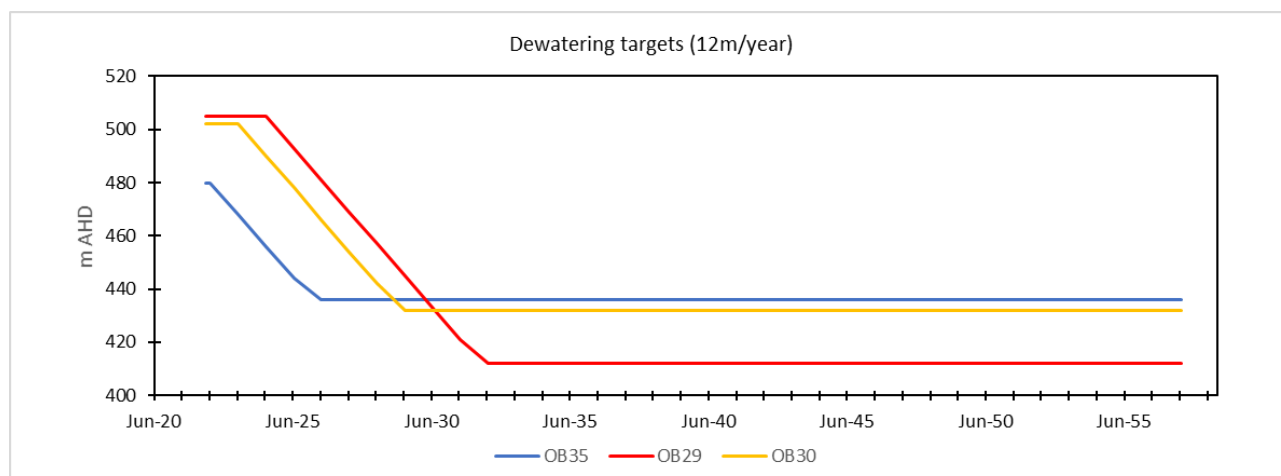


Figure O: Dewatering Targets for the 12 m/year Dewatering Scenario

For the 24 m/year dewatering scenario, the simulated total volume of water (Base Case model) abstracted by dewatering bores was calculated as 203.5 GL between 2022 and 2056 (predictive period) with a maximum dewatering rate of 61.6 ML/d during the financial year (FY) 2024-2025. Overall, the volumetric contribution from each orebody was calculated to be 56% from OB29, 16% from OB30 and 23% from OB35. Nonetheless, during the initial four financial years, i.e., until reaching the maximum abstraction rate in 2024-2025, OB35 contributes with 55% of the abstracted water, while OB30 with 23% and OB29 with 22% (Figure P).

For the 12 m/year dewatering scenario, the simulated total volume of water (Base Case model) abstracted by dewatering bores was calculated as 197.1 GL between 2022 and 2056 (predictive period) with a maximum dewatering rate of 44.1 ML/d during the FY 2025-2026. Overall, the volumetric contribution from each orebody was calculated to be 57% from OB29, 10% from OB30 and 33% from OB35. Nonetheless, during the initial five financial years, i.e., until reaching the maximum abstraction rate in 2025-2026, OB35 contributes with 82% of the abstracted water, while OB30 and OB29 with 9% (Figure Q).

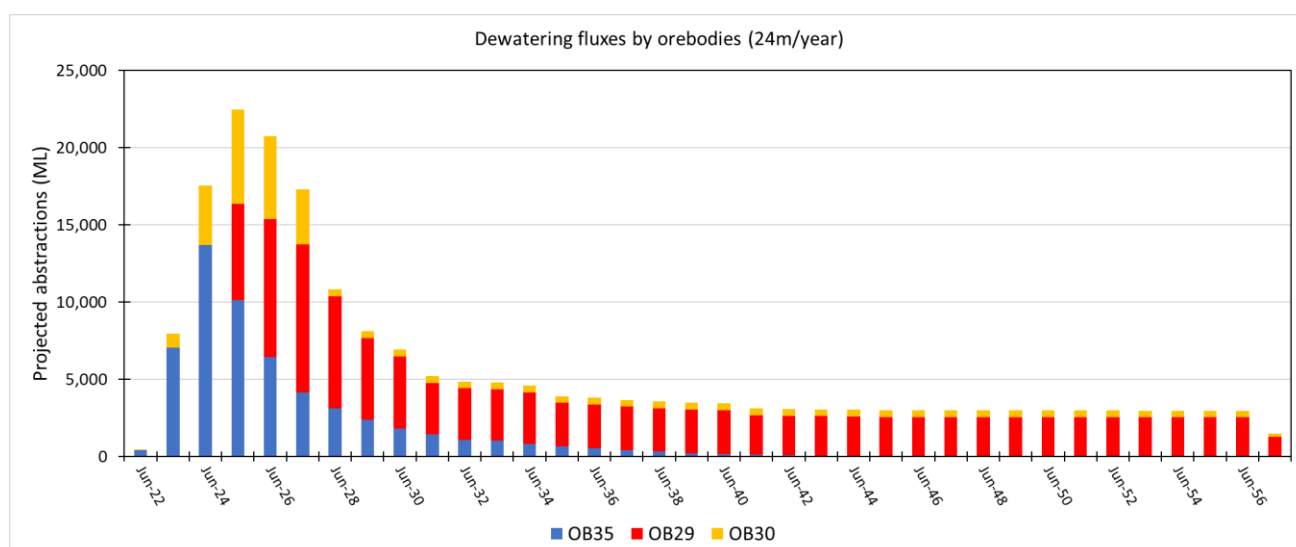


Figure P: Simulated Dewatering Rates for the 24 m/year Dewatering Scenario

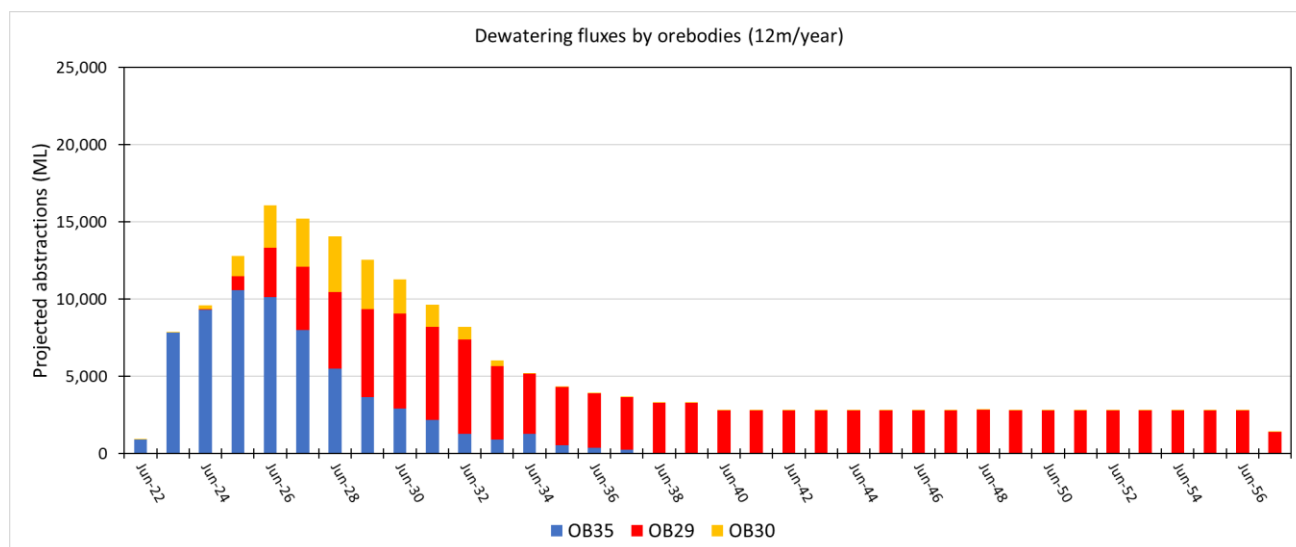


Figure Q: Simulated Dewatering Rates for the 12 m/year Dewatering Scenario.

Considering that the investigated geological scenarios did not produce important differences in the dewatering volumes using the 24 m/year dewatering scenario (Figure R), the 12 m/year dewatering scenario was only run for the Base Case model.

Figure S shows the comparison of the abstraction rates between the 12 and 24 m/year dewatering scenarios.

Overall, the model results honoured the observed heads across the model domain including OB29, OB30, OB35 and WR for the Base Case scenario. No major differences were observed within the geological scenarios. In all the tested scenarios, the predicted heads matched the dewatering targets, providing a well-determined gradient field to be used in the mixing assessment (see Figure T and Figure U for the 24 and 12 m/year scenarios, respectively).

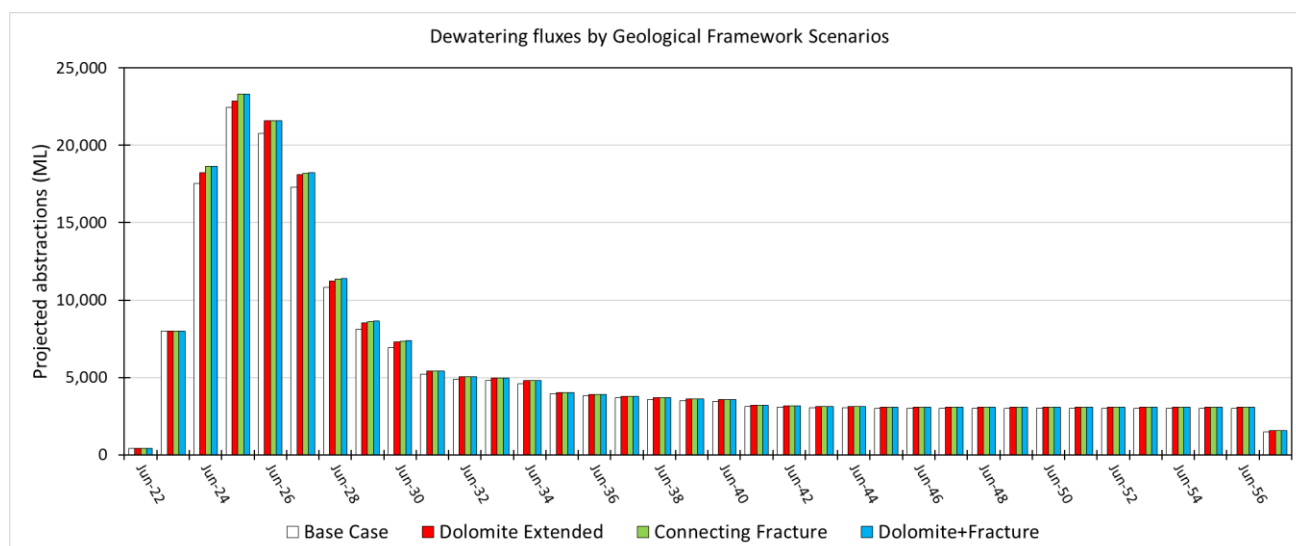


Figure R: Simulated Groundwater Dewatering Volumes within the Geological Scenarios

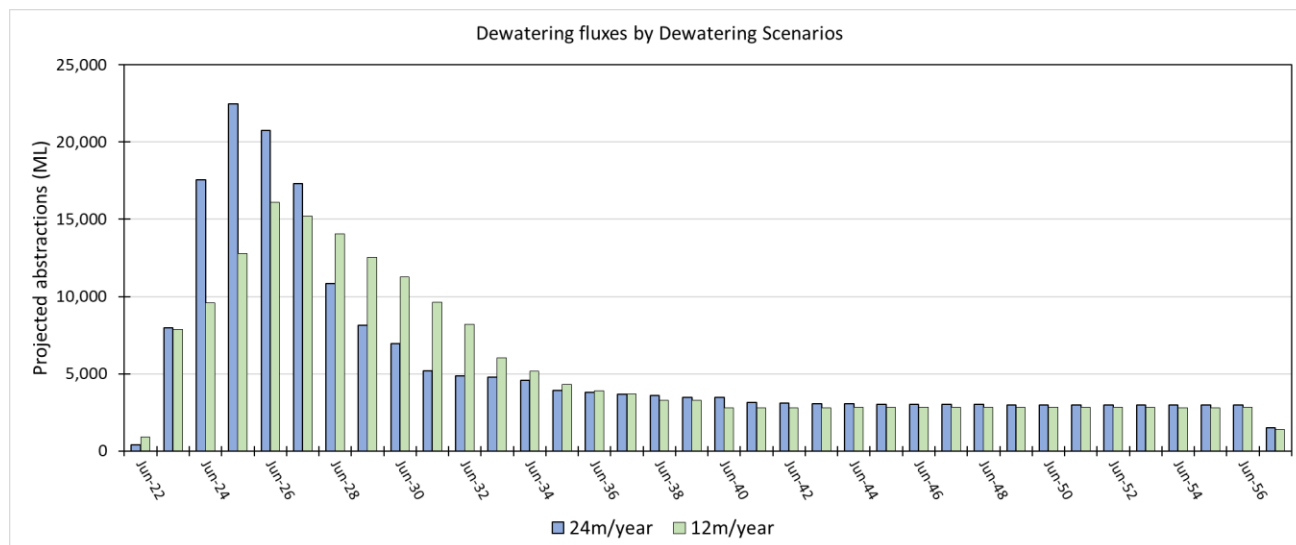


Figure S: Comparison Between Simulated Groundwater Dewatering Volumes by Dewatering Scenarios (12 vs 24 m/year)

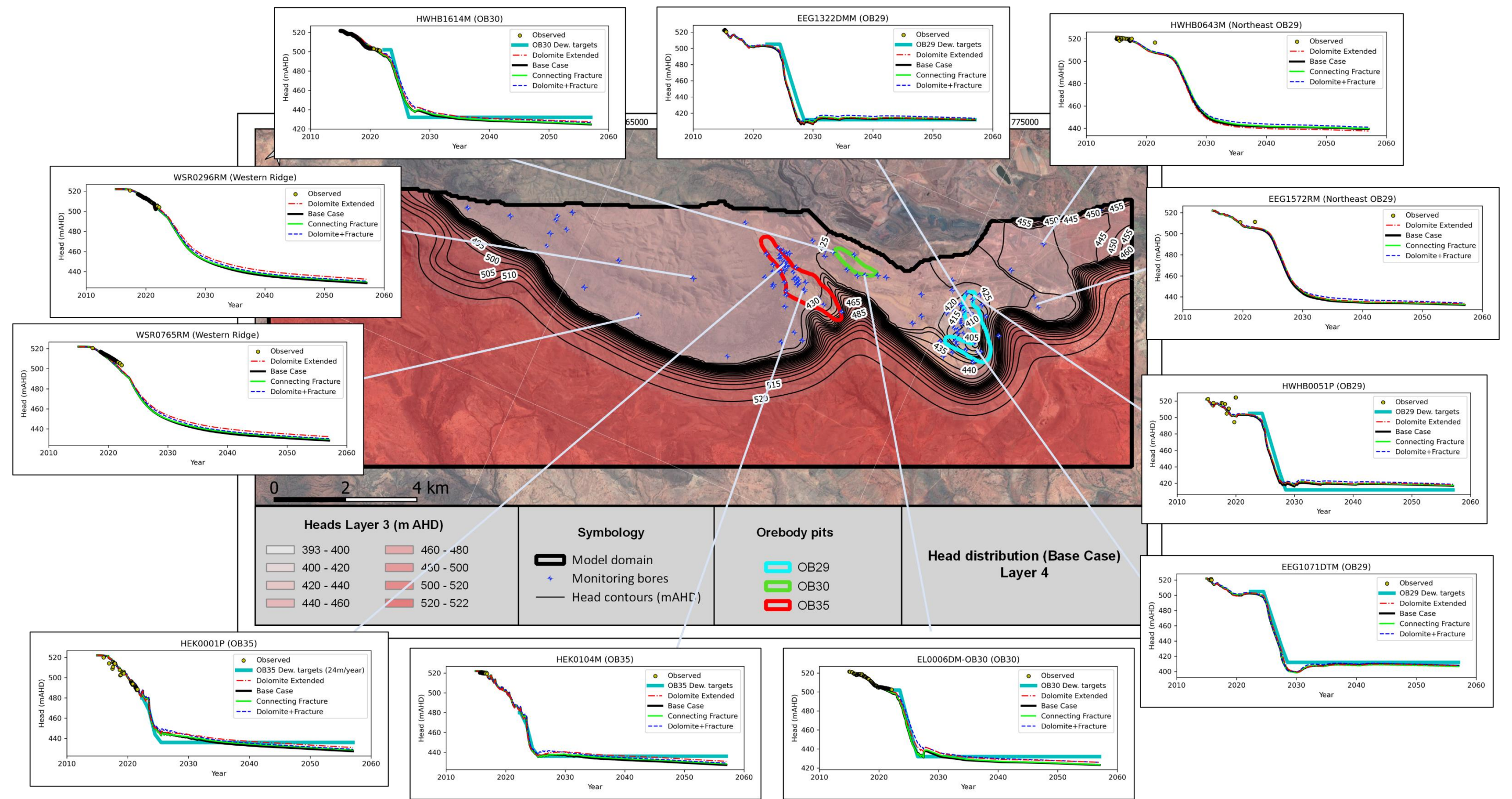


Figure T: Groundwater Level Contours (Base Case – year 2056) and Simulated Hydrographs (all model variations) at Selected Monitoring Bores Locations. Dewatering Targets Represented with a Cyan Line, while Measured Heads are Illustrated as Yellow Dots.

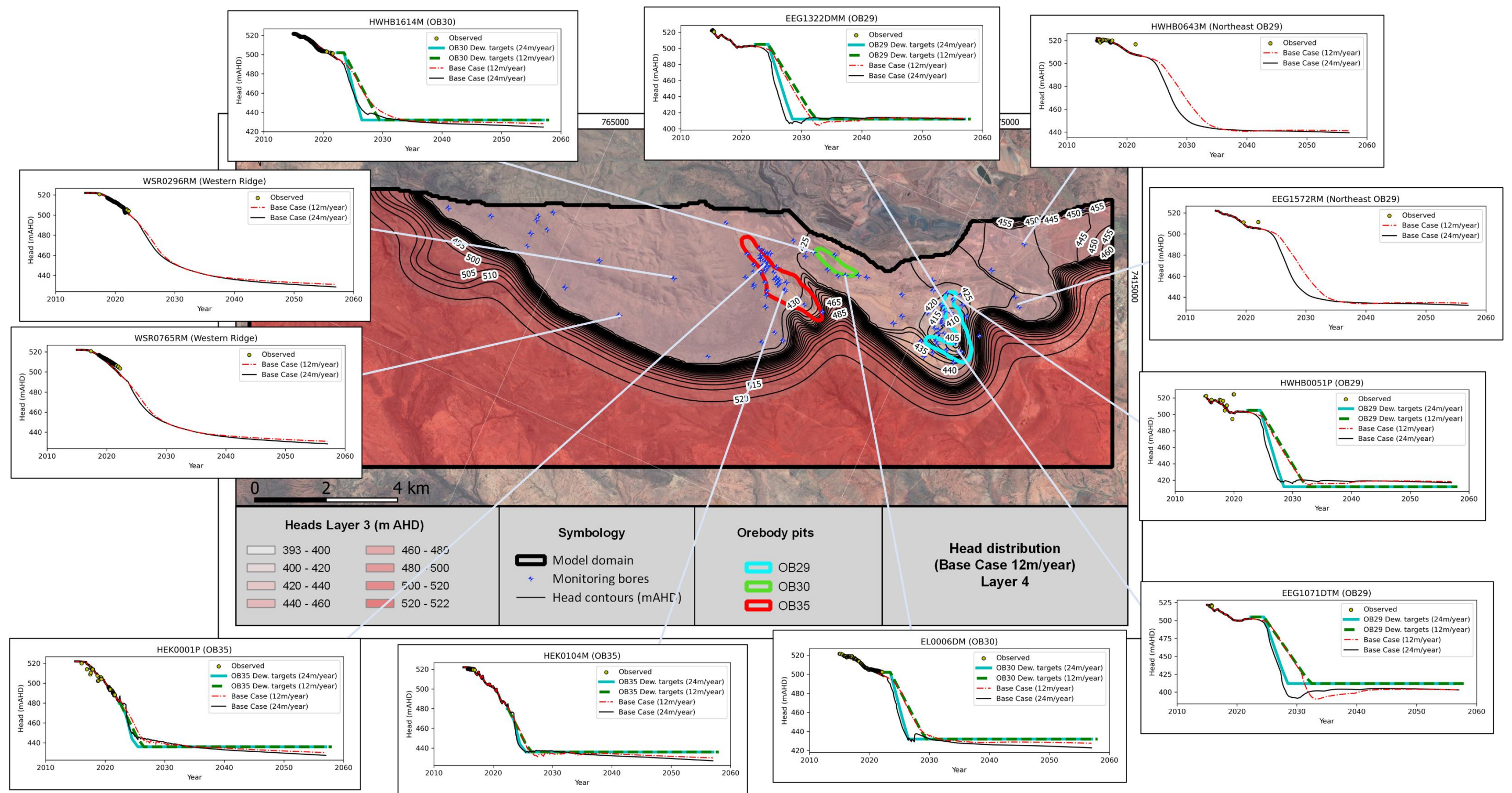


Figure U: Groundwater Level Contours (Base Case (12m/year) – year 2056) and Simulated Hydrographs (12 vs 24 m/year dewatering) at Selected Monitoring Bores Locations. Dewatering Targets for the 24m/year scenario Represented with a Cyan Line, while for the 12m/year Scenario Represented with a Green Dashed Line. Measured Heads are Illustrated as Yellow Dots.

6.0 ESTIMATION OF SUB-REGIONAL WATER BUDGETS

6.1 FlowSource

FlowSource (Black and Foley, 2013) is a post-processing utility which analyses groundwater flow fields computed by MODFLOW groundwater models. FlowSource can volumetrically delineate steady-state and quasi-steady-state capture zones. FlowSource takes MODFLOW drawdown, discretisation, and cell-by-cell files as inputs and then uses directed acyclic graphs (DAGs) to represent the groundwater flow path information but does not account for the travel time along the path. This enables estimation of the volume of groundwater that may ultimately reach a predefined 'destination' originating from each groundwater model cell. The 'destination' can be a single cell, or a group of cells and the cells need not be adjacent to one another.

For a specific "destination" model cell, FlowSource can be set up to calculate:

- Capture Fraction: The fraction of the flow through each model cell that will reach the destination cell.
- Volume From: The volume of water originating in each model cell that will reach the destination cell.
- Volume Through: The volume of water passing through each cell that will reach the destination cell.

Numerous other metrics can be calculated, but the three described above are considered to be the most relevant to this assessment. FlowSource has been widely used globally by industry, consultants, and regulators for a variety of purposes such as well head protection, pump and treat optimisation, and transient capture zone analysis (Black and Foley, 2013).

6.2 Analysis

The Volume From output from FlowSource was used to determine the volumetric contribution to a specific bore from each model cell during each stress period. The sum of this volumetric contribution was assumed to be exactly equal to the volume of water abstracted from each bore. Thus, this metric was used with the PFAS concentrations in each cell to estimate the contaminant mass load towards the bores.

To conduct this process, it was necessary to resize the plume maps to the same size and location as the model grid. In this way, the direct multiplication of Volume From and the PFAS concentration at each cell was assumed to represent the contaminant mass contribution to each bore during each stress period.

7.0 MIXING ESTIMATION RESULTS

7.1 Estimated Concentration at Individual Abstraction Wells

A mixing factor which is defined as the ratio of the volume of water reaching the abstraction bore from a contaminated region to that of the total volume of water being abstracted by the bore (Figure V), was calculated for each individual abstraction bore. It is important to estimate mixing because it provides critical information about the fluid dynamics within the groundwater system and shows how much the source has been mixed prior to reaching the abstraction bore.

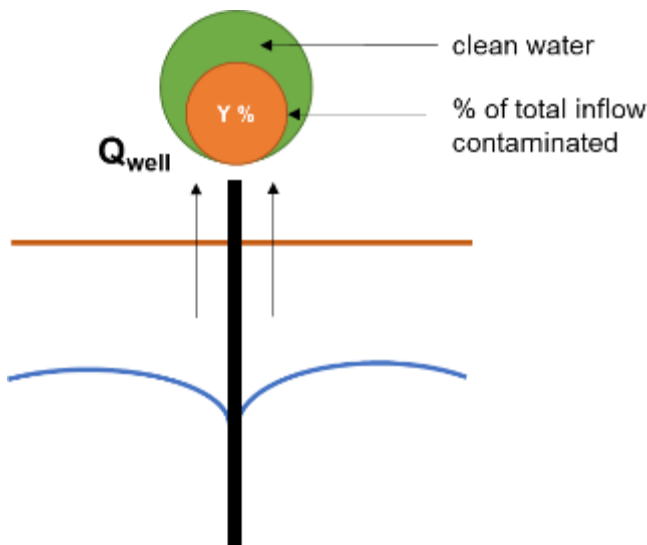


Figure V: Mixing Model.

Assuming no mixing or degradation of contaminants, the concentration of contaminants at each abstraction bore (C_{bore}) can be calculated as:

$$C_{bore} = \frac{\sum_{i=1}^n Vol_From_i \cdot C_i}{Q_{well}}$$

Where,

Q_{well} = Abstraction rate at well [L^3T^{-1}] (when there is no abstraction, C_{bore} is not calculated)

Vol_From_i = Volumetric contribution of the cell i that is finally abstracted at the dewatering bore [L^3T^{-1}]

C_i = Concentration of the assessed contaminant in the cell i [ML^{-3}]

The Mixing Factor (Y), defined as the inverse of the volumetric fraction of total inflow which is contaminated [-], is calculated as:

$$Y = \frac{Q_{well}}{\sum_{i=1}^n Vol_From_i} \text{ for cells } i \text{ with concentrations } C_i > 0.00023 \mu g/L$$

The individual abstraction bore assessment was carried out using the following approach for the proposed dewatering scenario:

- 1) A representative concentration for each cell in the model was determined based on the kriged contamination plume map.
- 2) For each model cell, the Volume From data from the FlowSource output was computed. A database was created for FlowSource outputs.
- 3) Mixing calculations were performed based on a source release mechanism. The product between the Volume From output from FlowSource and the PFAS concentration from the kriged plume at each model cell was calculated to determine the contaminant mass load at each model cell.
 - a) For cumulative Volume Through in a model cell greater than the total model cell volume, the concentration of contaminant in that model cell is assumed to be depleted and assigned a value of 0.0001 $\mu g/L$ (half the LOR).

- b) The plume concentrations were allowed to deplete based on the described methodology. The defined potential sources areas retain their concentrations constant during the entire simulation period.
- c) The total of the mass of contamination from all cells was then calculated by multiplying the concentration with the Volume From metric derived from the FlowSource postprocessing.
- d) To calculate the mixing factor, the sum of Volume From coming from model cells where the contaminant concentration is greater than the 99% species protection criterion ($0.00023 \mu\text{g/L}$) is considered to be the volume of water reaching the abstraction bores from an impacted region. On the other hand, the sum of Volume From coming cells with contamination concentration less than $0.00023 \mu\text{g/L}$ is considered as not impacted groundwater. The inverse of the mixing factor is then calculated as the sum of Volume From coming from contaminated areas divided by the actual abstraction at the bores to calculate, which corresponds to the sum of the Volume From coming from both, impacted and unimpacted regions.
- e) The total the mass of contaminant from all cells is then divided by the actual abstraction at the bores to compute the concentration of the contaminant at the bore.

7.2 Mixing Assessment Results

The estimation of potential concentrations of PFOS and PFOX+PFHxS from 2024 until 2056 was completed for each of the existing abstraction bores at OB29 and OB35, as well as the defined potential abstraction locations in OB30 (Appendix B). The dewatering bore locations are showed in Figure W. This process was conducted for the Base Case and the three geological model variations defined in Section 2.1 and the 12 m/year dewatering scenario. The analysis of these results is presented for the combined water from all dewatering bores within each orebody.

The assessment was carried out using the plume maps presented in Section 2.3 and assuming a constant source release mechanism. The plume thickness was defined as 1, 30, and 60 m for OB35, OB30 and OB29, respectively (refer to Section 2.3 for justification). The results have been screened against the 95% and 99% species protection criterion ($0.13 \mu\text{g/L}$ and $0.00023 \mu\text{g/L}$, respectively) and drinking water guideline ($0.07 \mu\text{g/L}$) (HEPA, 2020).

The results of the individual bores are presented in Attachment B while the results for the combined abstracted water from each orebody is presented in Figure X, Figure Y, and Figure Z.

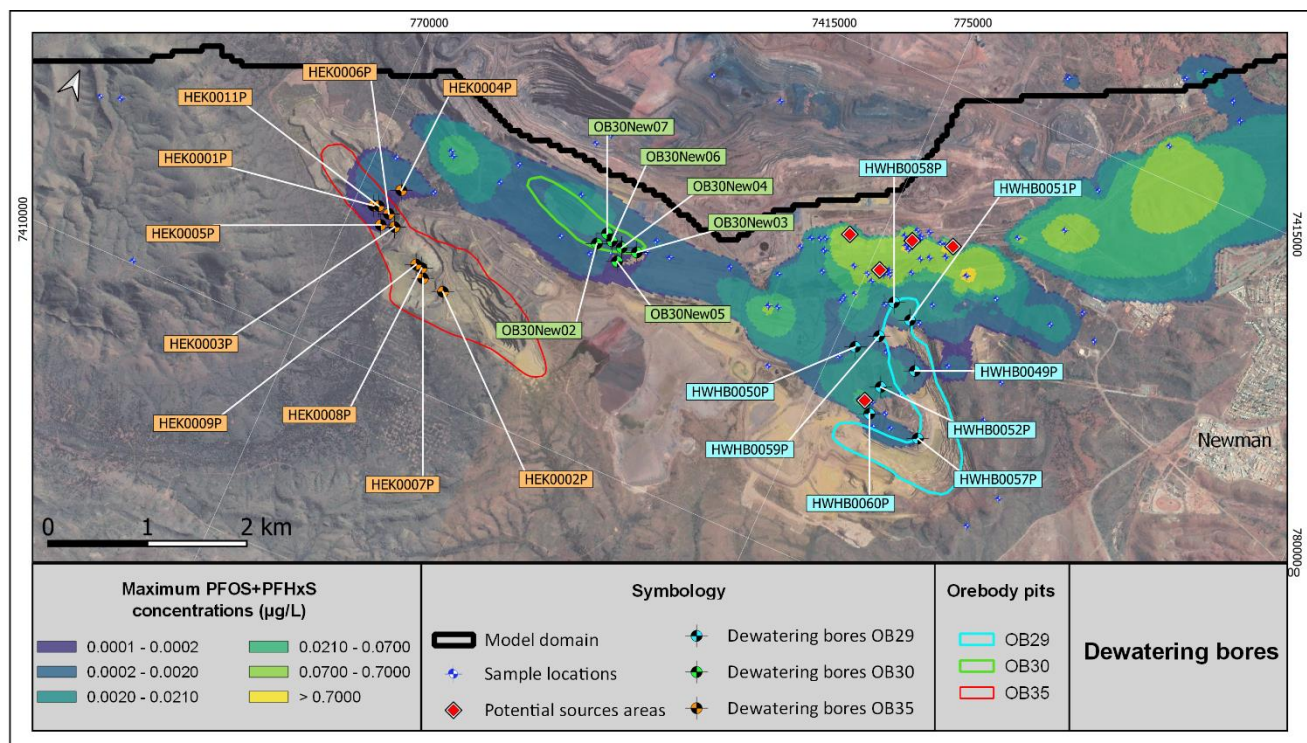


Figure W: Dewatering Bore Locations

During the entire period of dewatering activity, the predicted concentrations did not exceed the drinking water guideline for PFOS+PFHxS (0.07 µg/L) neither the screening value for the 95% species protection for PFOS (0.13 µg/L) for the combined water from each of the individual orebodies. However, it is predicted that during the initial four years of dewatering, PFOS concentration may exceed the screening value for the 99% species protection (0.00023 µg/L) in the combined water from OB29 and OB30. Similar results are observed for the individual bores in OB29 and OB30 where all of them showed predicted PFOS concentrations above the screening value for the 95% species (0.00023 µg/L) during the initial four years of dewatering. On the other hand, the PFOS concentrations of the combined abstracted water from OB35 and for their individual bore are predicted to below the 99% species protection (0.00023 µg/L) during the entire simulation time.

The following observation are made for the individual orebodies:

- For OB29 (Figure X), PFOS and PFOS+PFHxS concentrations are predicted to initially increase in the first year of dewatering for all the geological framework scenarios under the 24m/year dewatering scenario. This likely results from an increasing capture zone following the commencement of dewatering. A similar trend is observed for the 12m/year dewatering scenario; however, the increasing concentrations reach its peak three years following the commencement of dewatering. PFOS concentrations are predicted above the 99% species protection (0.00023 µg/L) during the first three years of the dewatering for all geological framework scenarios under the 24m/year dewatering scenario, and during the first five years under the 12 m/year dewatering scenario. This difference in the predictions between the dewatering scenarios is likely due to the smaller pumping rates during the 12 m/year scenario, which not only results in a slower propagation of the capture zone but also produces a slower plume depletion. After the predicted concentrations reach its peak, they rapidly decrease to values near half of LOR (0.0001 µg/L) by 2028 for all the geological framework scenarios. In comparison, for the 12 m/year dewatering scenario, PFOS and PFOS+PFHxS are predicted to decrease to values near half of LOR (0.0001 µg/L) by 2032.

- For OB30 (Figure Y), PFOS concentrations are predicted above the 99% species protection (0.00023 µg/L) during the first four years of the dewatering for all the geological framework scenarios under the 24 m/year dewatering scenario. On the other hand, under the 12 m/year dewatering scenario, PFOS concentrations are predicted above the 99% species protection (0.00023 µg/L) during the first eight years. After this, PFOS and PFOS+PFHxS concentrations are predicted decrease to values near half of LOR (0.0001 µg/L) by 2027 for the Base Case scenario, while for the rest of the geological scenarios, PFOS and PFOS+PFHxS are predicted to decrease to values near half of LOR (0.0001 µg/L) by 2028. For the 12m/year dewatering scenario, PFOS and PFOS+PFHxS concentrations are predicted to decrease to values near half of LOR (0.0001 µg/L) by 2030.
- For OB35 (Figure Z), PFOS and PFOS+PFHxS concentrations (2023) are predicted to be below the 99% species protection criterion (0.00023 µg/L) throughout the duration of the dewatering. There is an initial detection in the first year of dewatering; however, in subsequent years the concentrations decrease to values near half of LOR (0.0001 µg/L) for all the geological scenarios and the 12m/year dewatering scenario.

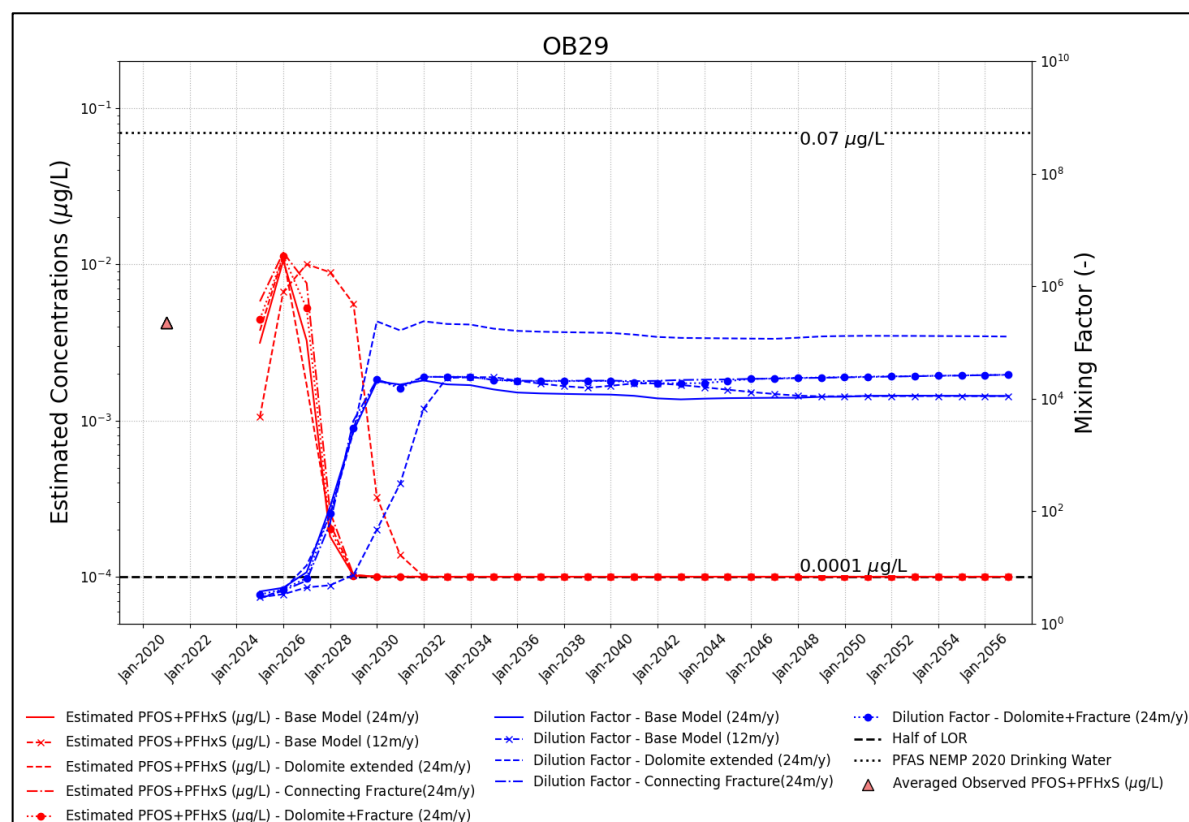
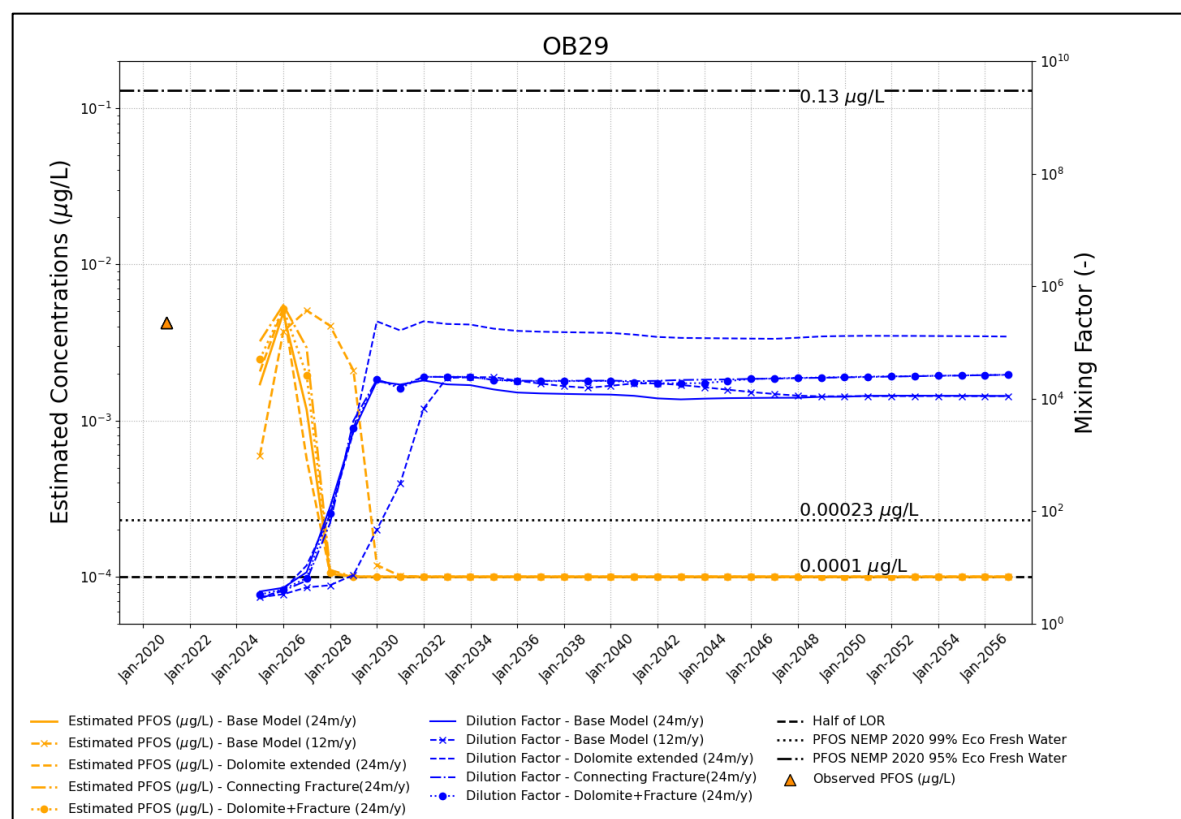


Figure X: Mixing Assessment Results for PFOS (top) and PFOS+PFHxS (bottom) for the Combined OB29 dewatering

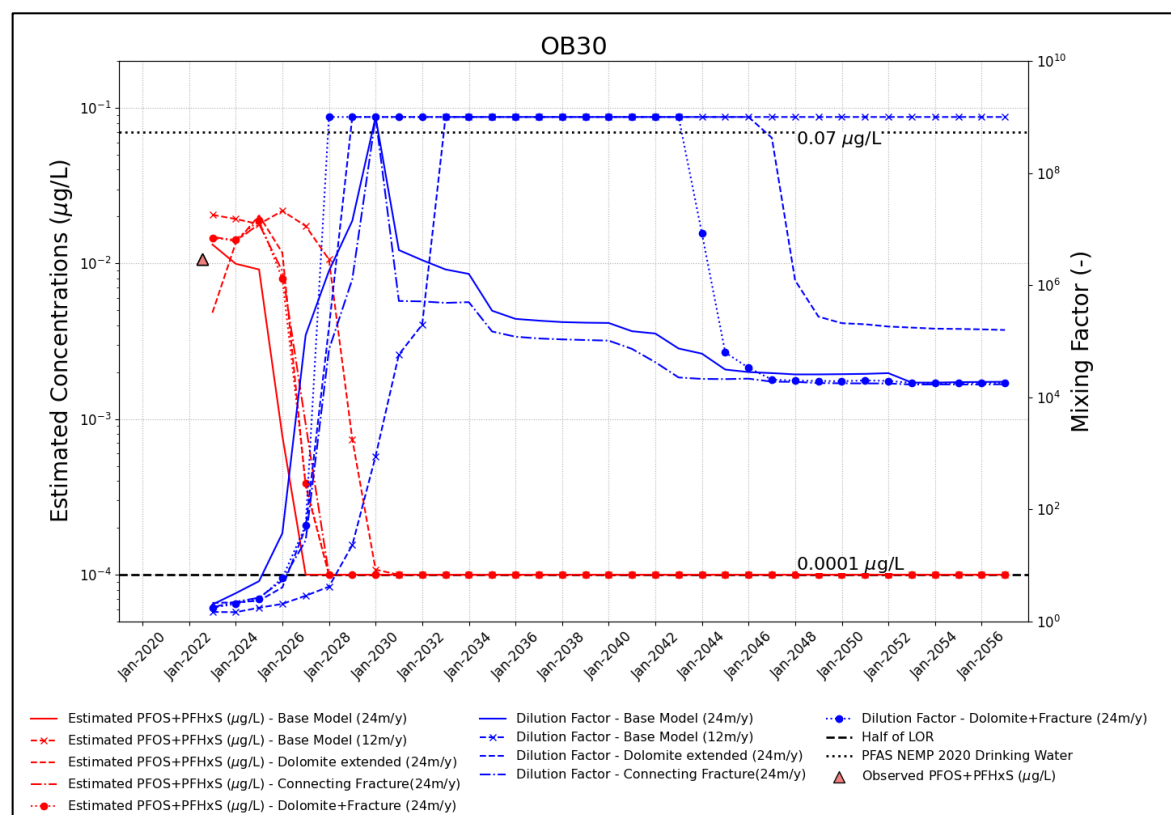
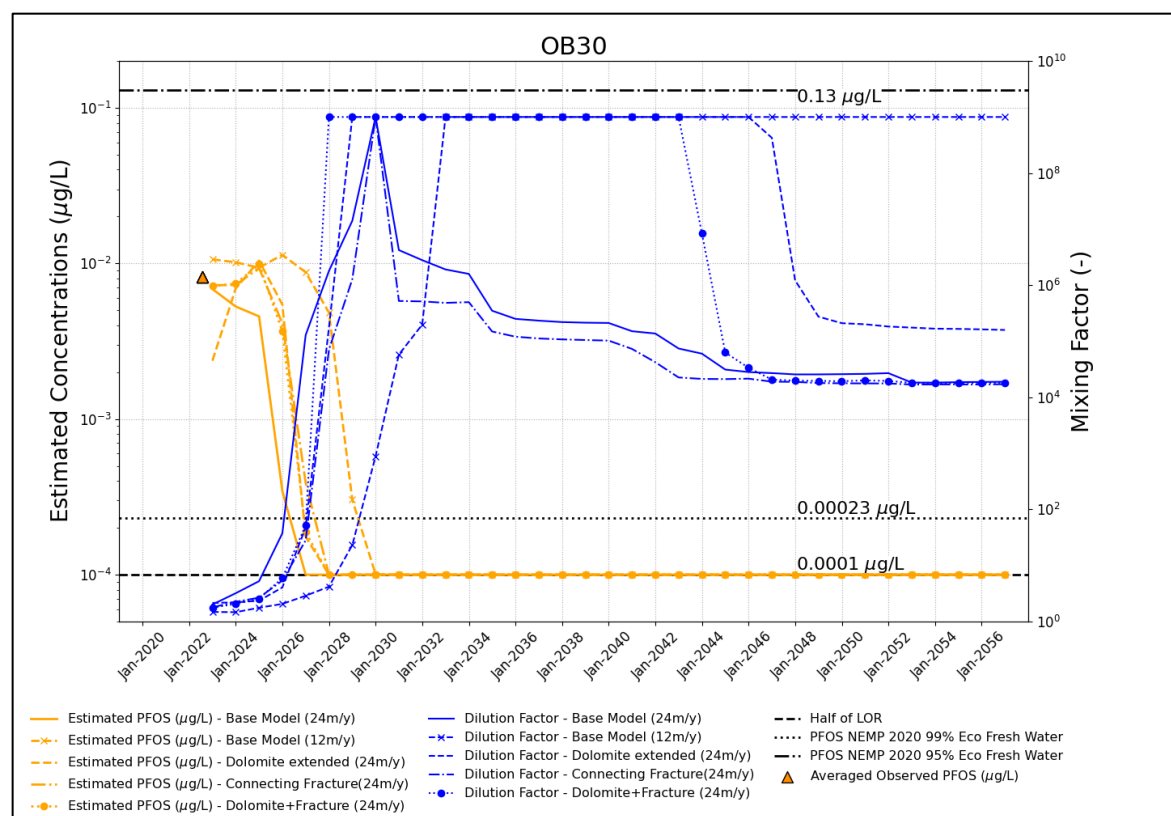


Figure Y: Mixing Assessment Results for PFOS (top) and PFOS+PFHxS (bottom) for the Combined OB30 dewatering

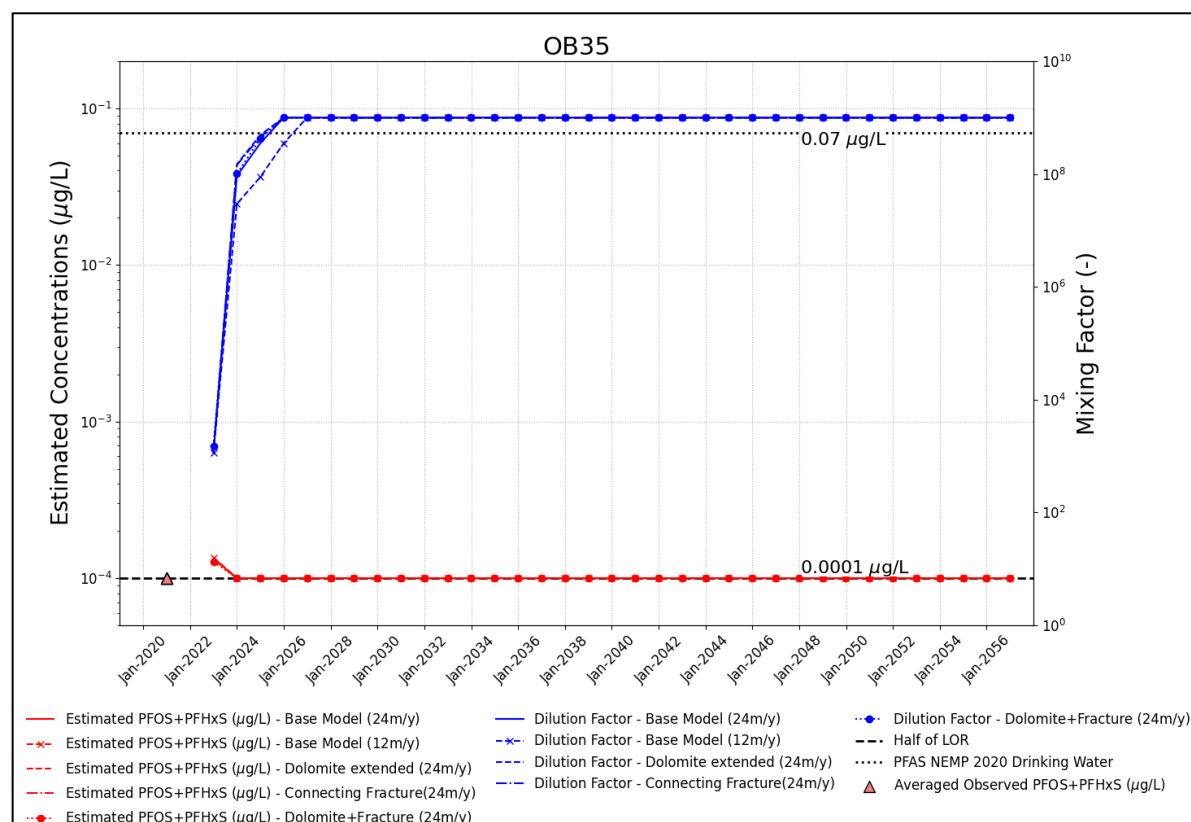
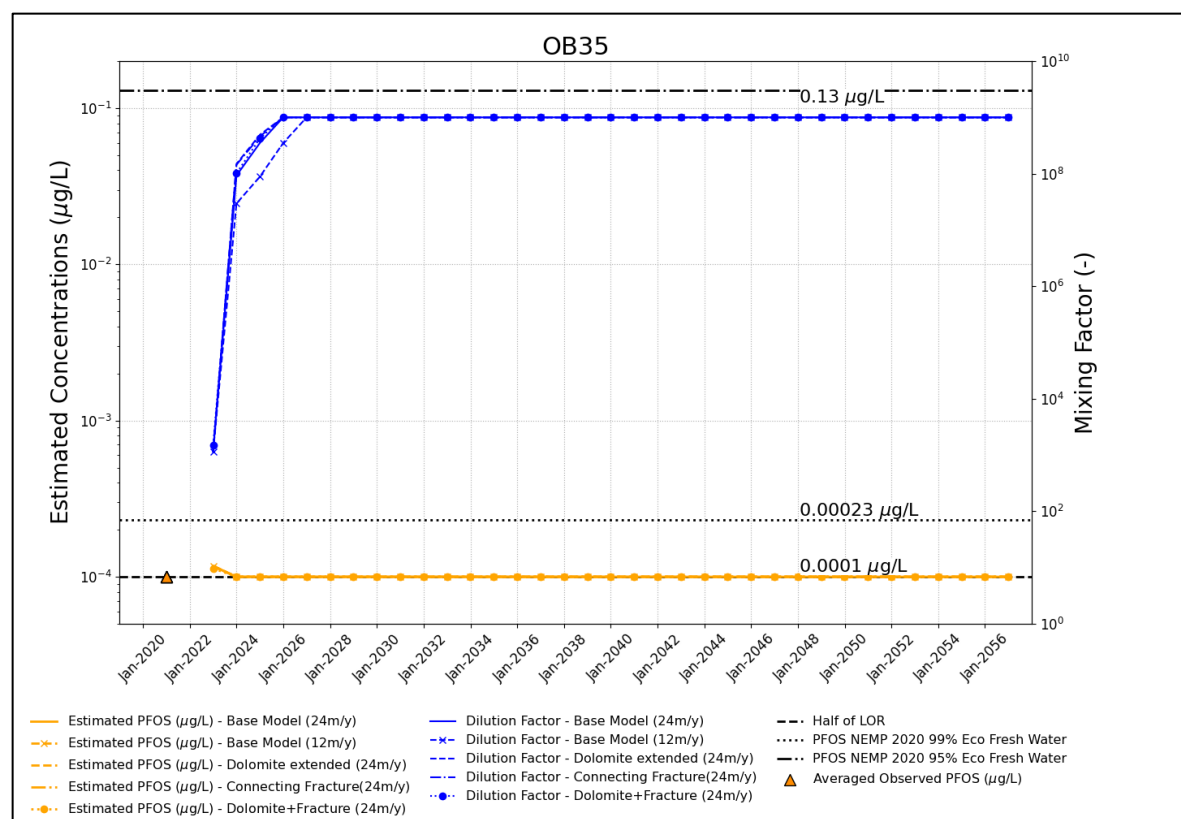


Figure Z: Mixing Assessment Results for PFOS (top) and PFOS+PFHxS (bottom) for the Combined OB35 dewatering

8.0 SUMMARY

BHP engaged WSP Golder to undertake a staged hydrogeological assessment to investigate the potential risk of PFAS migrating towards OB29, OB30 and OB35 dewatering bores and to support future decisions related to dewatering and management of the excess water at the site. To achieve the objectives, WSP Golder undertook a mixing assessment for PFOS and PFOS+PFHxS in the area.

The assessment used two main sources of information: the outputs of an updated and calibrated OB29/30/35 groundwater model, which was extended to the west to include Western Ridge; and the PFOS and PFOS+PFHxS concentrations from field sampling conducted at the site.

An updated version of the groundwater model developed as part of the 5C licence application was used to complete forward MODFLOW simulations to forecast groundwater flow in the region until 2056 (Section 2.1). Three alternative geological conceptual site models were evaluated using the 24 m/year dewatering scenario to explore the potential associated predictive uncertainty. The geological Base Case scenarios was also simulated using a 12 m/year dewatering scenario to observe the effect of potential uncertainties in the dewatering schedule.

The mixing assessment was calculated using both the volume of groundwater abstracted from each dewatering bore and the interpolated plume maps (Section 6.1). The plume maps were developed using the maximum PFOS and PFOS+PFHxS concentration at each sampling location (Section 2.3). Additional control interpolation points following the geologic contacts with low permeability units have been included to generate and delimit the plume maps. Although sampling locations are well distributed across the site, there is the potential that higher concentrations exist at the site.

The thickness of the plume (i.e., vertical delineation) was based on field data as well as calibrated to the average observed concentrations at dewatering bores or nearby monitoring wells. The results of this process suggested that the plume thickness is likely variable among the orebodies, with the most representative plume thicknesses of 1 m, 30 m and 60 m for OB35, OB30 and OB29, respectively. It is important to note that the plume thickness has a notable effect on the mixing assessment results, and therefore, these results should be reviewed if additional information related to the vertical delineation of PFAS becomes available.

The conservative assumption of a constant release from five known sources in the area was adopted for the assessment. The plumes have been allowed to deplete in areas outside these known sources. If additional sources are identified in the area, or ongoing concentrations are noted during dewatering these results would need to be reviewed.

The mixing assessment results for the combined dewatering water had PFOS+PFHxS concentrations below the drinking water guideline value (0.07 µg/L) and PFOS concentrations below the 95% species protection (0.13 µg/L). However, PFOS concentrations are initially predicted to be above the screening value for the 99% species protection (0.00023 µg/L) in the combined water from OB29 and OB30, however after four and five years of dewatering, for OB30 and OB29, respectively, concentrations decrease to levels close to half of LOR (0.0001 µg/L). In the case of OB35, the predicted PFOS concentrations for the entire simulation time were below the 99% species protection (0.00023 µg/L).

The results from the mixing assessment showed minimal variation among the geological scenarios evaluated. Therefore, while uncertainty exists regarding the geological conceptual site model in the vicinity of OB30 it does not appear to affect the resulting PFAS concentrations at dewatering bores at site. In comparison, the results appear to be more sensitive to the dewatering schedule, with the 12 m/year scenario predicting concentrations in OB29 and OB30 would be similar in magnitude to the 24 m/year scenario but only delayed due to the smaller pumping rates assigned.

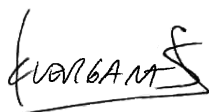
The reduced dewatering scenario did not vary the results at OB35. It is important to note that these results are valid under the assumptions that the actual abstraction rates, the contamination plume areas, thickness, and concentrations, as well as the plume depletion are similar to those described in this assessment.

9.0 IMPORTANT INFORMATION

Your attention is drawn to the document titled – “Important Information Relating to this Report”, which is included in Attachment C of this report. The statements presented in that document are intended to inform a reader of the report about its proper use. There are important limitations as to who can use the report and how it can be used. It is important that a reader of the report understands and has realistic expectations about those matters. The Important Information document does not alter the obligations Golder has under the contract between it and its client.

Yours sincerely

GOLDER ASSOCIATES PTY LTD



Claudio Vergara-Saez
Senior Hydrogeologist



Shane Hyde
Principal Environmental Scientist

CVS/KM/hn

Attachments: A – Mixing Assessment Results (Plume Thickness Variability)
B – Mixing Assessment Results
C – Important Information

[https://golderassociates.sharepoint.com/sites/150095/project files/6 deliverables/016-l ob29/21481693-016-l-rev0 final.docx](https://golderassociates.sharepoint.com/sites/150095/project%20files/6%20deliverables/016-l%20ob29/21481693-016-l-rev0%20final.docx)

REFERENCES

Black A. and Foley C. (2013). FlowSource: A program to efficiently delineate volumetric capture areas pathways and source areas in groundwater models. In MODFLOW and More 2013: Translating Science into Practice.

BHP (2020) OB32 Numerical Modelling (taken from H3 report January 2020).

Doherty, J. (2010) PEST, Model-Independent Parameter Estimation—User Manual. 5th Edition, with Slight Additions, Watermark Numerical Computing, Brisbane.

Harbaugh, A.W. (1990). A computer program for calculating subregional water budgets using results from the U.S. Geological Survey modular three-dimensional ground-water flow model: U.S. Geological Survey Open-File Report 90-392, 46 p., <https://doi.org/10.3133/ofr90392>.

Harbaugh, A.W. (2005). MODFLOW-2005, the U.S. Geological Survey modular ground-water model -- the Ground-Water Flow Process: U.S. Geological Survey Techniques and Methods 6-A16.

HEPA (2020). PFAS National Environmental Management Plan 2.0.

ATTACHMENT A

Mixing Assessment Results (Plume Thickness Variability)

1.0 INDIVIDUAL DEWATERING BORES IN OB29 (PLUME THICKNESS OF 1, 10, 30 AND 60 M)

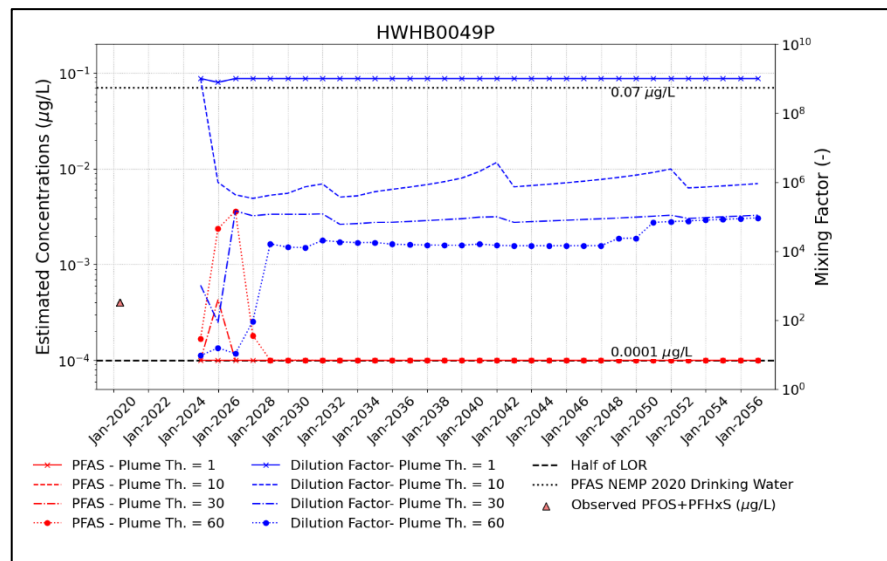
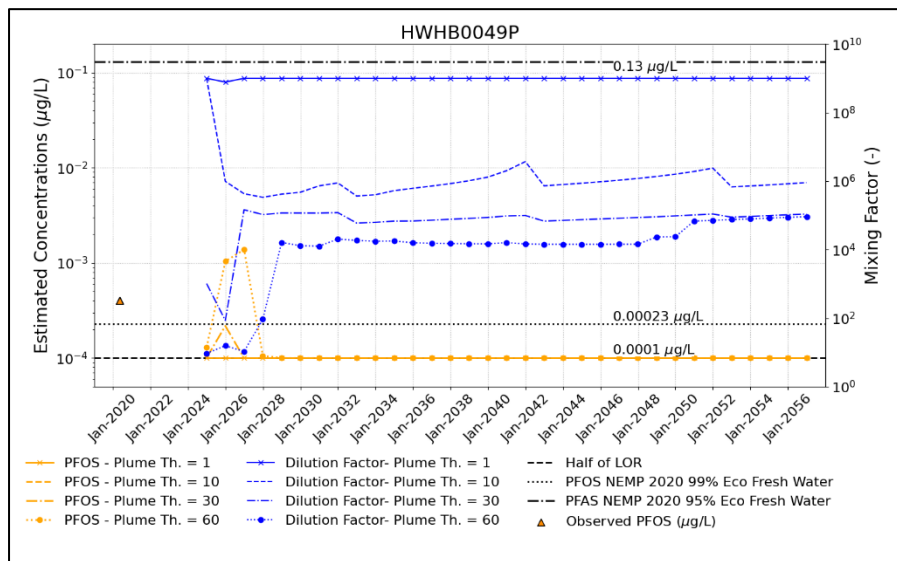


Figure A: Mixing Assessment Results for the bore HWHB0049P in OB29. PFOS (left) and PFOS+PFHxS (right).

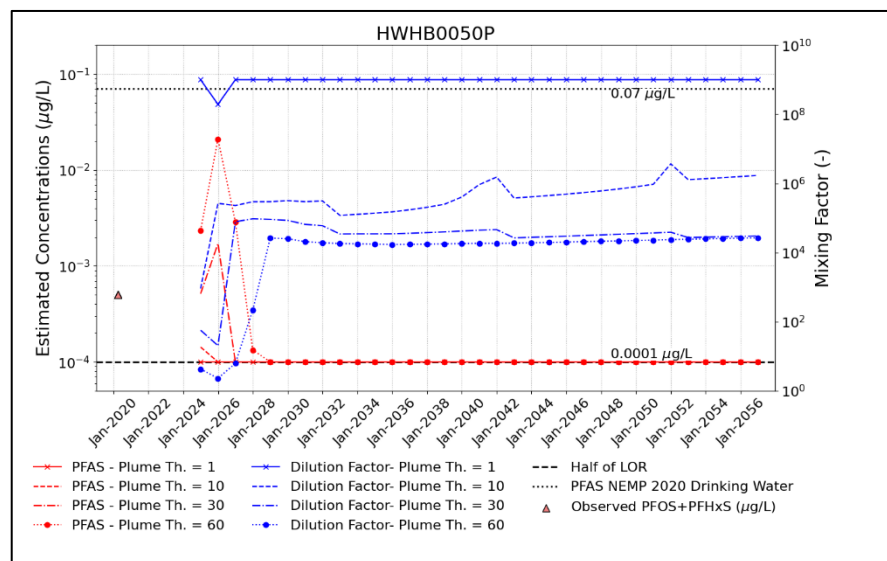
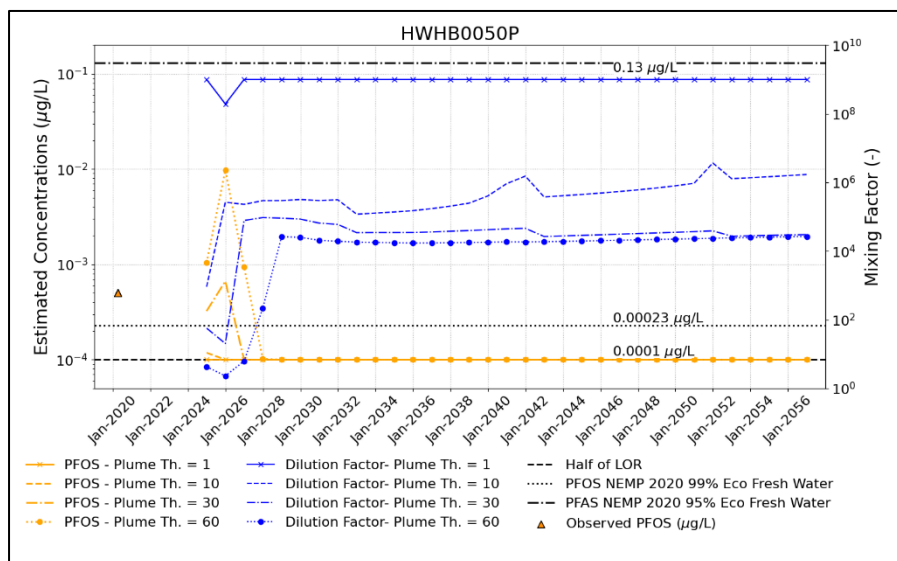


Figure B: Mixing Assessment Results for the bore HWHB0050P in OB29. PFOS (left) and PFOS+PFHxS (right).

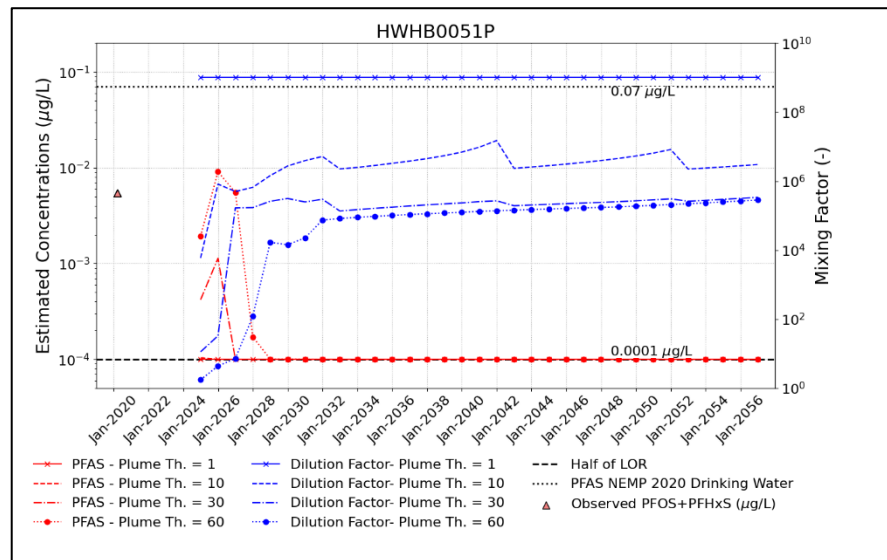
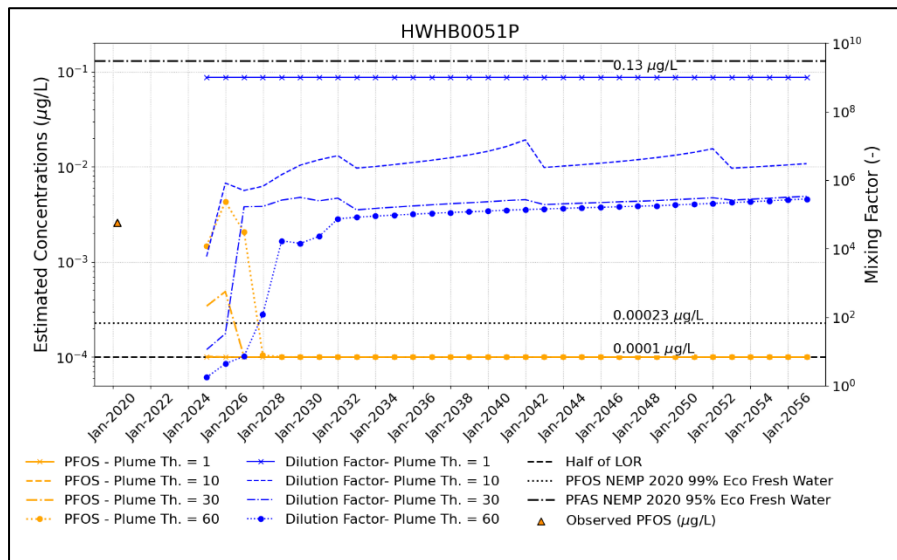


Figure C: Mixing Assessment Results for the bore HWHB0051P in OB29. PFOS (left) and PFOS+PFHxS (right).

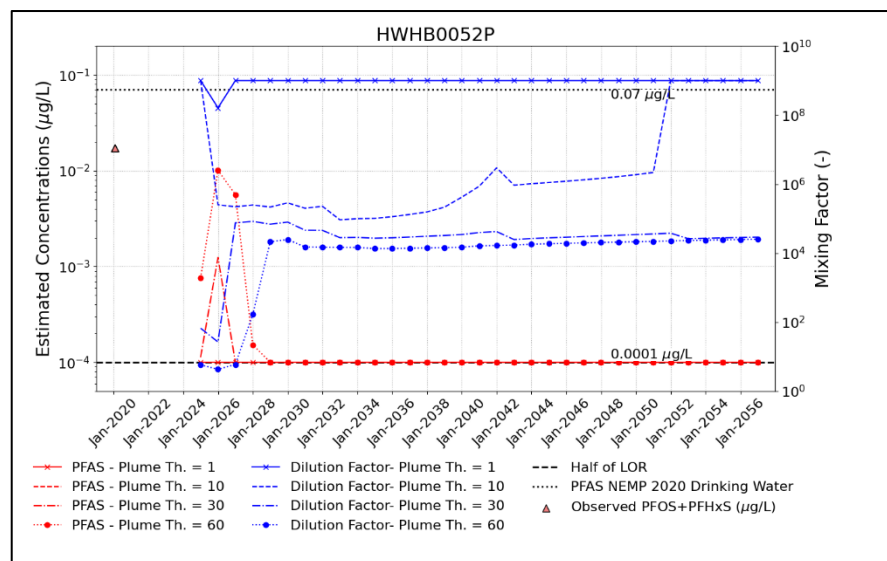
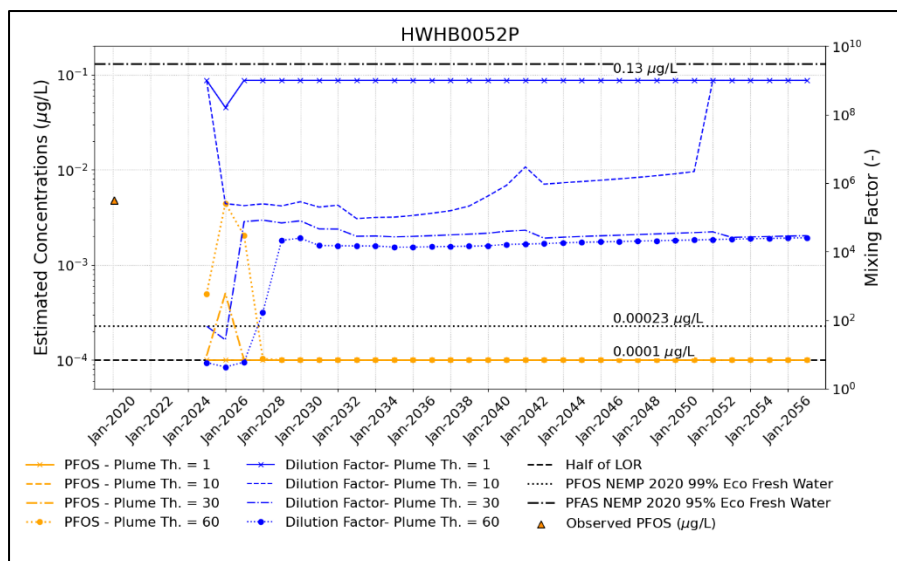


Figure D: Mixing Assessment Results for the bore HWHB0052P in OB29. PFOS (left) and PFOS+PFHxS (right).

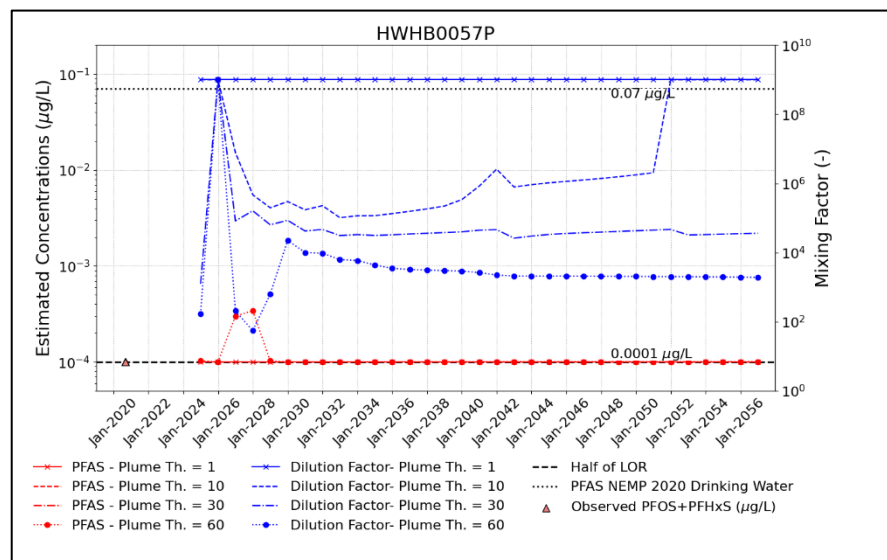
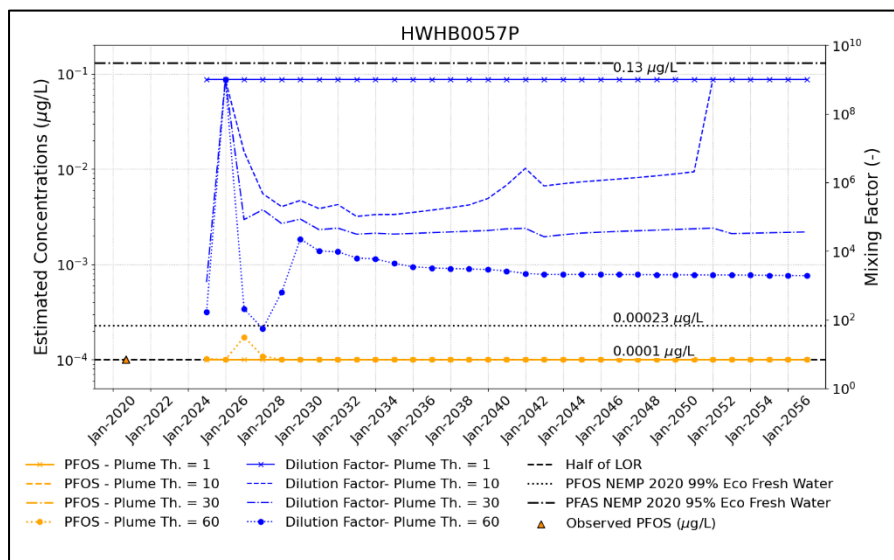


Figure E: Mixing Assessment Results for the bore HWHB0057P in OB29. PFOS (left) and PFOS+PFHxS (right).

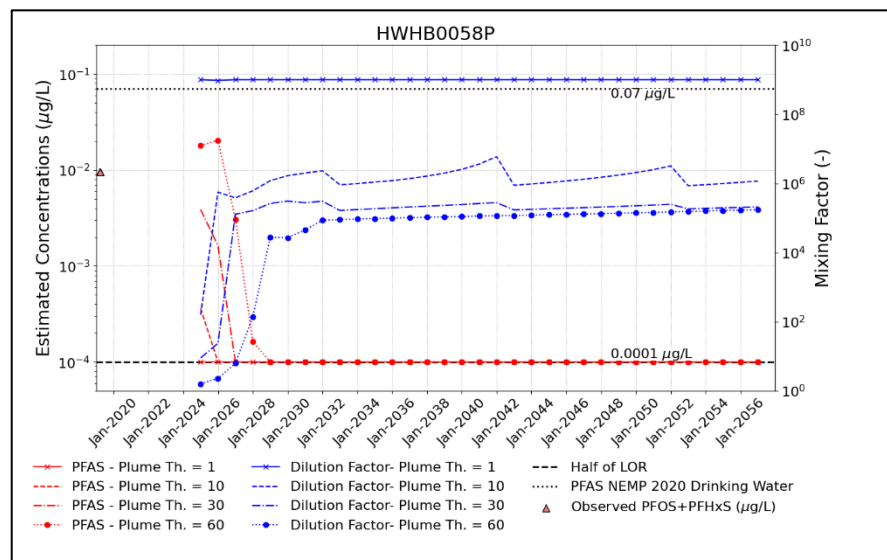
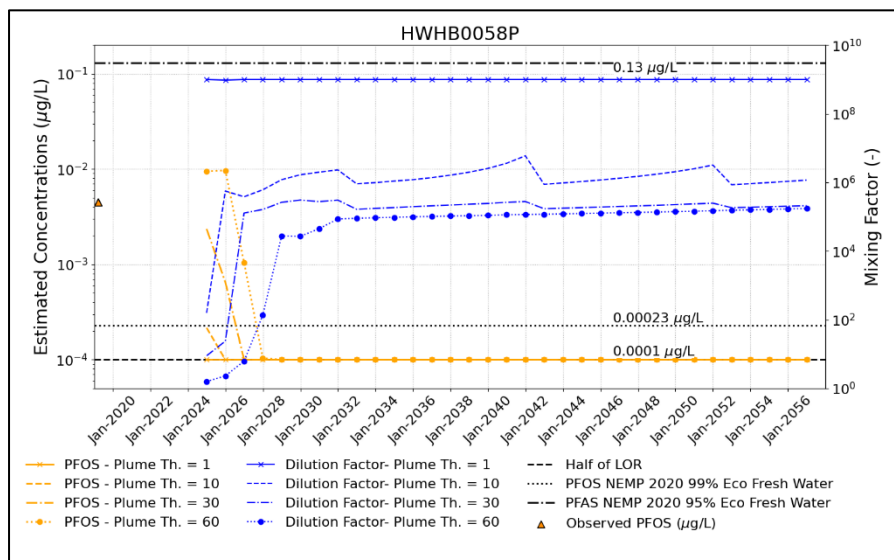


Figure F: Mixing Assessment Results for the bore HWHB0058P in OB29. PFOS (left) and PFOS+PFHxS (right).

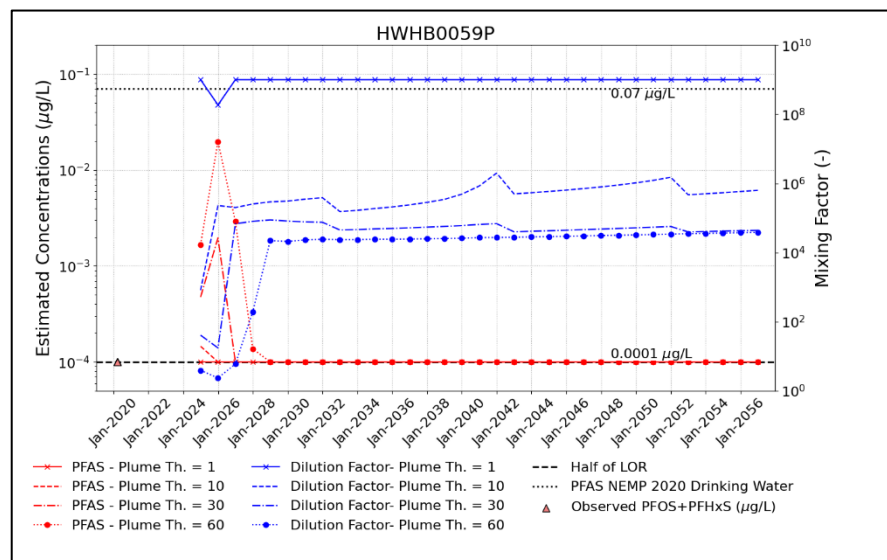
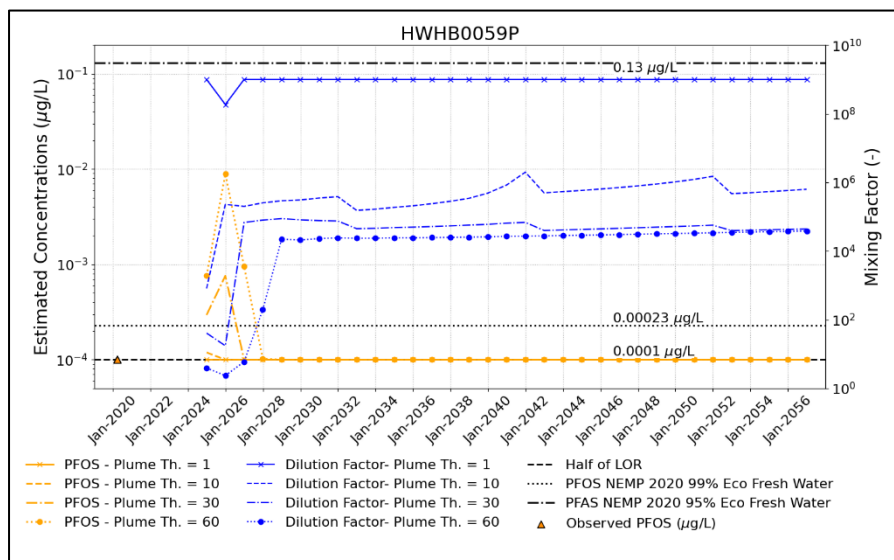


Figure G: Mixing Assessment Results for the bore HWHB0059P in OB29. PFOS (left) and PFOS+PFHxS (right).

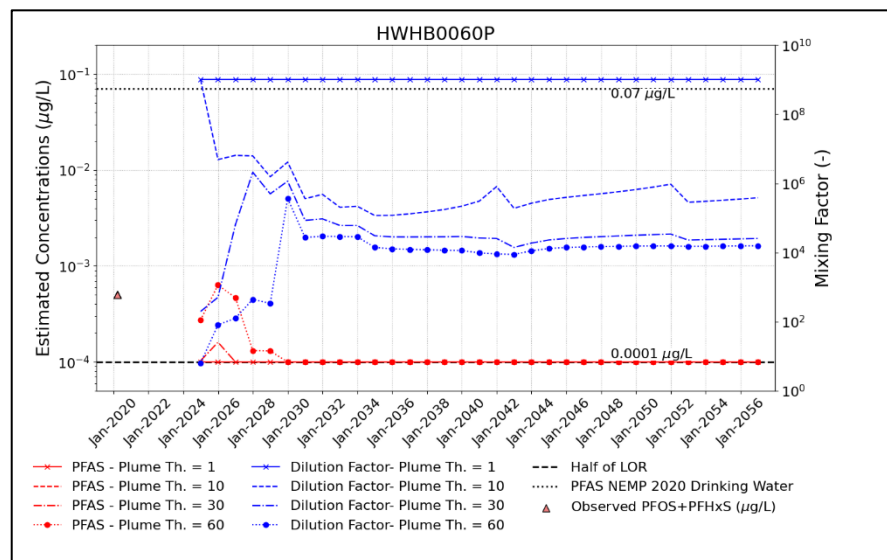
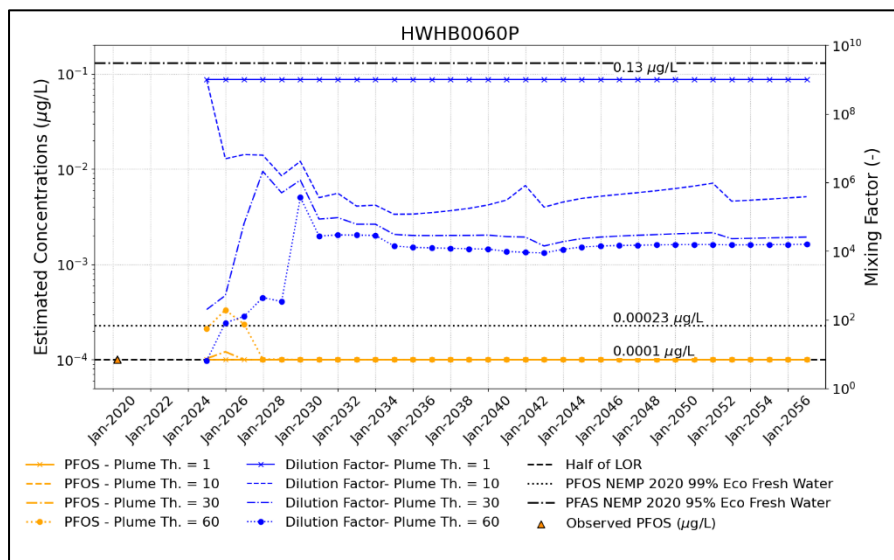


Figure H: Mixing Assessment Results for the bore HWHB0060P in OB29. PFOS (left) and PFOS+PFHxS (right).

2.0 INDIVIDUAL DEWATERING BORES IN OB30 (PLUME THICKNESS OF 1, 10, 30 AND 60 M)

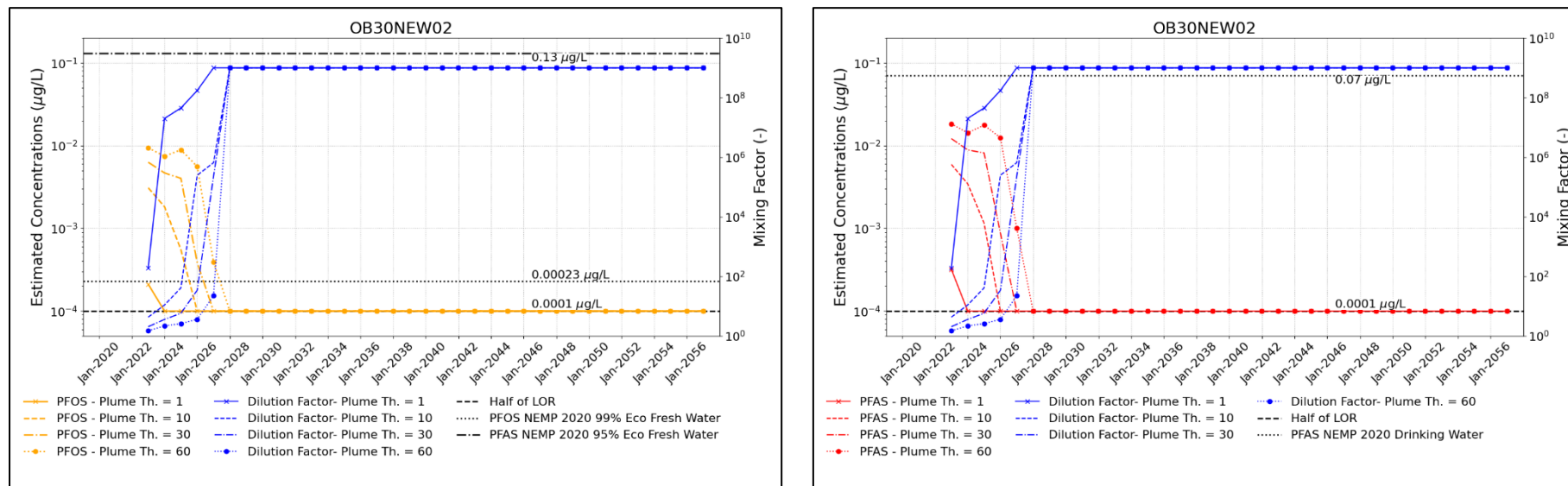


Figure I: Mixing Assessment Results for the potential bore location OB30NEW02 in OB30. PFOS (left) and PFOS+PFHxS (right).

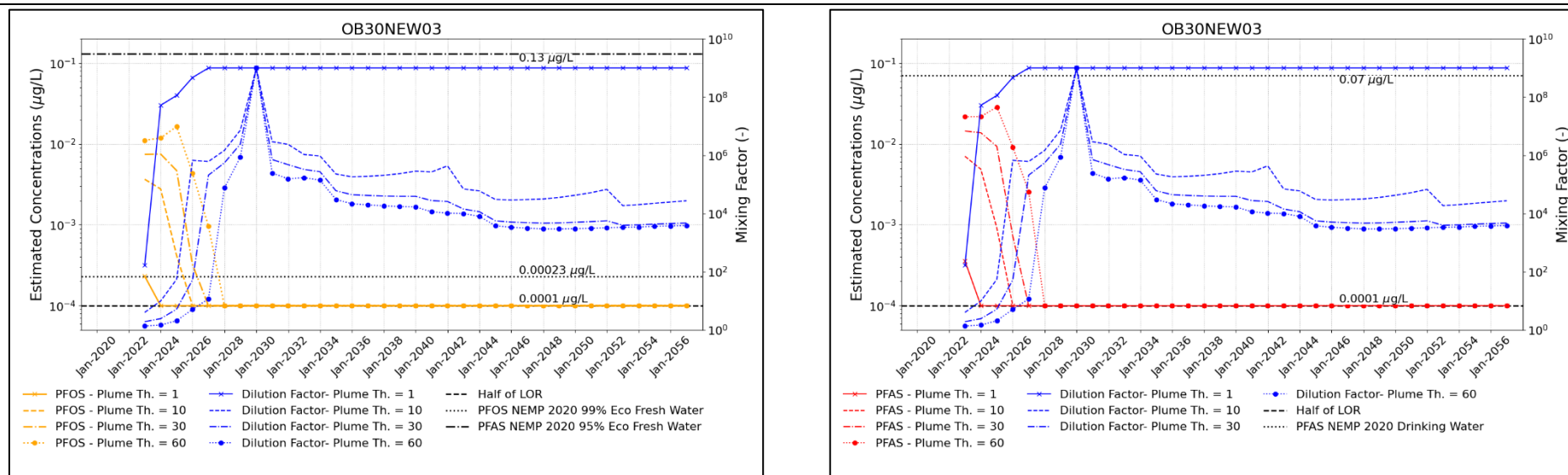


Figure J: Mixing Assessment Results for the potential bore location OB30NEW03 in OB30. PFOS (left) and PFOS+PFHxS (right).

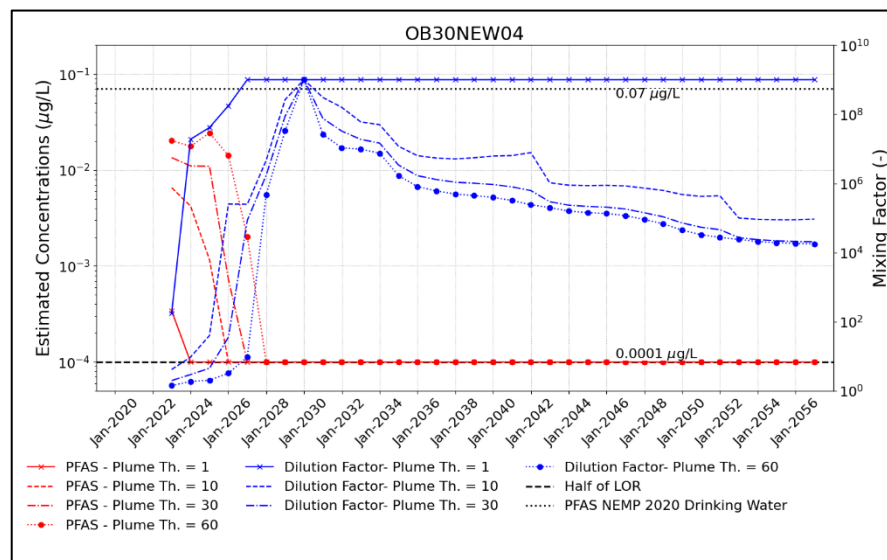
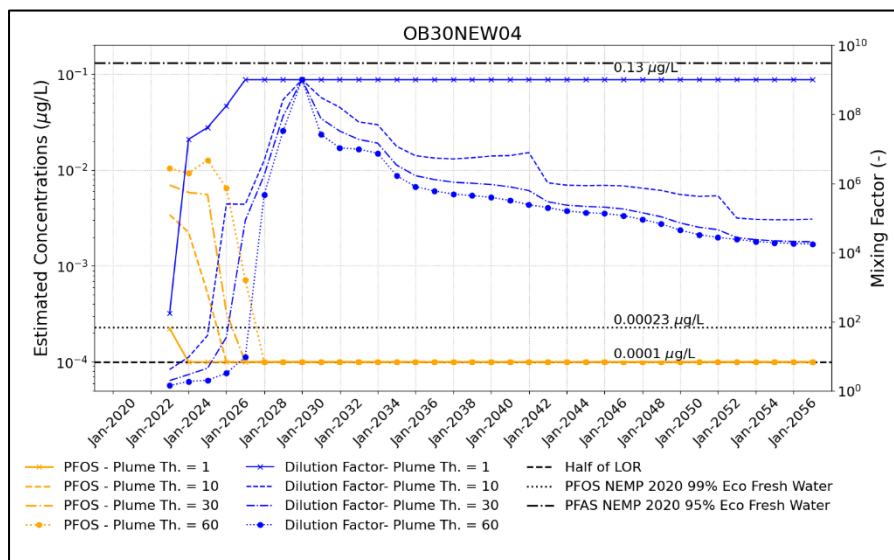


Figure K: Mixing Assessment Results for the potential bore location OB30NEW04 in OB30. PFOS (left) and PFOS+PFHxS (right).

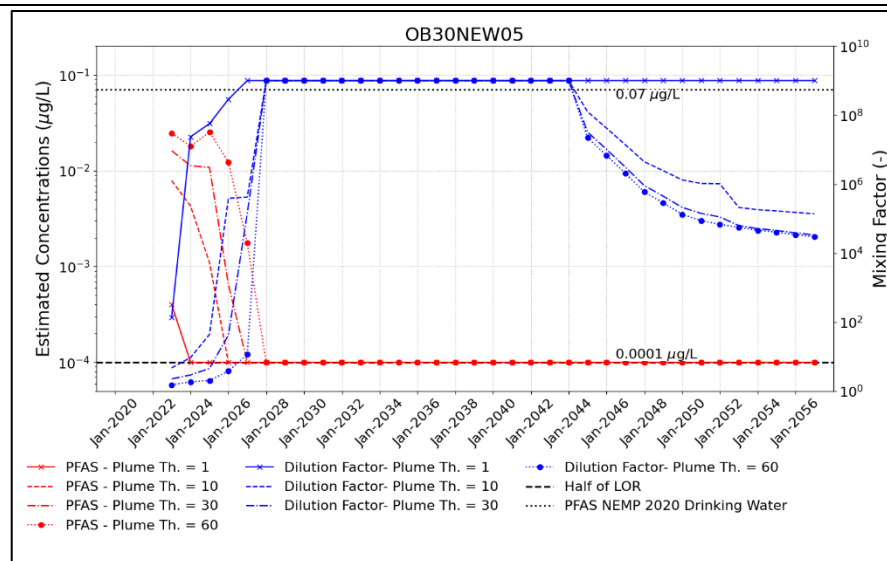
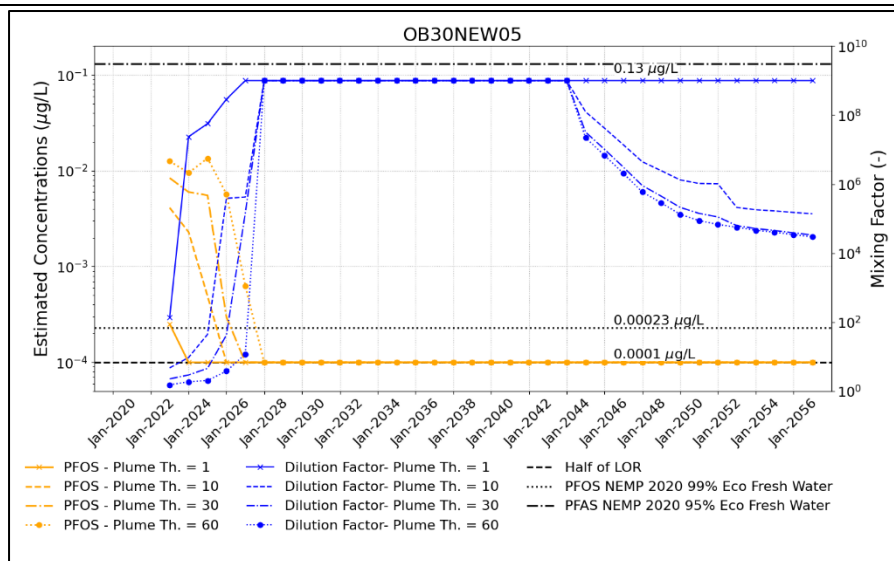


Figure L: Mixing Assessment Results for the potential bore location OB30NEW05 in OB30. PFOS (left) and PFOS+PFHxS (right).

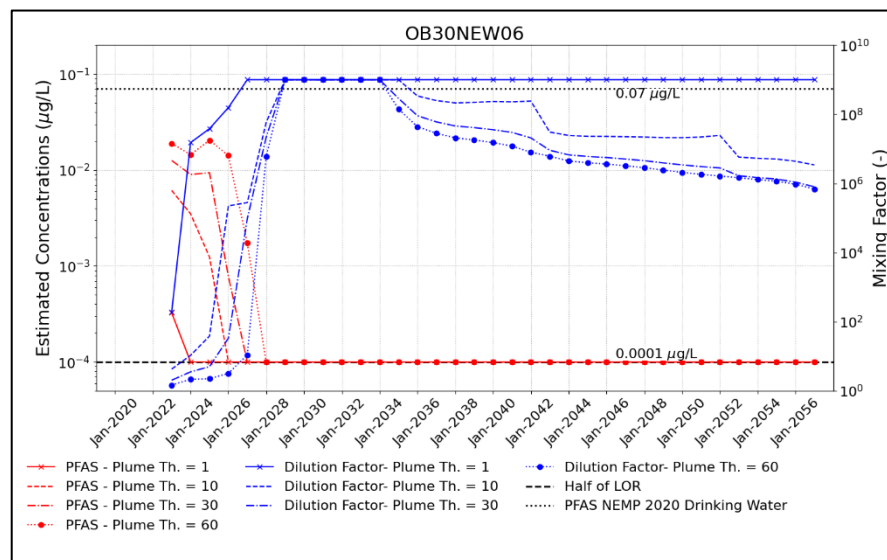
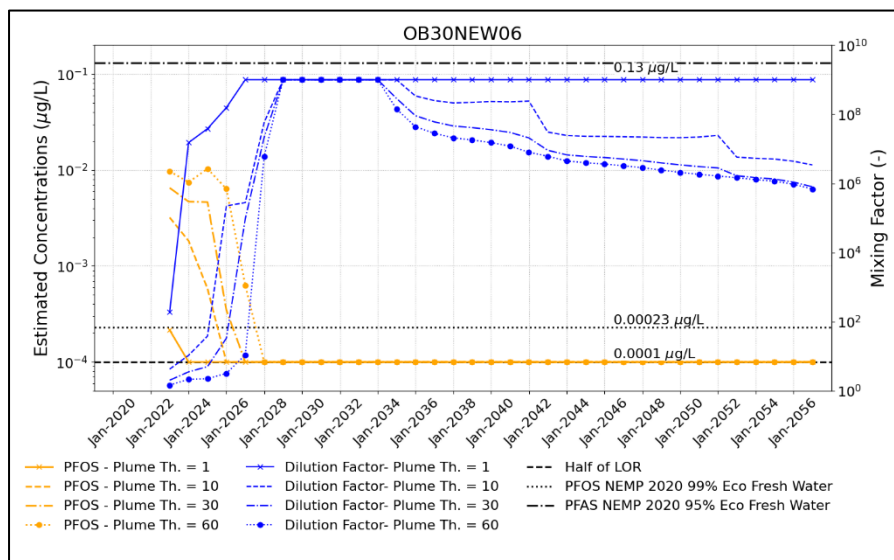


Figure M: Mixing Assessment Results for the potential bore location OB30NEW06 in OB30. PFOS (left) and PFOS+PFHxS (right).

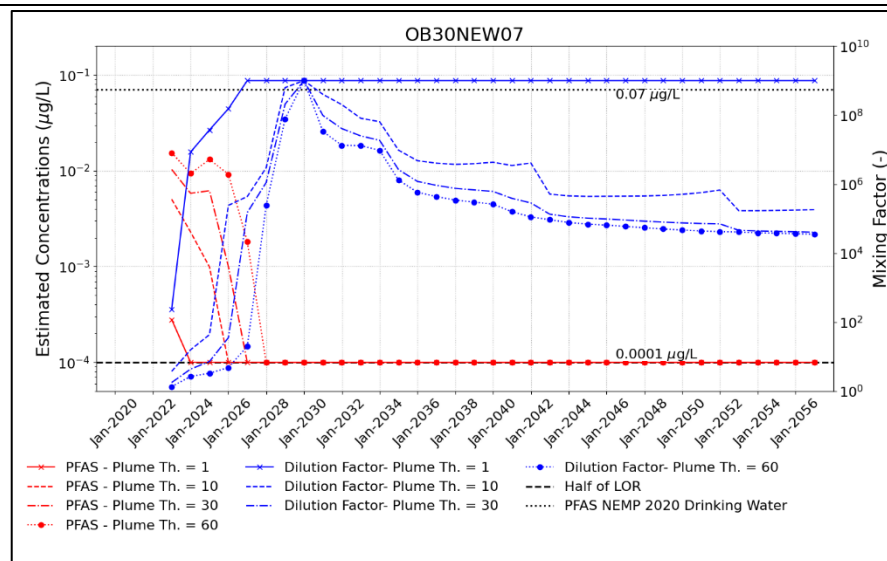
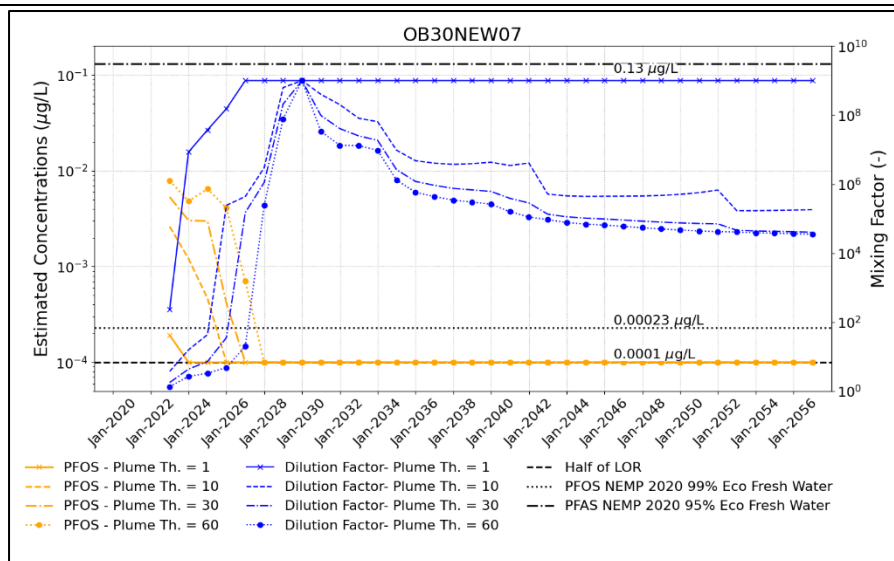


Figure N: Mixing Assessment Results for the potential bore location OB30NEW07 in OB30. PFOS (left) and PFOS+PFHxS (right).

3.0 INDIVIDUAL DEWATERING BORES IN OB35 (PLUME THICKNESS OF 1, 10, 30 AND 60 M)

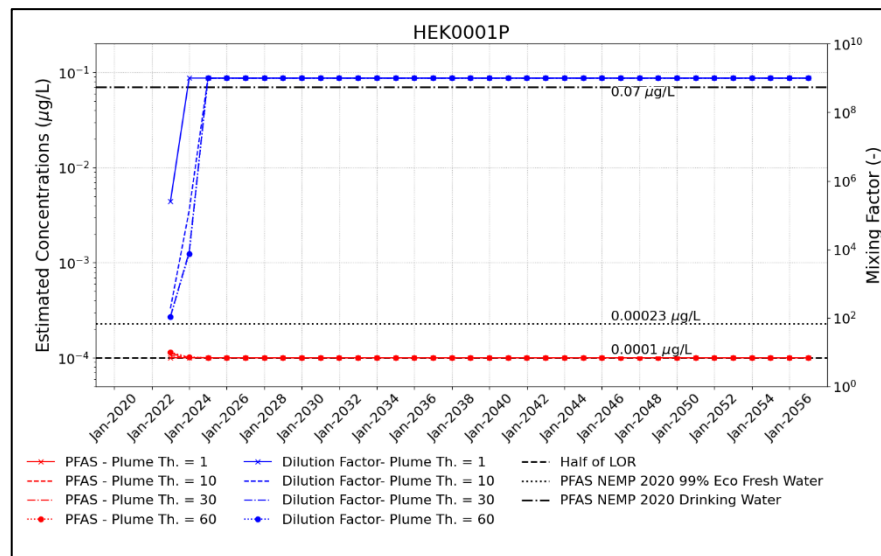
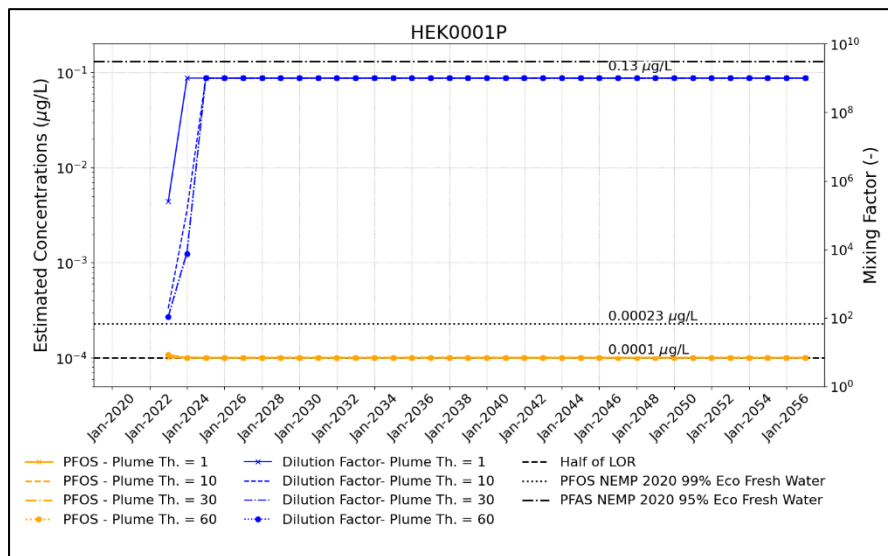


Figure O: Mixing Assessment Results for the bore HEK0001P in OB35. PFOS (left) and PFOS+PFHxS (right).

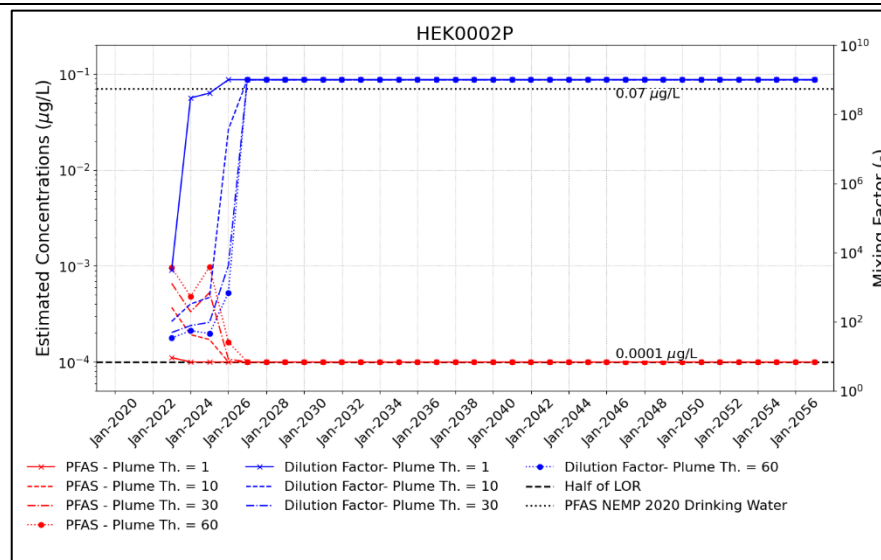
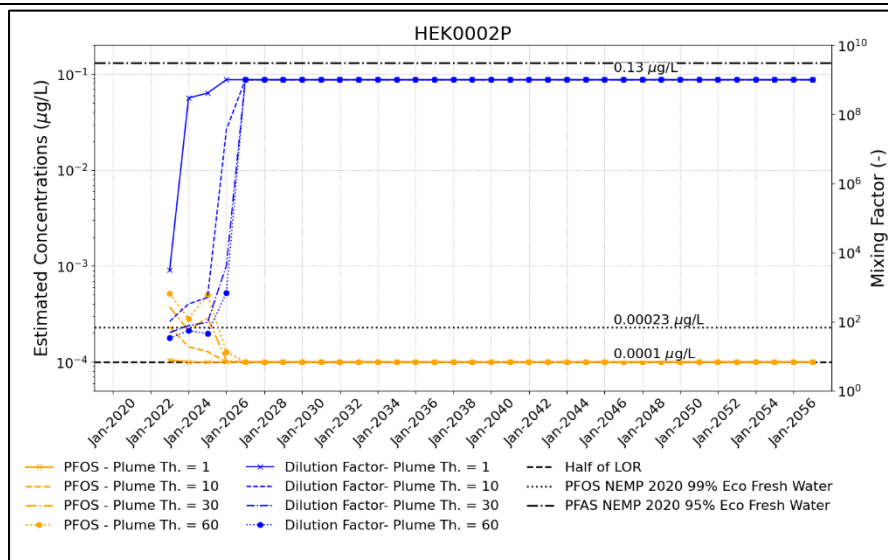


Figure P: Mixing Assessment Results for the bore HEK0002P in OB35. PFOS (left) and PFOS+PFHxS (right).

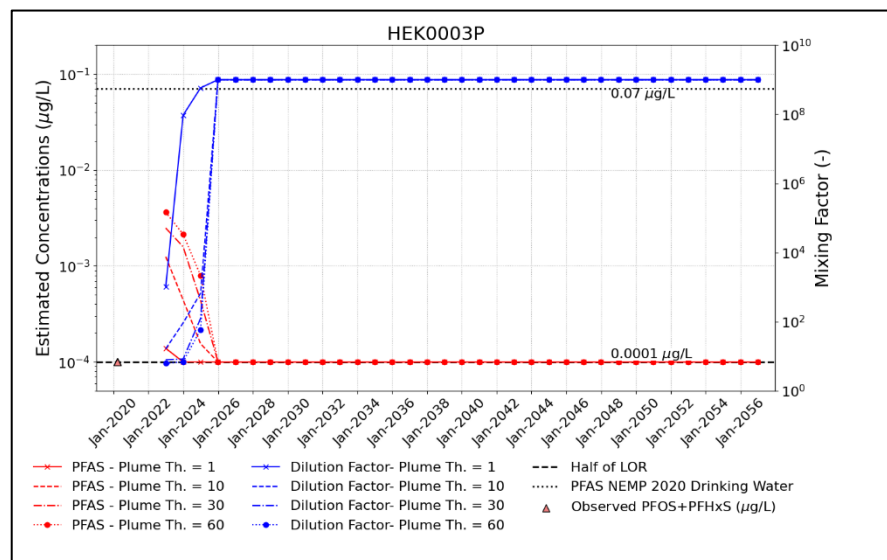
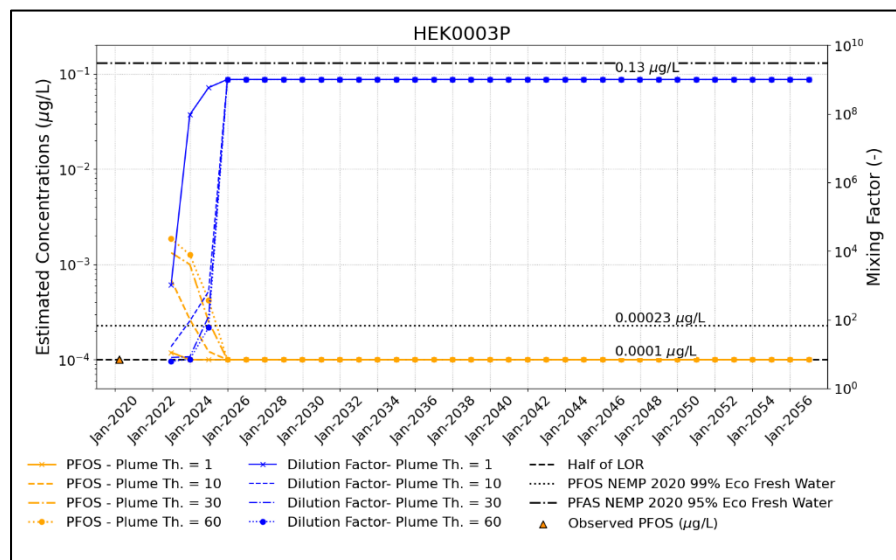


Figure Q: Mixing Assessment Results for the bore HEK0003P in OB35. PFOS (left) and PFOS+PFHxS (right).

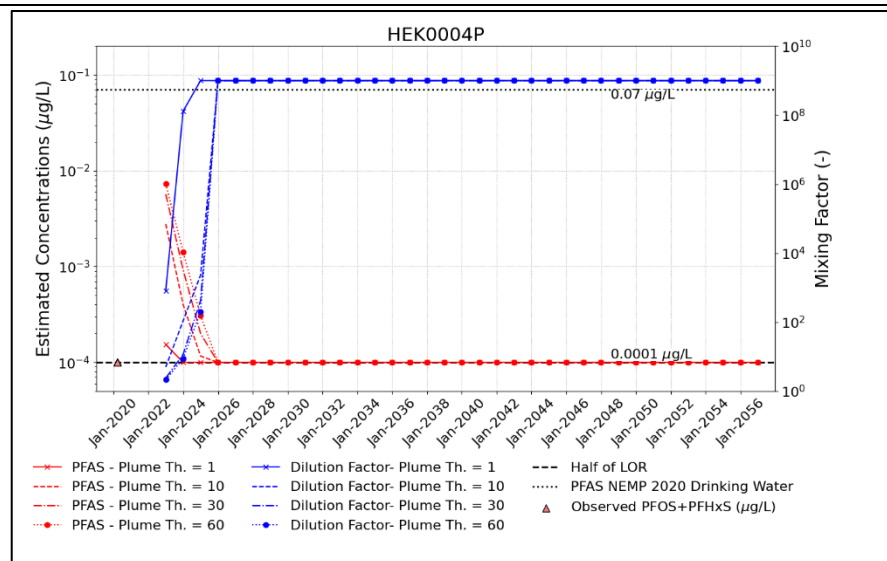
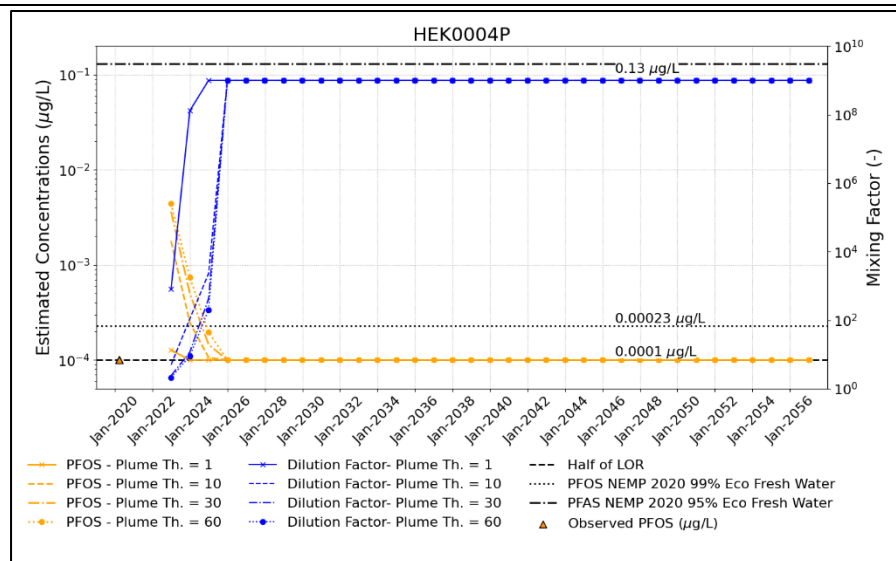


Figure R: Mixing Assessment Results for the bore HEK0004P in OB35. PFOS (left) and PFOS+PFHxS (right).

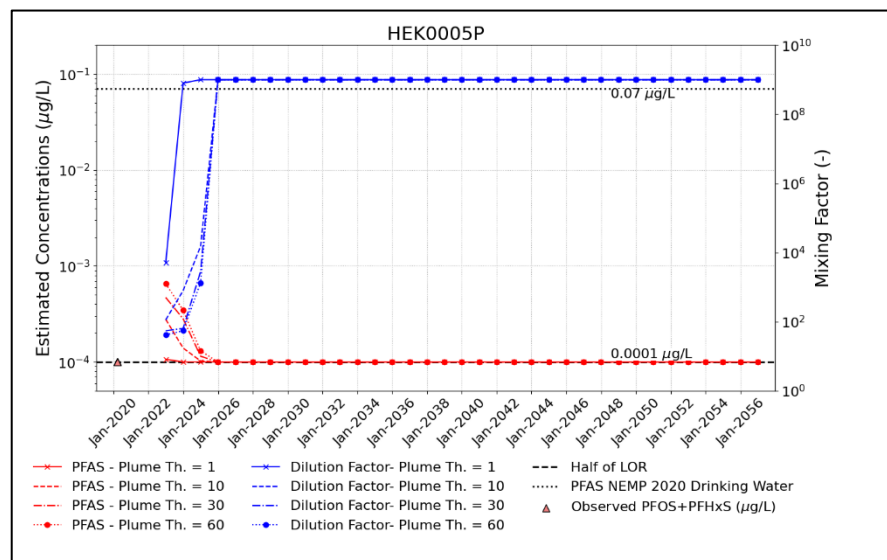
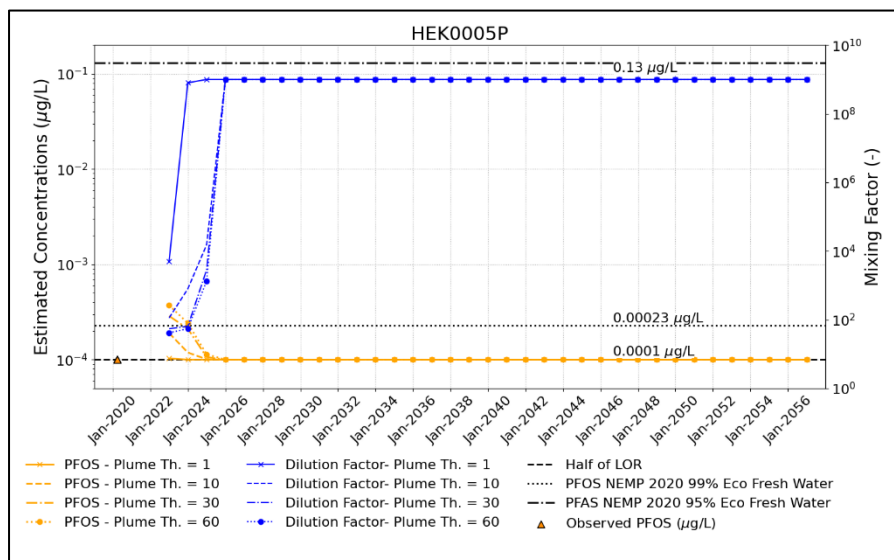


Figure S: Mixing Assessment Results for the bore HEK0005P in OB35. PFOS (left) and PFOS+PFHxS (right).

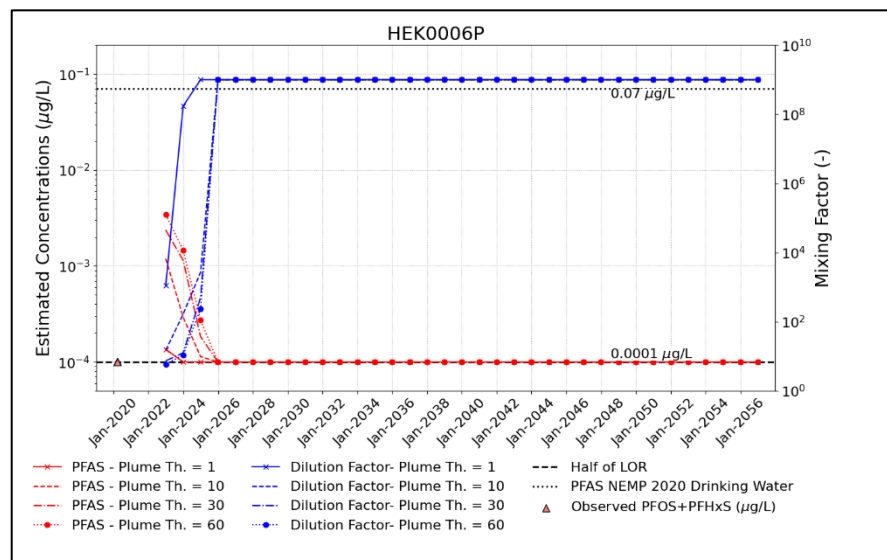
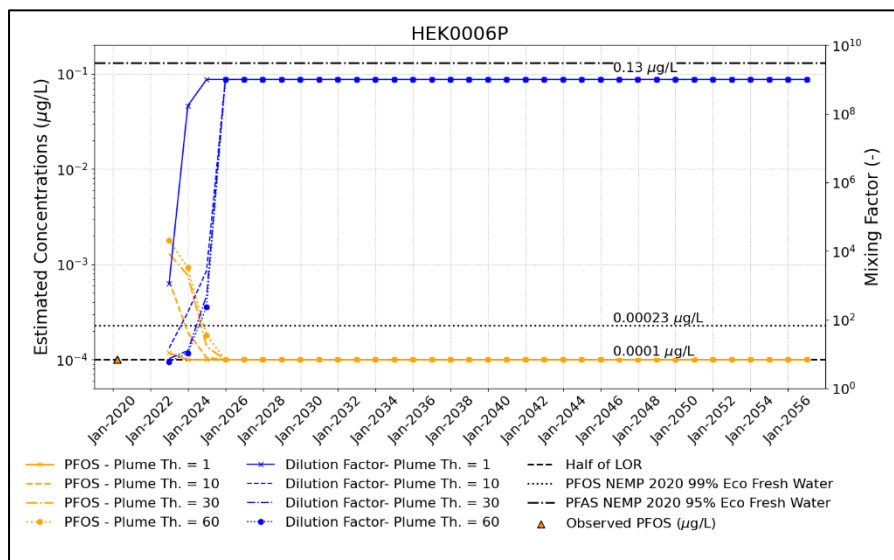


Figure T: Mixing Assessment Results for the bore HEK0006P in OB35. PFOS (left) and PFOS+PFHxS (right).

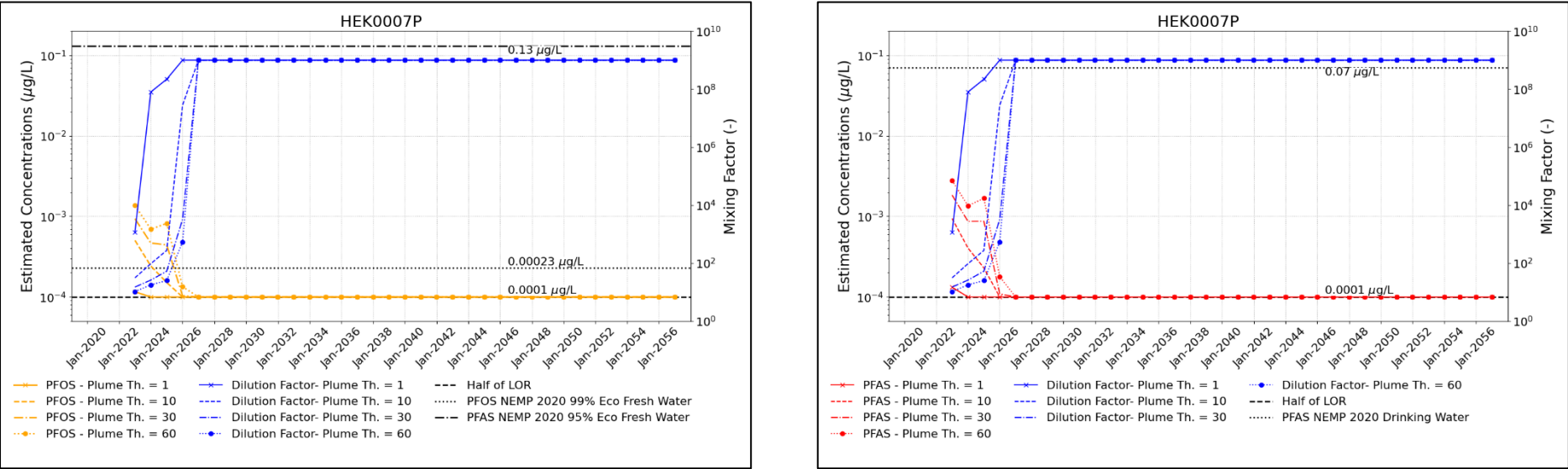


Figure U: Mixing Assessment Results for the bore HEK0007P in OB35. PFOS (left) and PFOS+PFHxS (right).

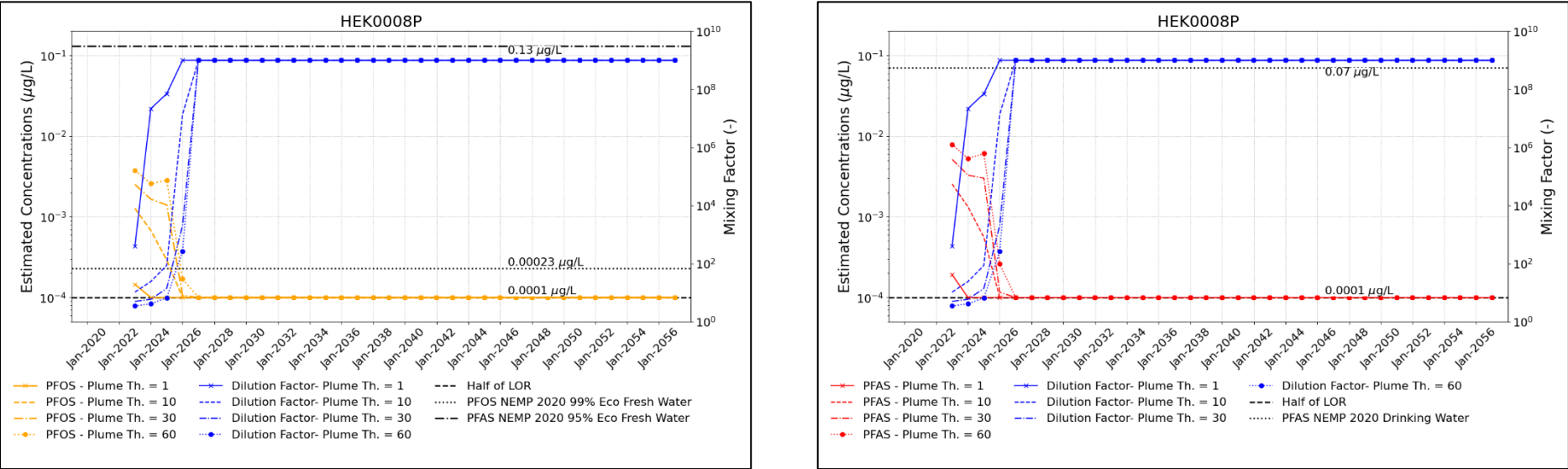
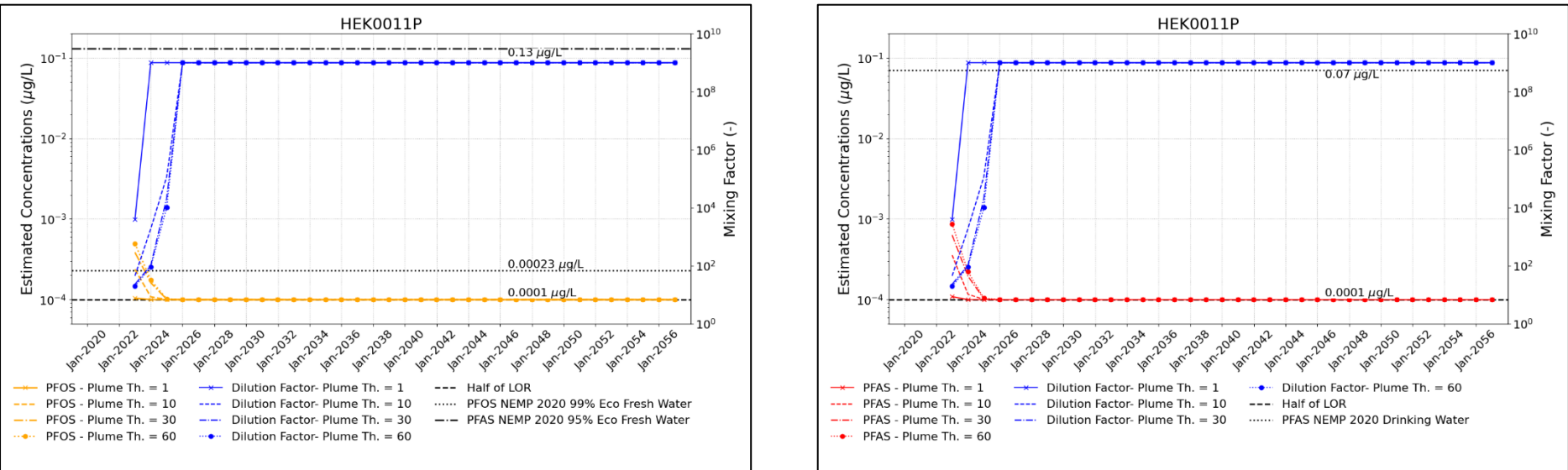
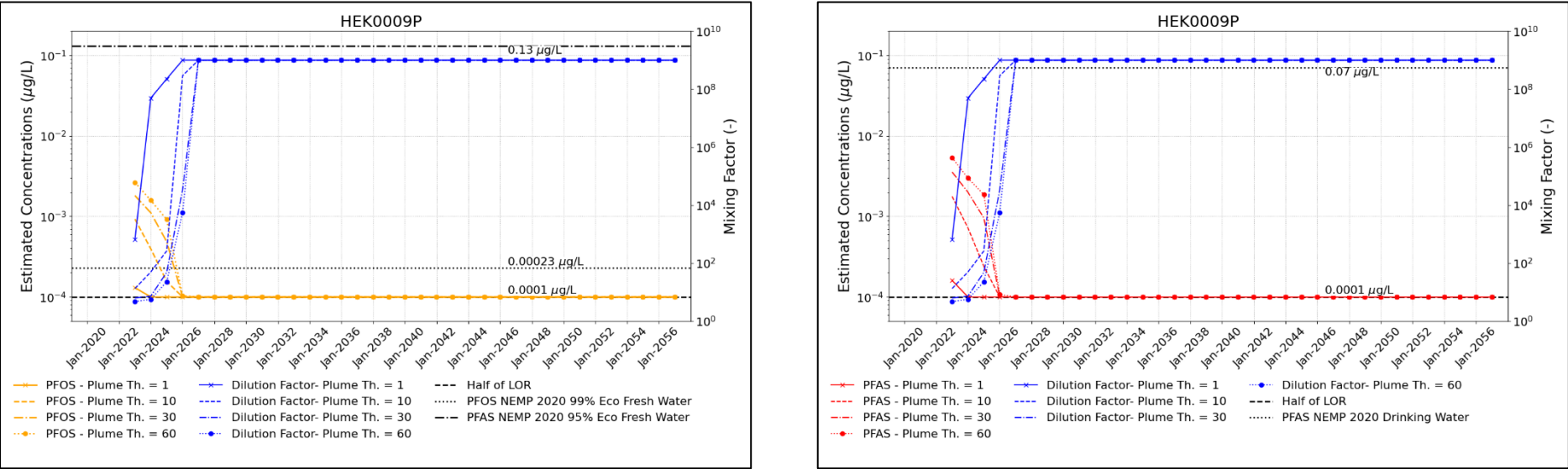


Figure V: Mixing Assessment Results for the bore HEK0008P in OB35. PFOS (left) and PFOS+PFHxS (right).



ATTACHMENT B

Mixing Assessment Results

1.0 INDIVIDUAL DEWATERING BORES IN OB29

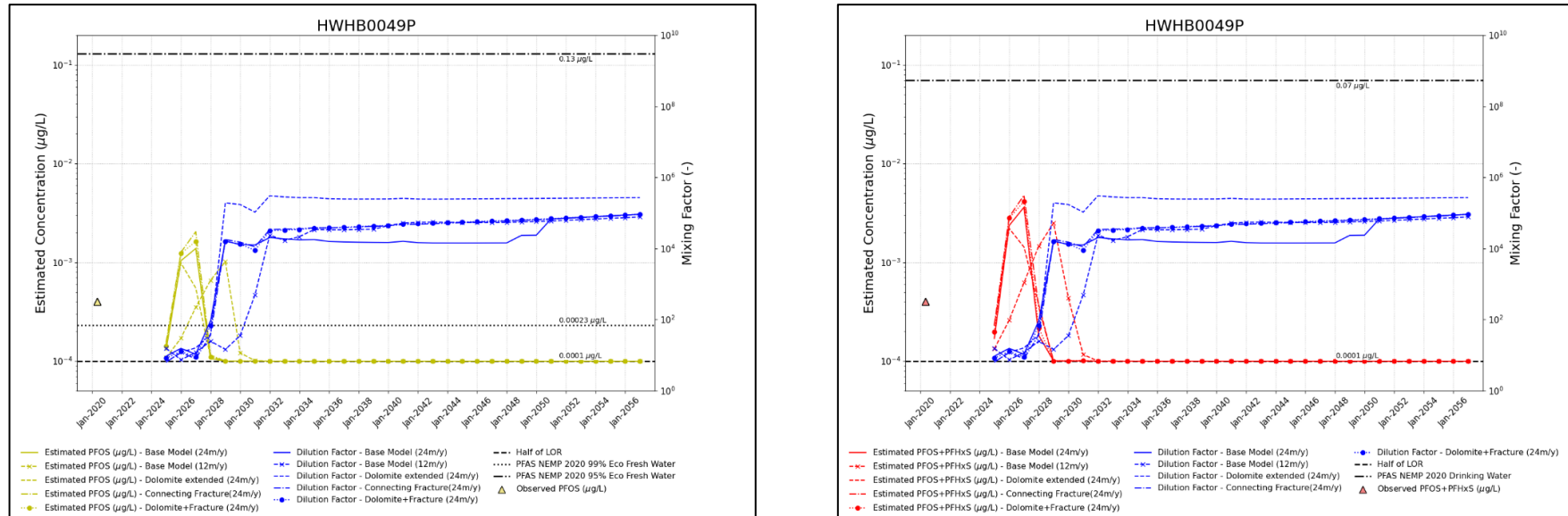


Figure A: Mixing Assessment Results for the bore HWHB0049P in OB29. PFOS (left) and PFOS+PFHxS (right).

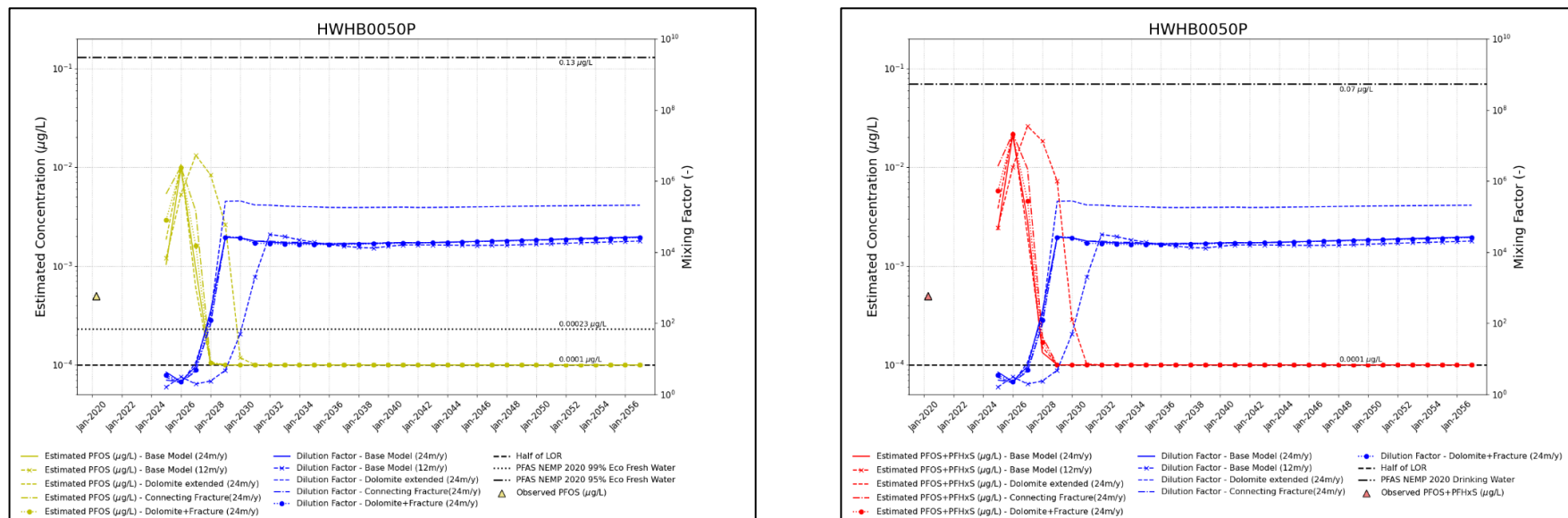


Figure B: Mixing Assessment Results for the bore HWHB0050P in OB29. PFOS (left) and PFOS+PFHxS (right).

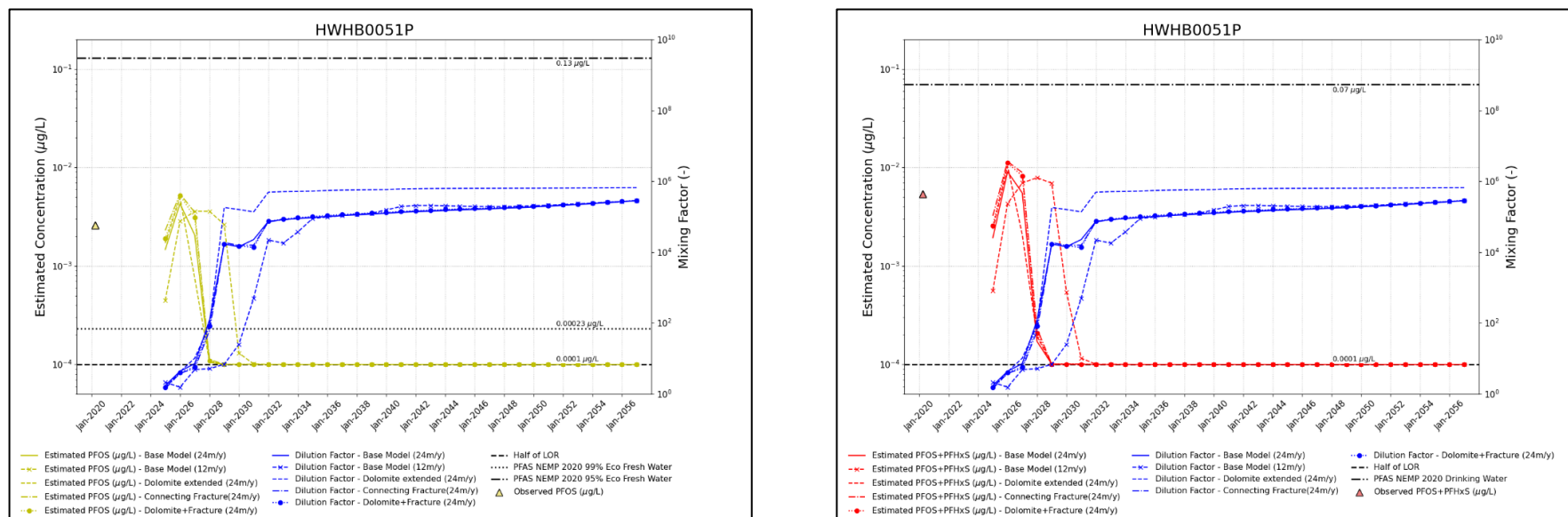


Figure C: Mixing Assessment Results for the bore HWHB0051P in OB29. PFOS (left) and PFOS+PFHxS (right).

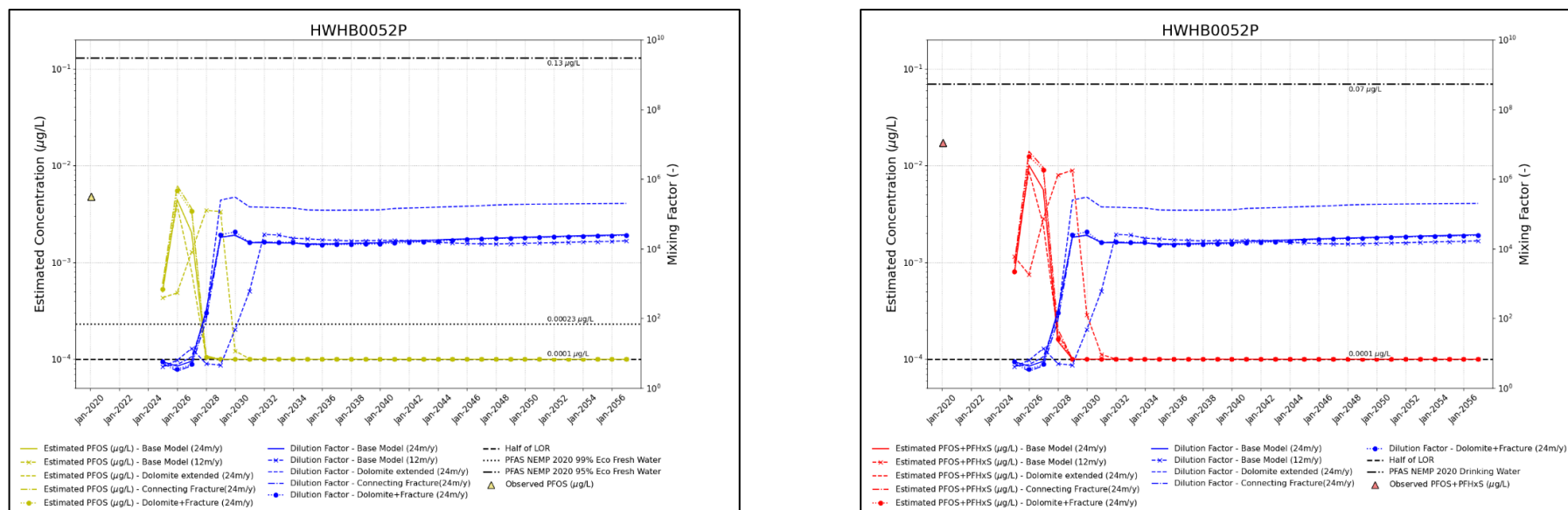


Figure D: Mixing Assessment Results for the bore HWHB0052P in OB29. PFOS (left) and PFOS+PFHxS (right).

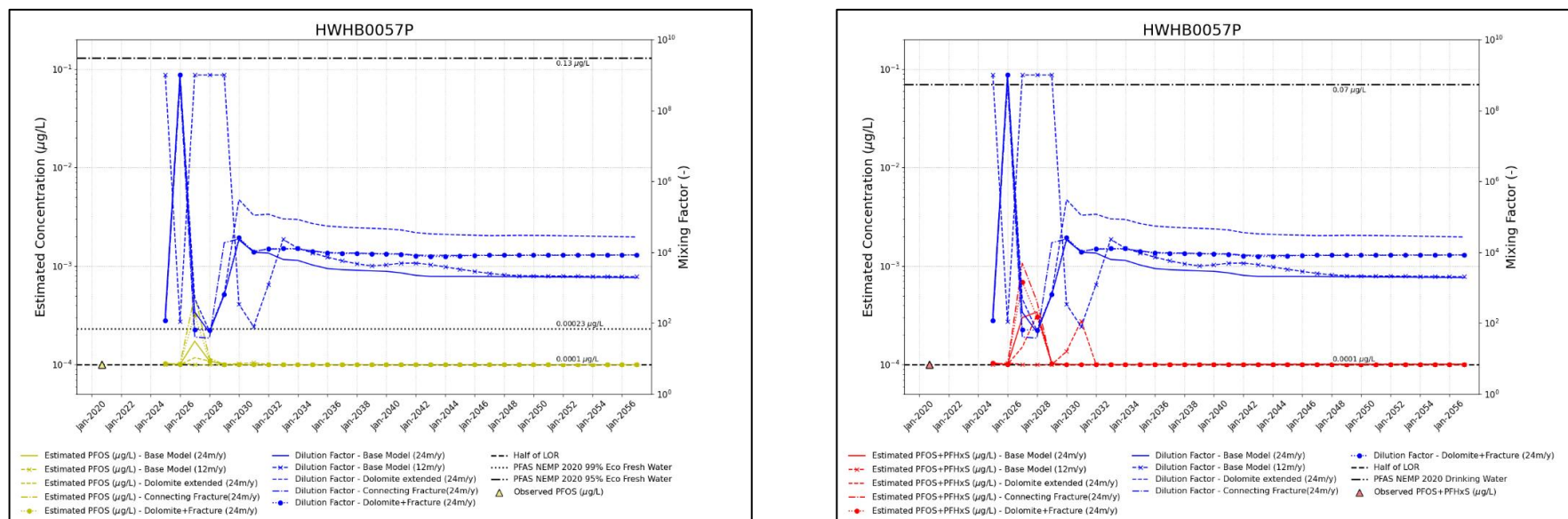


Figure E: Mixing Assessment Results for the bore HWHB0057P in OB29. PFOS (left) and PFOS+PFHxS (right).

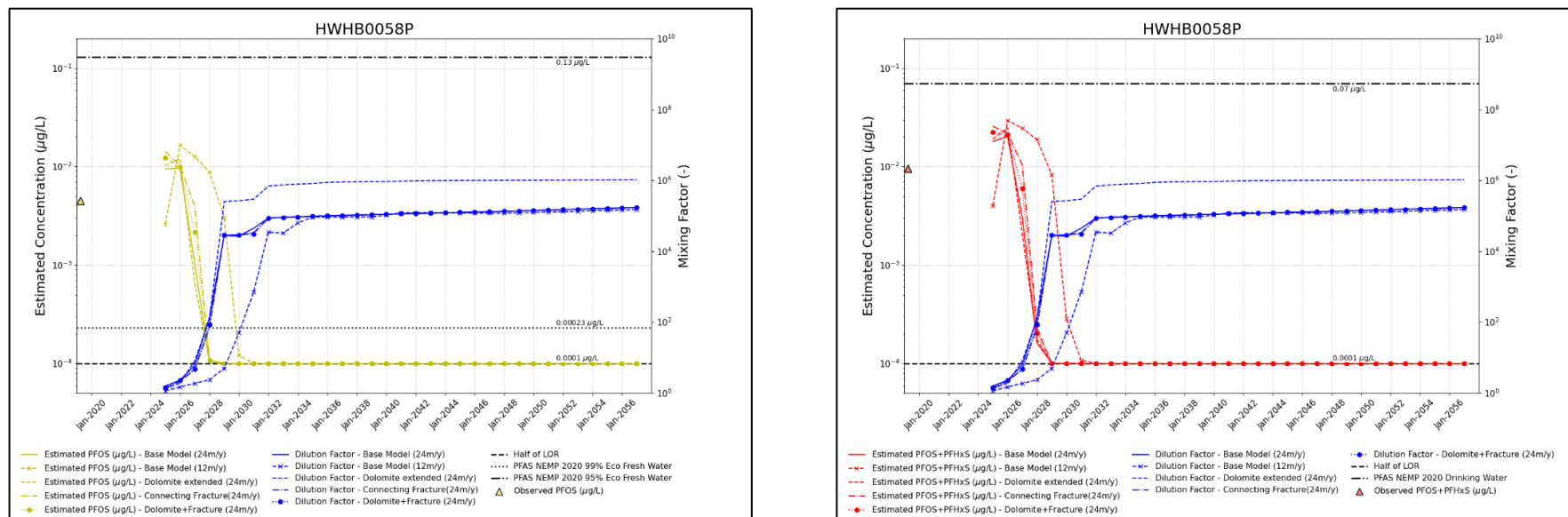


Figure F: Mixing Assessment Results for the bore HWHB0058P in OB29. PFOS (left) and PFOS+PFHxS (right).

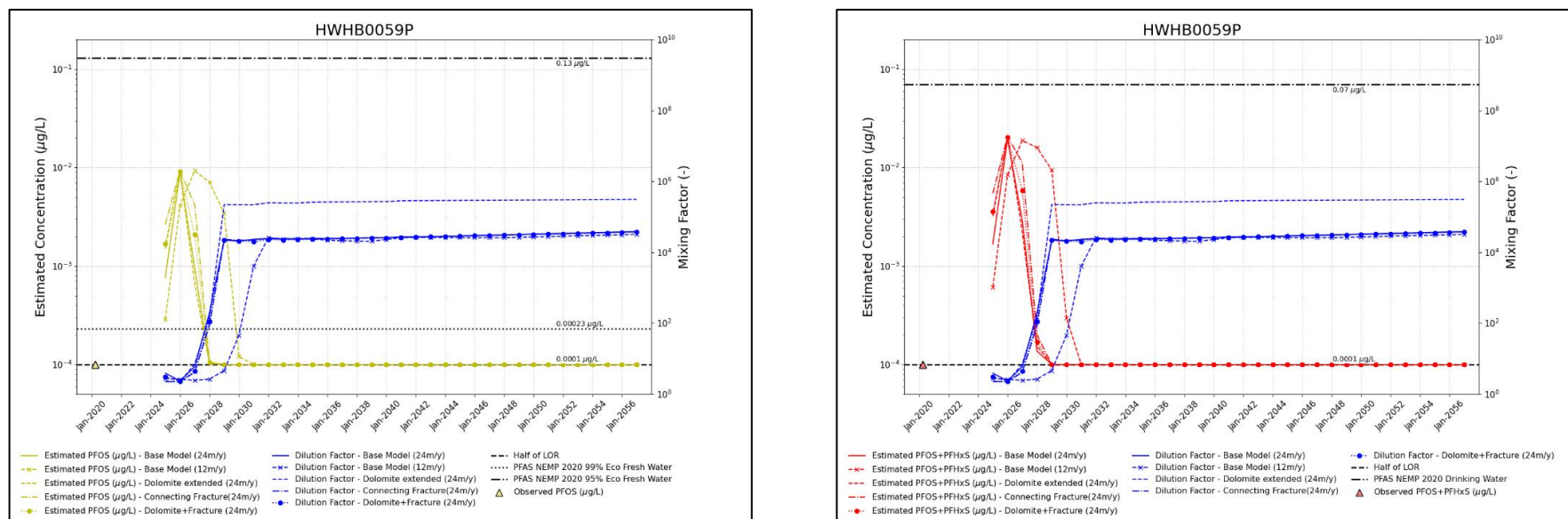


Figure G: Mixing Assessment Results for the bore HWHB0059P in OB29. PFOS (left) and PFOS+PFHxS (right).

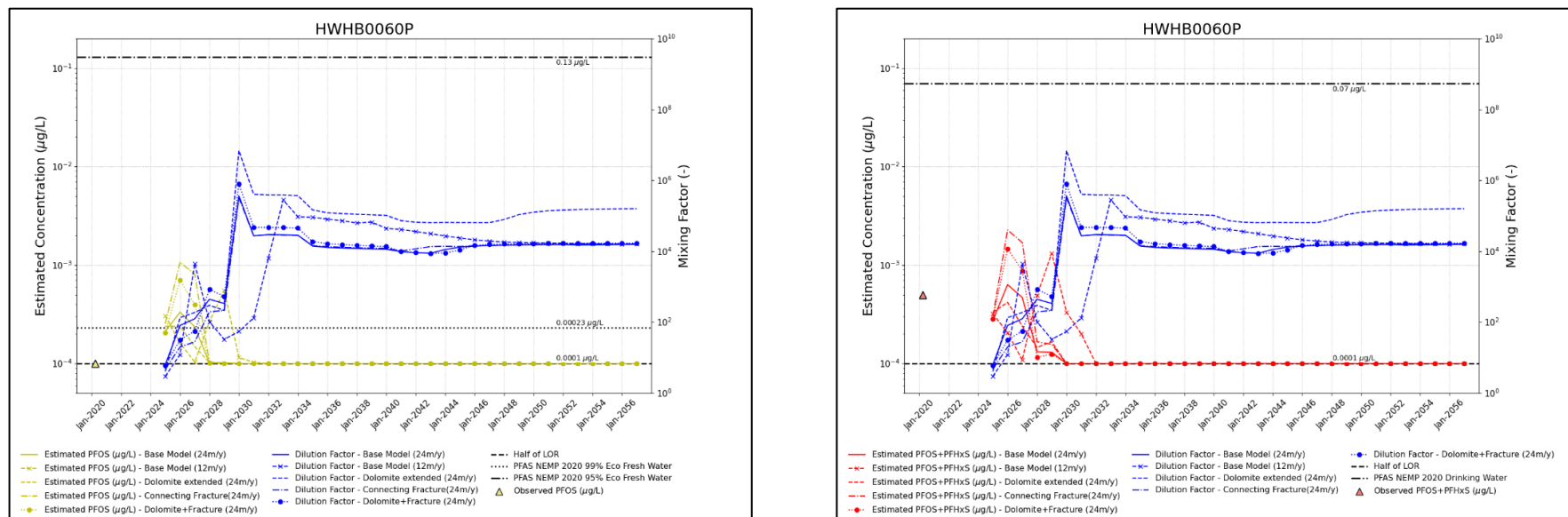


Figure H: Mixing Assessment Results for the bore HWHB0060P in OB29. PFOS (left) and PFOS+PFHxS (right).

2.0 INDIVIDUAL DEWATERING POTENTIAL LOCATIONS IN OB30

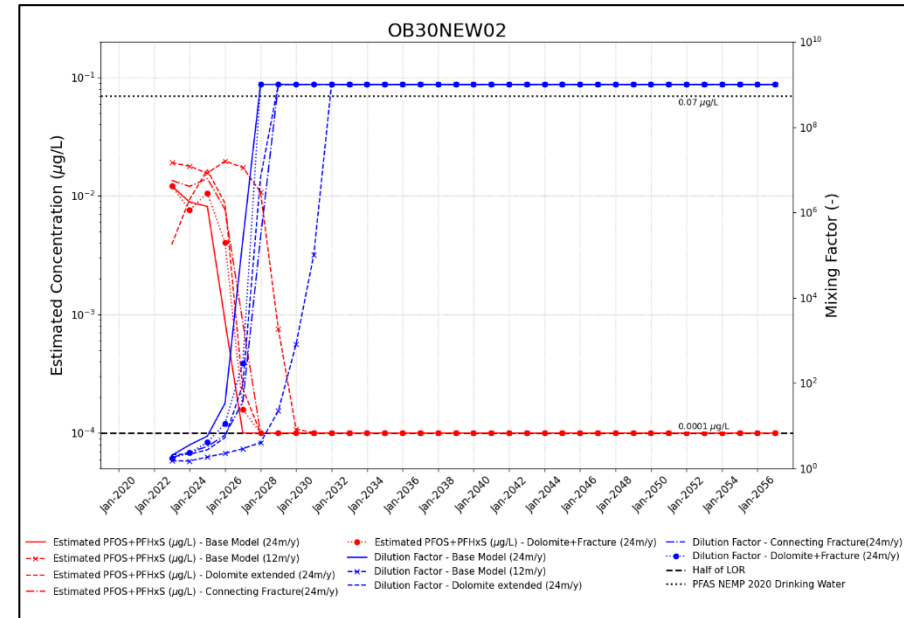
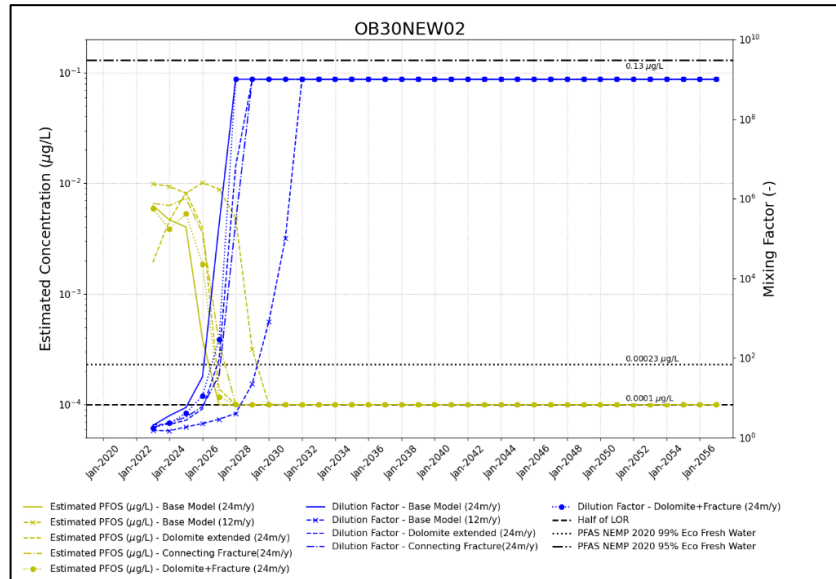


Figure I: Mixing Assessment Results for the potential bore location OB30NEW02 in OB30. PFOS (left) and PFOS+PFHxS (right).

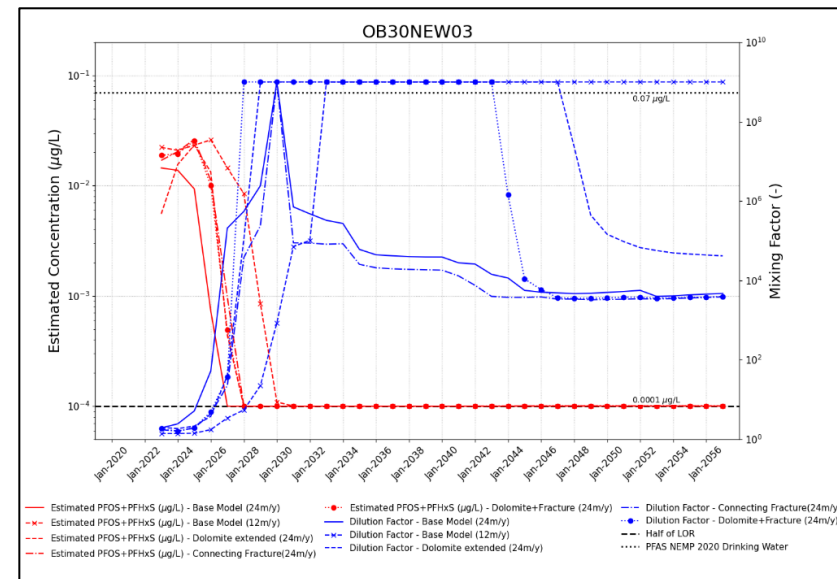
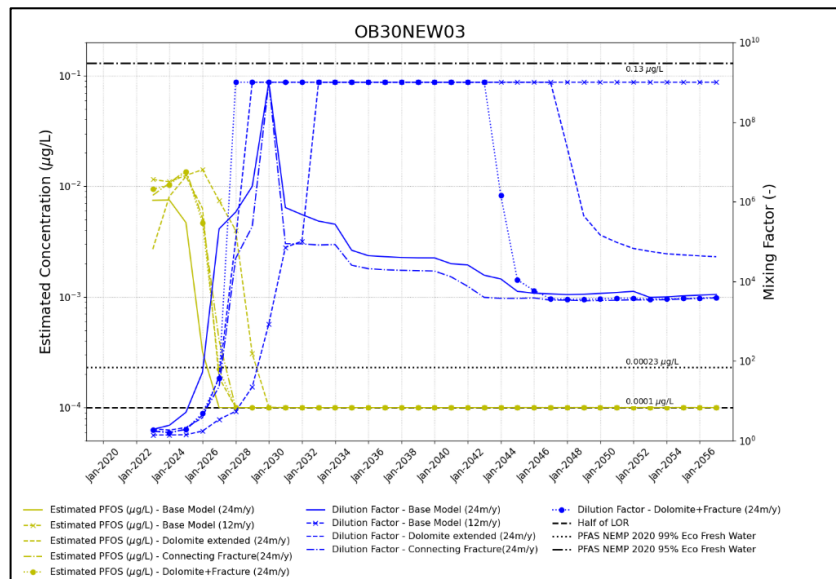
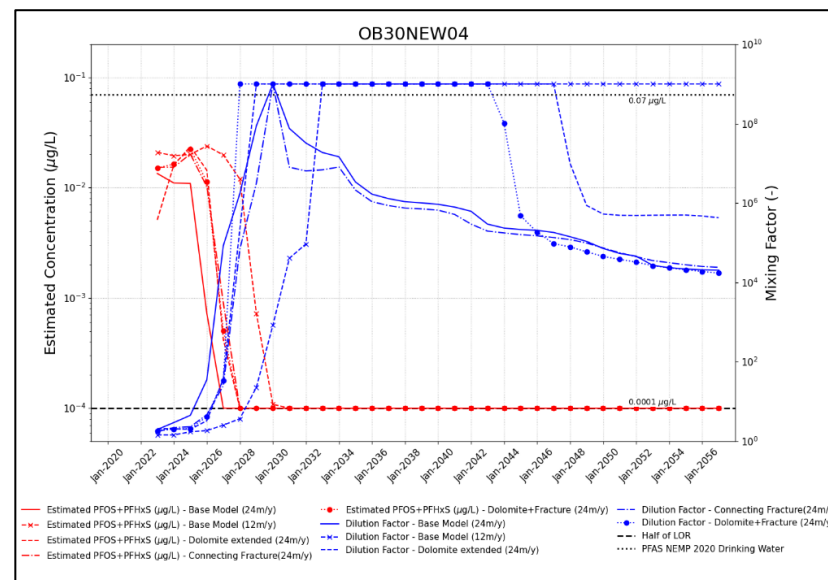
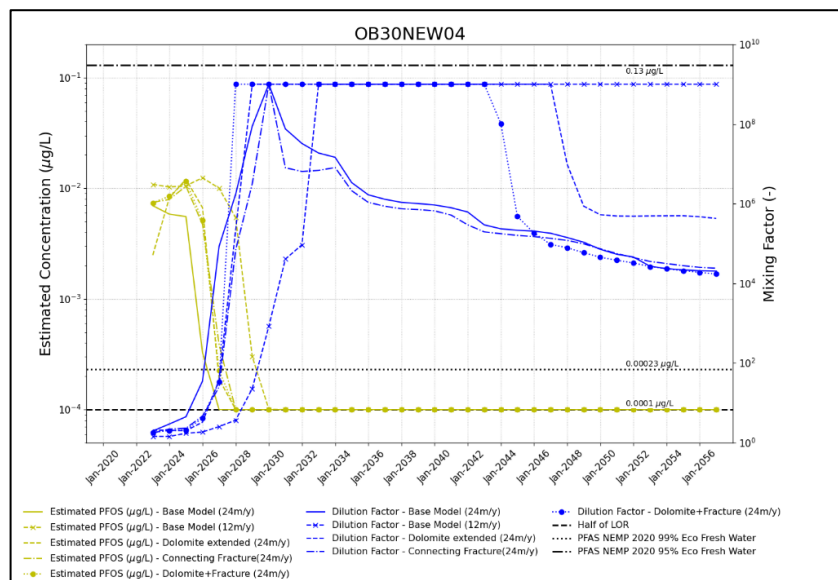
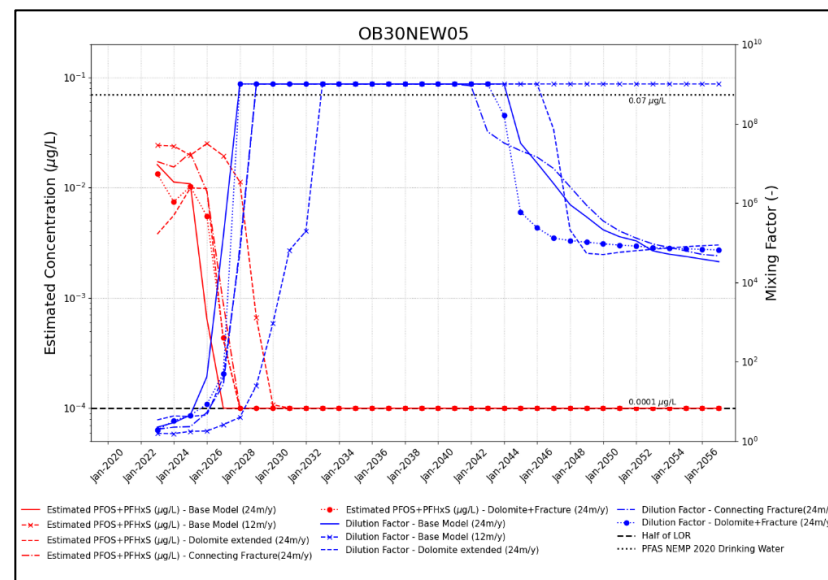
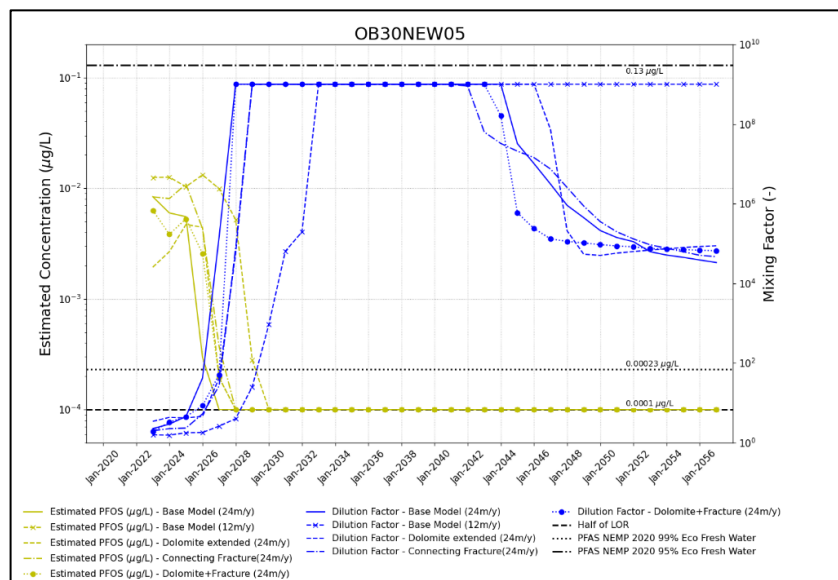


Figure J: Mixing Assessment Results for the potential bore location OB30NEW03 in OB30. PFOS (left) and PFOS+PFHxS (right).**Figure K: Mixing Assessment Results for the potential bore location OB30NEW04 in OB30. PFOS (left) and PFOS+PFHxS (right).****Figure L: Mixing Assessment Results for the potential bore location OB30NEW05 in OB30. PFOS (left) and PFOS+PFHxS (right).**

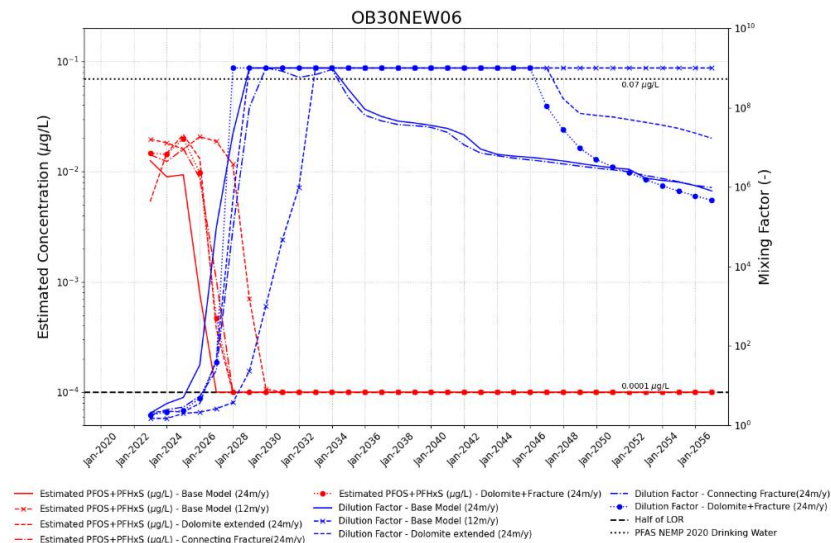
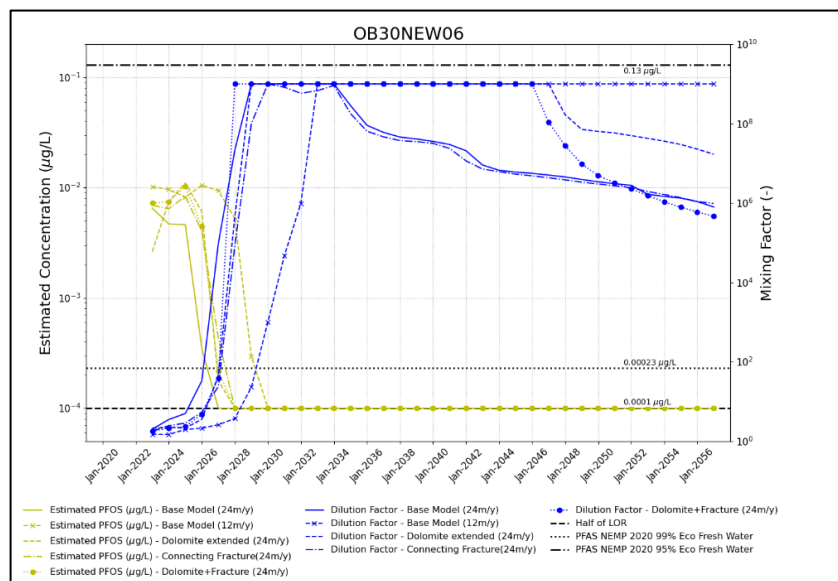


Figure M: Mixing Assessment Results for the potential bore location OB30NEW06 in OB30. PFOS (left) and PFOS+PFHxS (right).

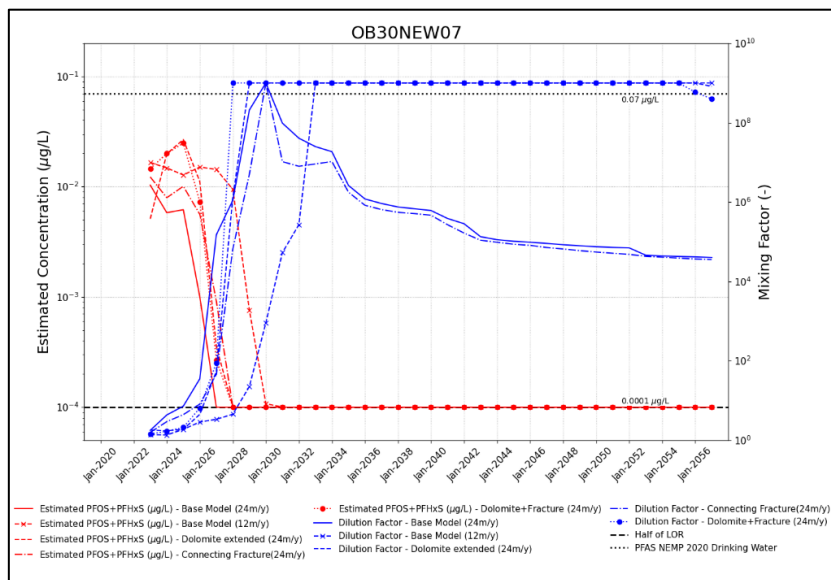
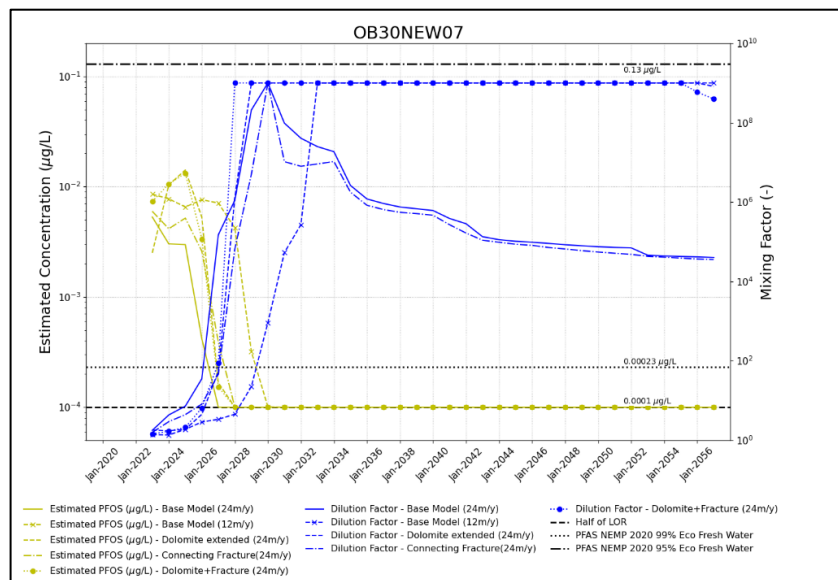


Figure N: Mixing Assessment Results for the potential bore location OB30NEW07 in OB30. PFOS (left) and PFOS+PFHxS (right).

3.0 INDIVIDUAL DEWATERING BORES IN OB35

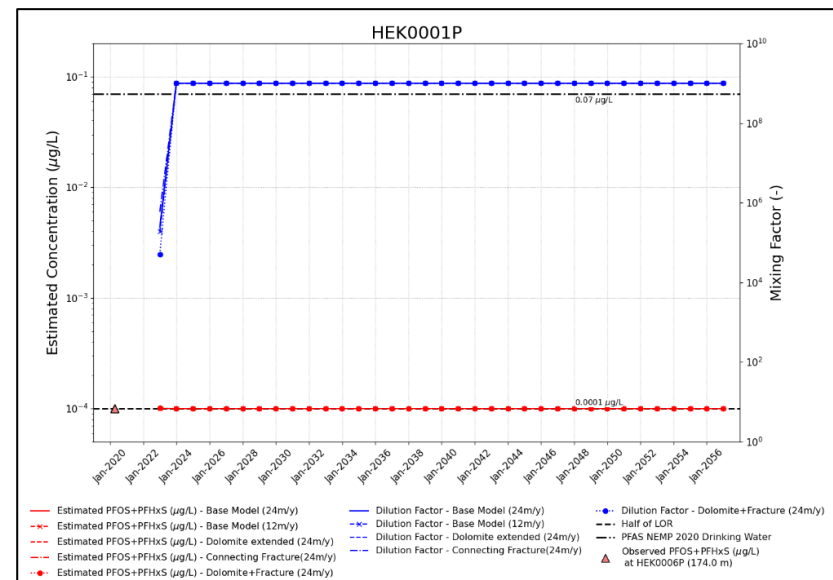
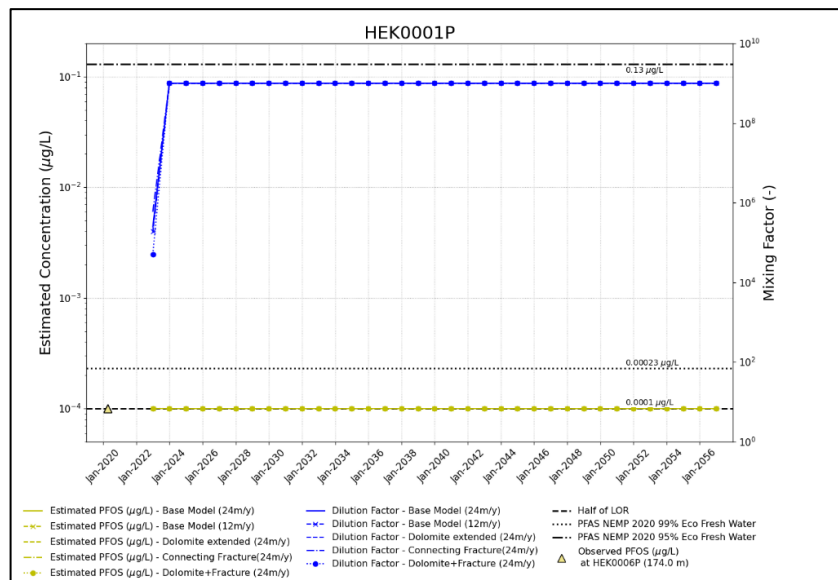


Figure O: Mixing Assessment Results for the bore HEK0001P in OB35. PFOS (left) and PFOS+PFHxS (right).

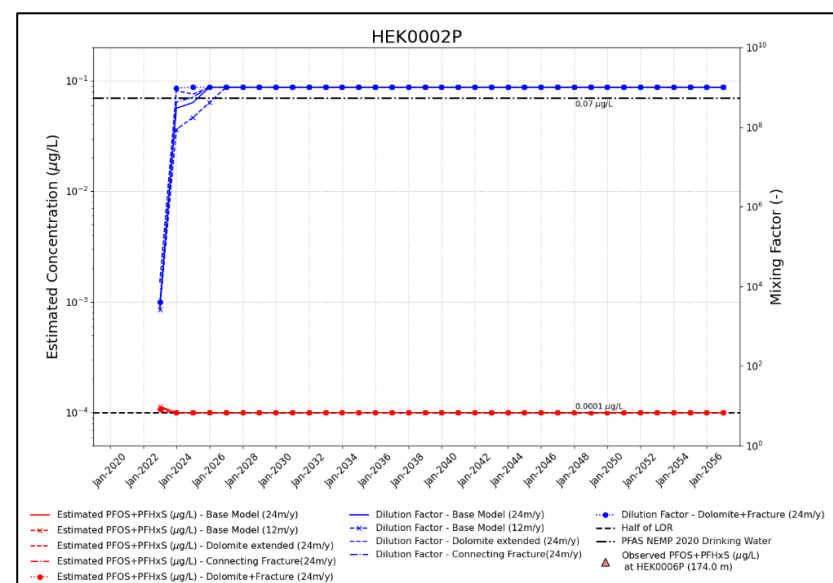
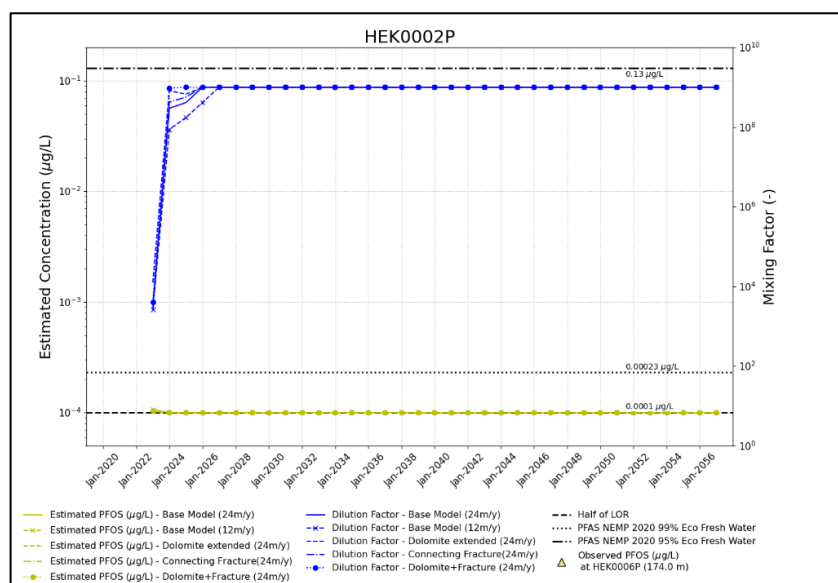


Figure P: Mixing Assessment Results for the bore HEK0002P in OB35. PFOS (left) and PFOS+PFHxS (right).

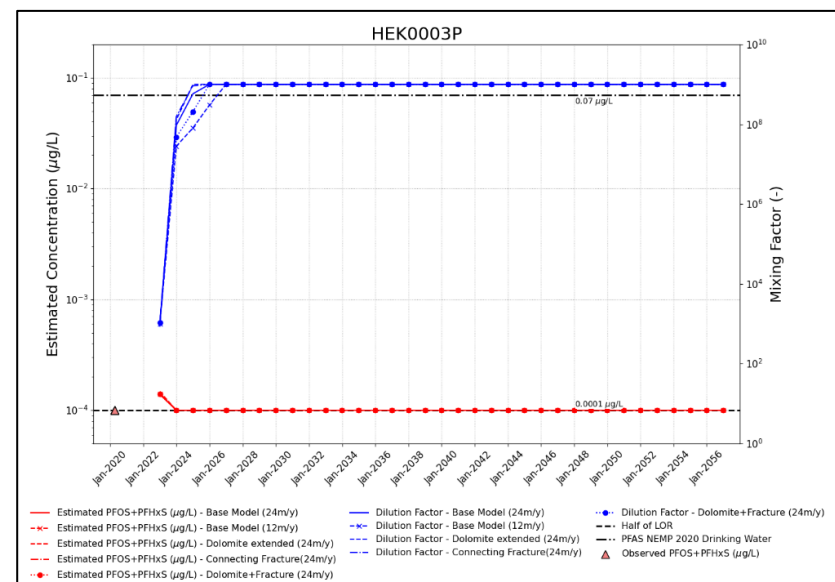
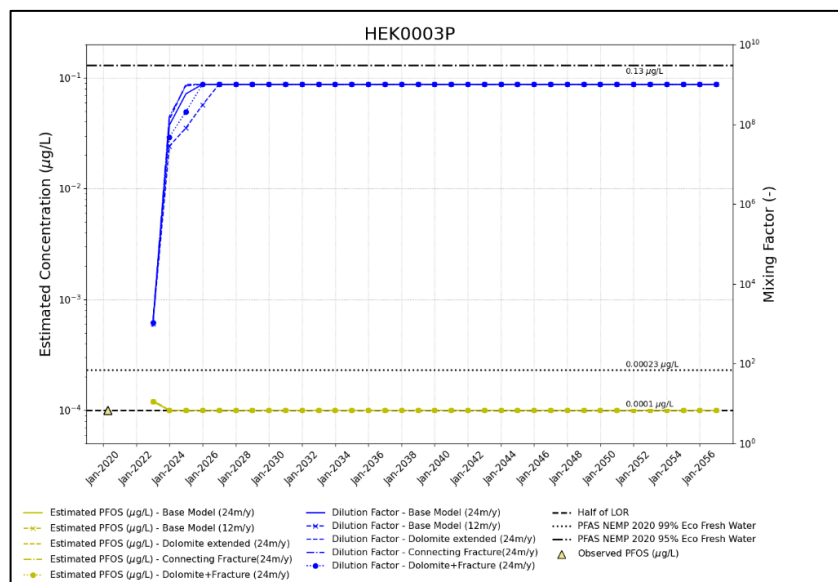


Figure Q: Mixing Assessment Results for the bore HEK0003P in OB35. PFOS (left) and PFOS+PFHxS (right).

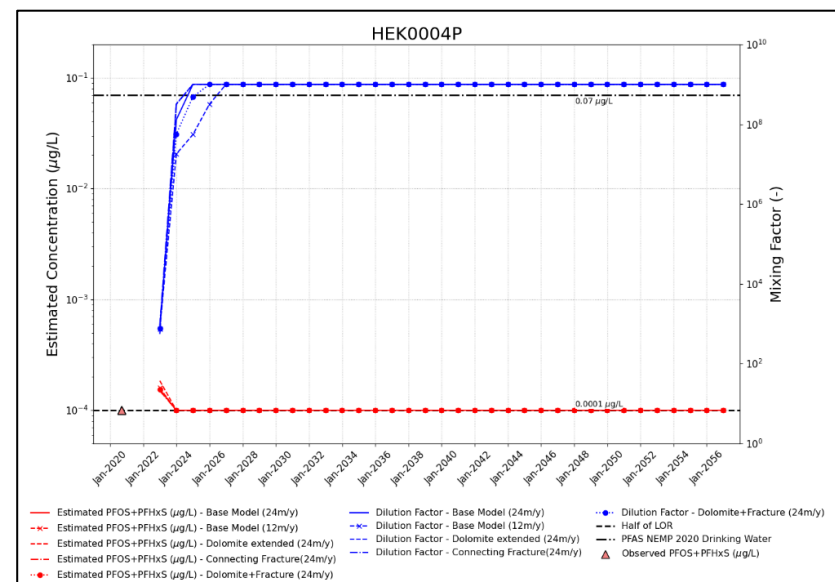
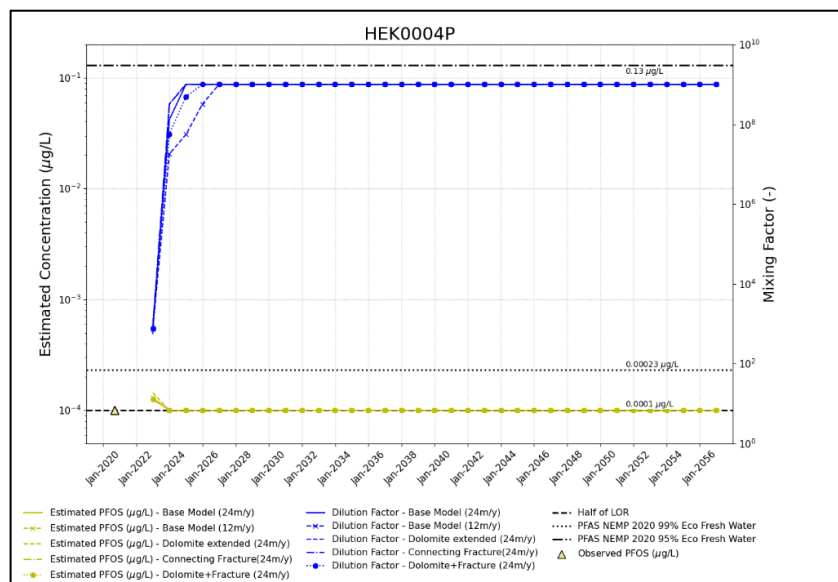


Figure R: Mixing Assessment Results for the bore HEK0004P in OB35. PFOS (left) and PFOS+PFHxS (right).

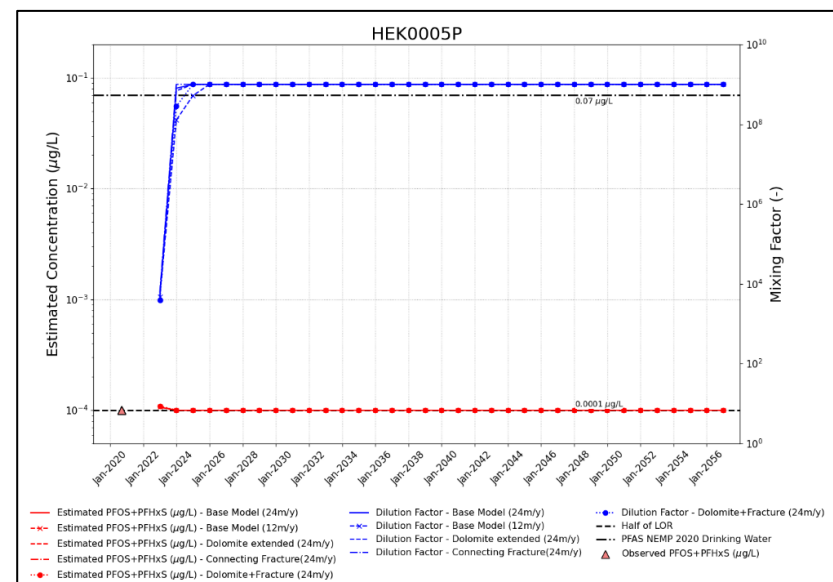
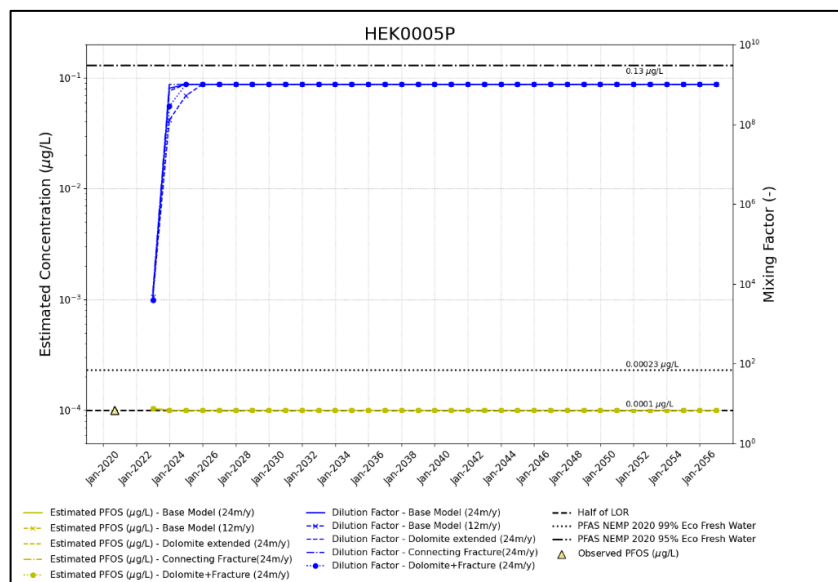


Figure S: Mixing Assessment Results for the bore HEK0005P in OB35. PFOS (left) and PFOS+PFHxS (right).

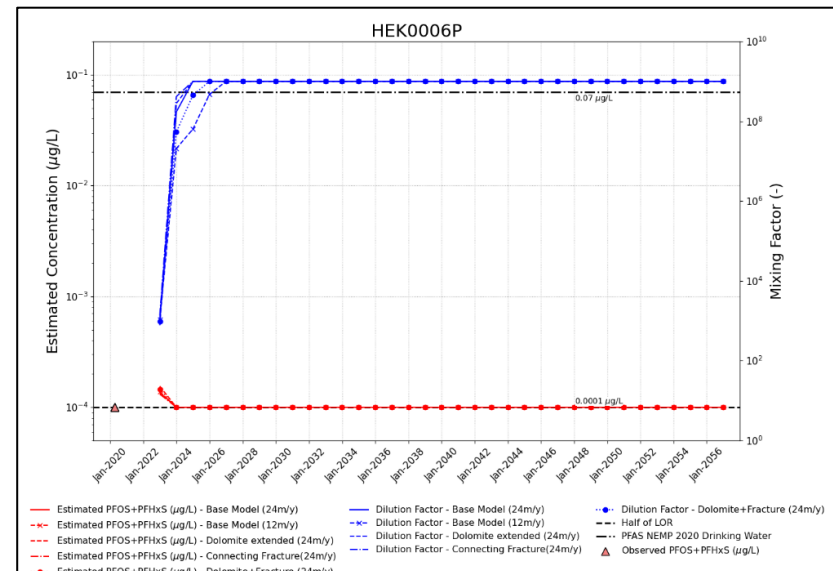
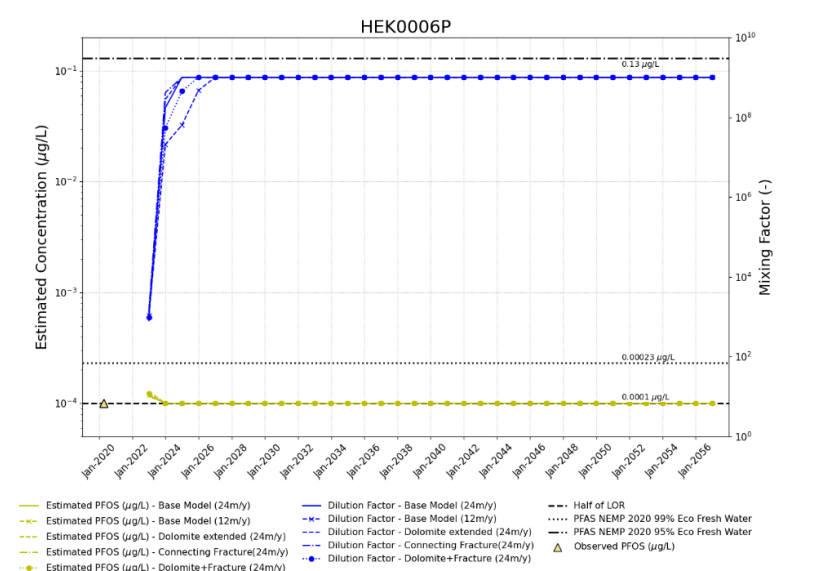


Figure T: Mixing Assessment Results for the bore HEK0006P in OB35. PFOS (left) and PFOS+PFHxS (right).

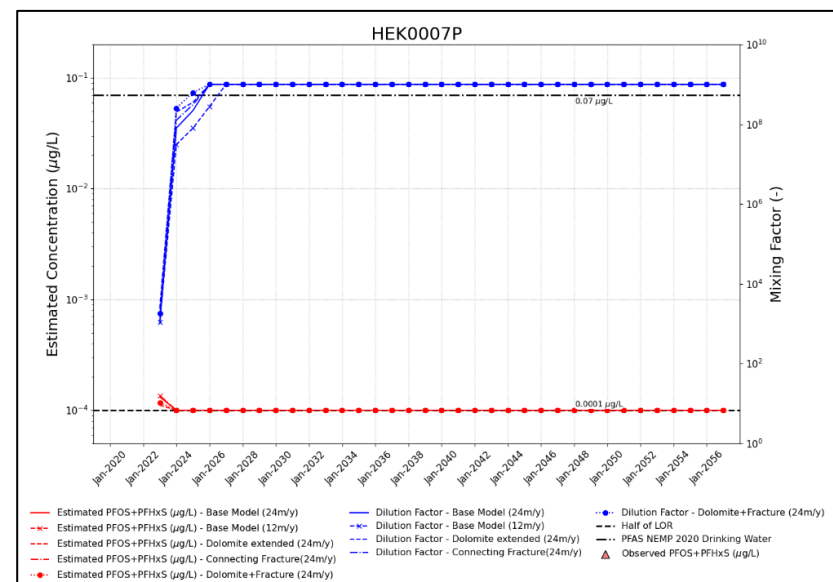
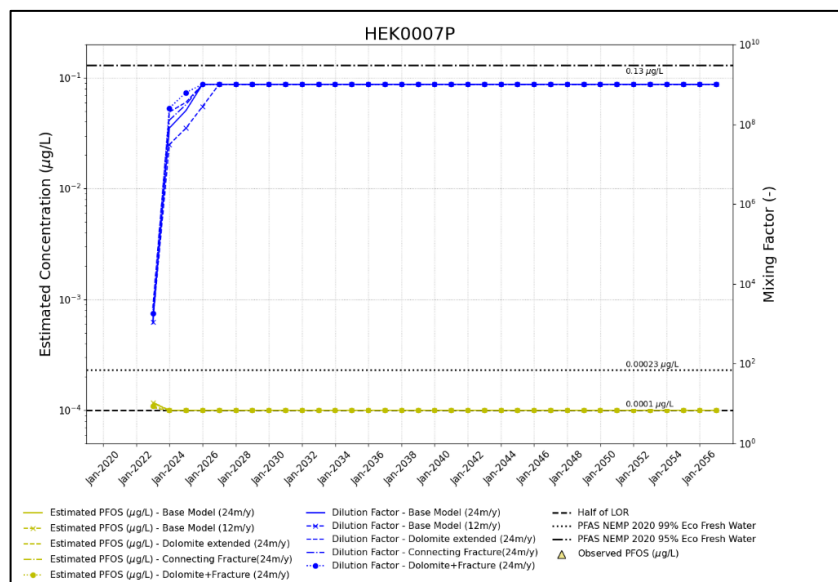


Figure U: Mixing Assessment Results for the bore HEK0007P in OB35. PFOS (left) and PFOS+PFHxS (right).

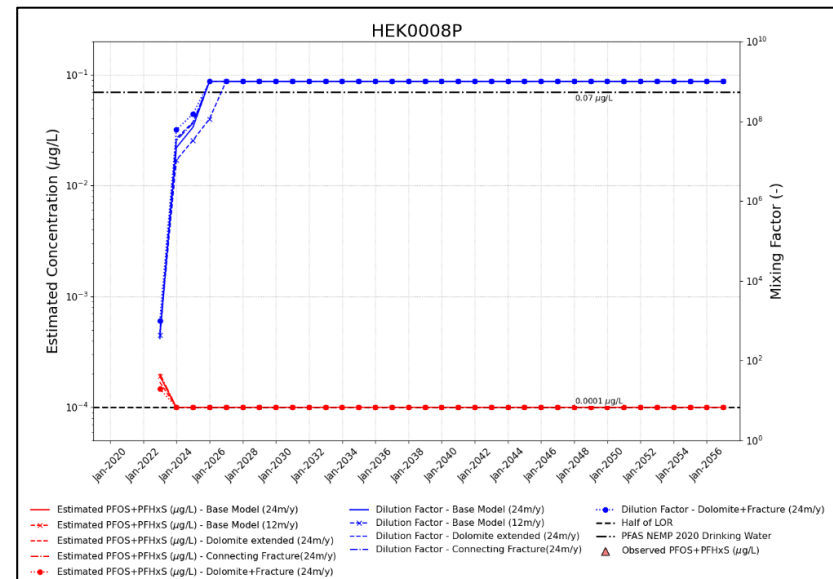
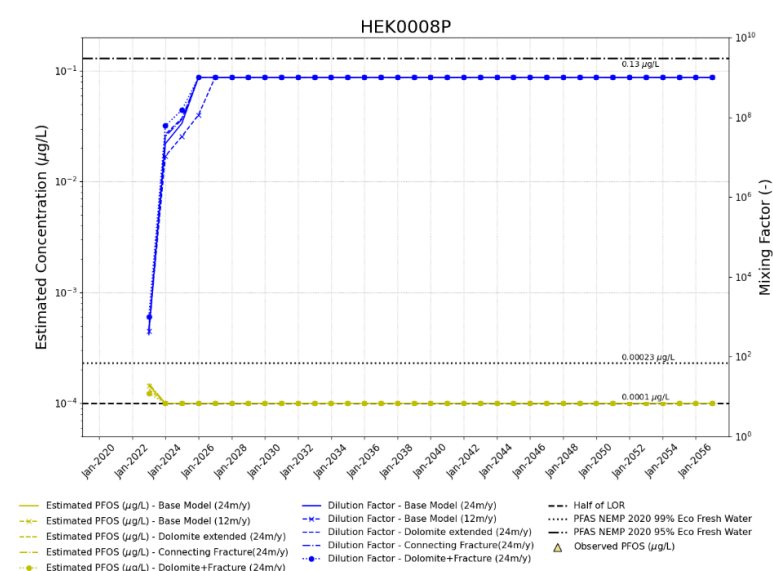


Figure V: Mixing Assessment Results for the bore HEK0008P in OB35. PFOS (left) and PFOS+PFHxS (right).

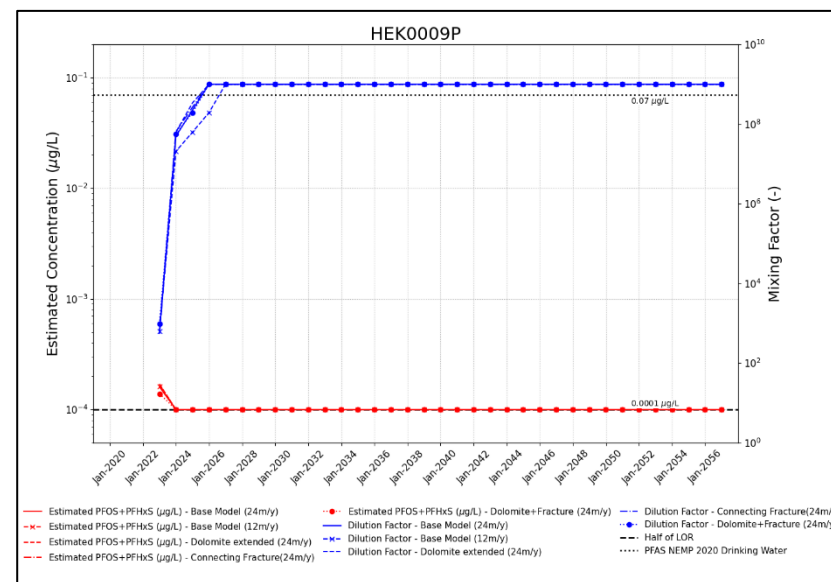
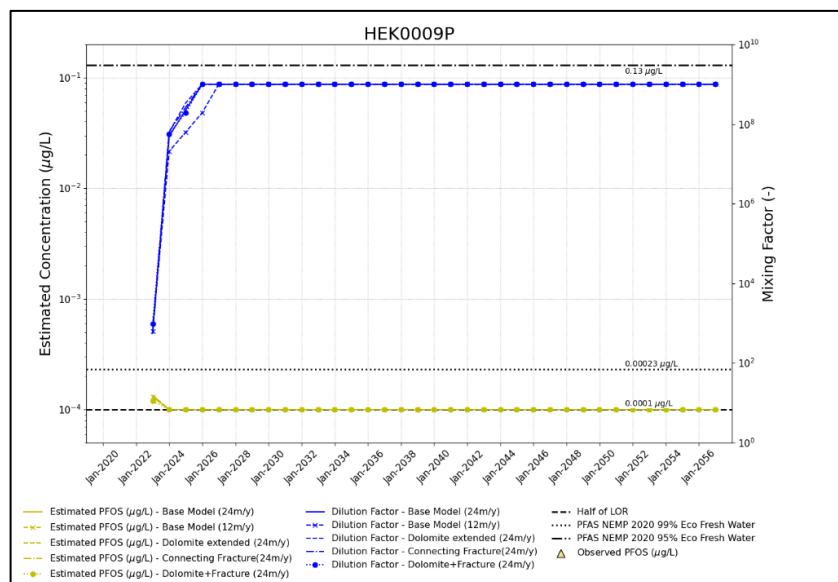


Figure W: Mixing Assessment Results for the bore HEK0009P in OB35. PFOS (left) and PFOS+PFHxS (right).

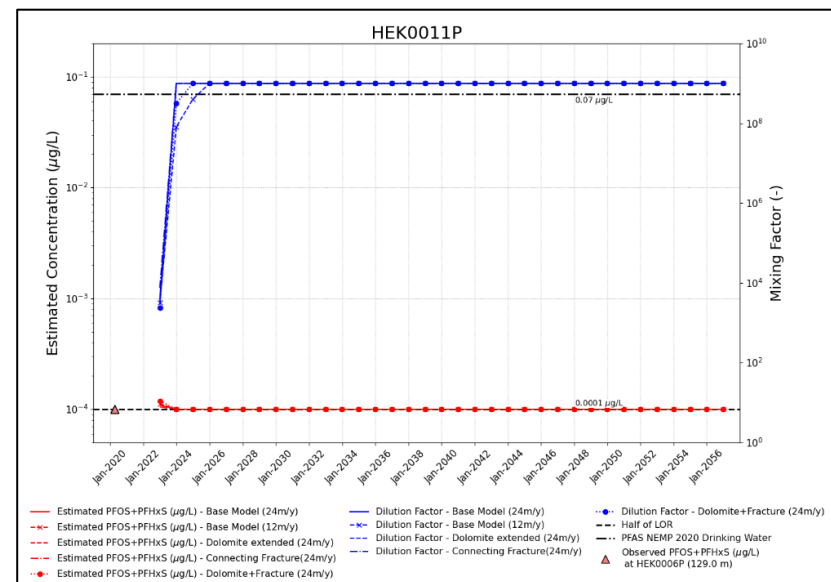
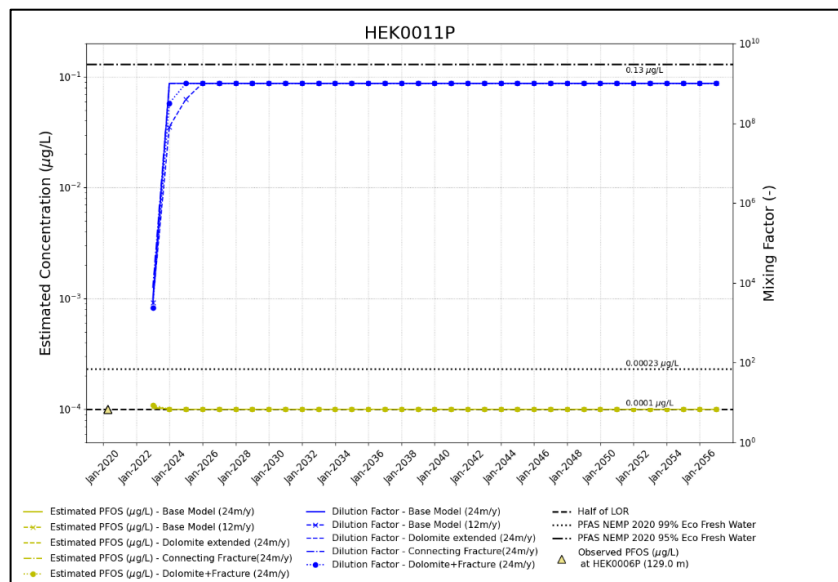


Figure X: Mixing Assessment Results for the bore HEK0011P in OB35. PFOS (left) and PFOS+PFHxS (right).

ATTACHMENT C

Important Information

The document ("Report") to which this page is attached and which this page forms a part of, has been issued by Golder Associates Pty Ltd ("Golder") subject to the important limitations and other qualifications set out below.

This Report constitutes or is part of services ("Services") provided by Golder to its client ("Client") under and subject to a contract between Golder and its Client ("Contract"). The contents of this page are not intended to and do not alter Golder's obligations (including any limits on those obligations) to its Client under the Contract.

This Report is provided for use solely by Golder's Client and persons acting on the Client's behalf, such as its professional advisers. Golder is responsible only to its Client for this Report. Golder has no responsibility to any other person who relies or makes decisions based upon this Report or who makes any other use of this Report. Golder accepts no responsibility for any loss or damage suffered by any person other than its Client as a result of any reliance upon any part of this Report, decisions made based upon this Report or any other use of it.

This Report has been prepared in the context of the circumstances and purposes referred to in, or derived from, the Contract and Golder accepts no responsibility for use of the Report, in whole or in part, in any other context or circumstance or for any other purpose.

The scope of Golder's Services and the period of time they relate to are determined by the Contract and are subject to restrictions and limitations set out in the Contract. If a service or other work is not expressly referred to in this Report, do not assume that it has been provided or performed. If a matter is not addressed in this Report, do not assume that any determination has been made by Golder in regards to it.

At any location relevant to the Services conditions may exist which were not detected by Golder, in particular due to the specific scope of the investigation Golder has been engaged to undertake. Conditions can only be verified at the exact location of any tests undertaken. Variations in conditions may occur between tested locations and there may be conditions which have not been revealed by the investigation and which have not therefore been taken into account in this Report.

Golder accepts no responsibility for and makes no representation as to the accuracy or completeness of the information provided to it by or on behalf of the Client or sourced from any third party. Golder has assumed that such information is correct unless otherwise stated and no responsibility is accepted by Golder for incomplete or inaccurate data supplied by its Client or any other person for whom Golder is not responsible. Golder has not taken account of matters that may have existed when the Report was prepared but which were only later disclosed to Golder.

Having regard to the matters referred to in the previous paragraphs on this page in particular, carrying out the Services has allowed Golder to form no more than an opinion as to the actual conditions at any relevant location. That opinion is necessarily constrained by the extent of the information collected by Golder or otherwise made available to Golder. Further, the passage of time may affect the accuracy, applicability or usefulness of the opinions, assessments or other information in this Report. This Report is based upon the information and other circumstances that existed and were known to Golder when the Services were performed and this Report was prepared. Golder has not considered the effect of any possible future developments including physical changes to any relevant location or changes to any laws or regulations relevant to such location.

Where permitted by the Contract, Golder may have retained subconsultants affiliated with Golder to provide some or all of the Services. However, it is Golder which remains solely responsible for the Services and there is no legal recourse against any of Golder's affiliated companies or the employees, officers or directors of any of them.

By date, or revision, the Report supersedes any prior report or other document issued by Golder dealing with any matter that is addressed in the Report.

Any uncertainty as to the extent to which this Report can be used or relied upon in any respect should be referred to Golder for clarification